
Article:
Keenan, Tessa, Dowle, Adam, Bates, Rachel et al. (1 more author) (2019) Characterisation of the Streptomyces coelicolor glycoproteome reveals glycoproteins important for cell wall biogenesis. MBio. e01092. ISSN 2150-7511

Characterisation of the *Streptomyces coelicolor* glycoproteome reveals glycoproteins important for cell wall biogenesis.

Tessa Keenan[1], Adam Dowle[2], Rachel Bates[2] and Margaret C. M. Smith*[1]

[1] *Department of Biology, University of York, York, YO10 5DD, UK.*

[2] *Bioscience Technology Facility, University of York, York, YO10 5DD, UK.*

Corresponding author: Margaret C. M. Smith, Department of Biology, University of York, York, YO10 5DD, UK. Maggie.smith@york.ac.uk

Keywords: *Streptomyces coelicolor*, glycosylation, cell wall biosynthesis, antibiotics.

Abstract

The physiological role of protein O-glycosylation in prokaryotes is poorly understood, due to our limited knowledge of the extent of their glycoproteomes. In Actinobacteria, defects in protein O-mannosyl transferase (Pmt)-mediated protein O-glycosylation have been shown to significantly retard growth (*Mycobacterium tuberculosis*, *Corynebacterium glutamicum*) or result in increased sensitivities to cell-wall targeting antibiotics (*Streptomyces coelicolor*) suggesting that protein O-glycosylation may have an important role in cell physiology. Only a single glycoprotein (SCO4142, PstS) has been identified to date in *S. coelicolor*. Combining biochemical and MS-based approaches, we have isolated and characterised the membrane glycoproteome in *S. coelicolor*. A total of ninety-five high confidence glycopeptides were identified which mapped to thirty-seven new *S. coelicolor* glycoproteins and a deeper understanding of glycosylation sites in PstS. Glycosylation sites were found to be modified with up to three hexose residues, consistent with what has been observed previously in other Actinobacteria. *S. coelicolor* glycoproteins have diverse roles, including solute binding, polysaccharide hydrolases, ABC transporters and cell wall biosynthesis, the latter being of potential relevance to the antibiotic-sensitive phenotype of *pmt*$^{-}$ mutants. Null mutants in genes encoding a putative D-Ala-D-Ala carboxypeptidase (SCO4847) and an L, D transpeptidase (SCO4934) were hypersensitive to cell-wall targeting antibiotics. Additionally, the *sco4847*$^{-}$ mutants displayed an increased susceptibility to lysozyme treatment. These findings strongly suggest that both glycoproteins are required for maintaining cell wall integrity and that glycosylation could be affecting enzyme function.

Importance

In prokaryotes, the role of protein glycosylation is poorly understood due to our limited understanding of their glycoproteomes. In some Actinobacteria, defects in protein O-glycosylation have been shown to retard growth and result in hypersensitivity to cell-wall targeting antibiotics, suggesting that this modification may be important for maintaining cell wall structure. Here, we have characterised the glycoproteome in *Streptomyces coelicolor* and shown that glycoproteins have diverse roles including solute binding, ABC transporters and cell wall biosynthesis. We have generated mutants encoding two putative cell-wall active glycoproteins and shown them to be hypersensitive to cell-wall targeting antibiotics. These findings strongly suggest that both glycoproteins are required for maintaining cell wall integrity and that glycosylation could be affecting enzyme function.

Introduction

Protein modification by glycosylation is a process that occurs in all domains of life (1, 2). Glycan moieties, which can be extremely diverse in structure and composition, are most commonly attached to either asparagine (N-glycosylation) or to serine/threonine (O-glycosylation) in the peptide chain. The presence of the glycan changes the physico-chemical properties of the protein and has been shown to have effects on cellular localisation, ligand binding and stability (1). The enzymes mediating N- and O-glycosylation are conserved between kingdoms, but studies on protein glycosylation in prokaryotes lags behind that of eukaryotes. Consequently, with a few exceptions (3-5), the extent and functions of the glycoproteome in most prokaryotes are unclear.

Recent reports have described the phenotypes of bacteria lacking a protein-O-mannosyl transferase (Pmt) and they are either strongly retarded in growth (*Mycobacterium tuberculosis*, *Corynebacterium glutamicum*) or have increased sensitivities to several antibiotics that target the cell wall, including vancomycin and β-lactams (*Streptomyces coelicolor*) (6-8). These three bacterial species are all within the Actinobacteria where the occurrence of Pmt is prevalent. In the case of *Streptomyces,* the *pmt*$^-$ mutants have also become resistant to infection by the phage ϕC31, implying that the glycans could perform a role in ligand recognition (9). The O-glycoproteome from *Mycobacterium tuberculosis* (*M. tuberculosis)* has been extensively explored; in particular the culture filtrate consists of more than forty glycoproteins, including potential cell-wall active glycoproteins such as a putative glycosyl hydrolase (Rv1096) and a β-lactamase BlaC (Rv2068c) (10-14). In contrast only a single glycoprotein (SCO4142; PstS) has been identified to date in *S. coelicolor* (15). Given that the Pmt mediated O-glycosylation system is a general glycosylation system in

other bacteria and fungi, we hypothesise the presence of a glycoproteome in *S. coelicolor* and one of its roles is in cell wall biogenesis.

Pmt is a predicted integral membrane protein and in *M. tuberculosis* has been shown to mannosylate unfolded proteins as they are secreted through the Sec system (16). The sugar donor for Pmt is polyprenol phosphate mannose (PPM), which is made intra-cytoplasmically via the transfer of mannose from GDP-mannose to polyprenol phosphate by polyprenol phosphate mannose synthase (Ppm1) (15, 17). PPM is then thought to be flipped in the membrane so that the mannose moiety can be presented to Pmt for transfer to the target proteins. *S. coelicolor ppm1*$^-$ mutants, and mutants (*manB*$^-$ and *manC*$^-$) with depleted enzymes that supply GDP-mannose to Ppm1, all have phenotypes that resemble that of the *pmt*$^-$ mutants but display more extreme antibiotic sensitivities (6, 18).

The phenotypes of the *pmt*$^-$ mutants imply that glycosylation has an important role in cell physiology. The increased sensitivity of the *S. coelicolor pmt*$^-$ mutants to the antibiotics vancomycin and some b-lactams suggest that glycosylation might affect the function of enzymes in cell wall biogenesis, possibly in peptidoglycan crosslinking. Here we investigate the *Streptomyces* glycoproteome, focussing on the membrane and membrane-associated proteins with a view to elucidating the mechanism that underpins the antibiotic sensitivity. Using enrichment of the glycoproteome by lectin chromatography followed by mass spectrometry, a total of ninety-five, high-confidence glycopeptides were characterised from thrity-eight glycoproteins. *S. coelicolor* mutants were constructed in genes encoding glycoproteins that could be involved in peptidoglycan biosynthesis and were found to have an antibiotic-sensitive phenotype. These data indicate that protein glycosylation might have a role in the functions of multiple periplasmic proteins.

Results and Discussion

Enrichment and detection of a glycoproteome in S. coelicolor

To investigate the glycoproteome in *S. coelicolor*, membrane protein fractions were isolated from the *S. coelicolor* parent strain J1929, and the glycosylation deficient strains DT1025 (*pmt*$^-$) and DT3017 (*ppm1*$^-$). The strains were cultivated in defined, phosphate limited (F134), liquid medium as expression of the previously characterised *S. coelicolor* glycoprotein SCO4142 (PstS) was known to be induced on phosphate depletion (15, 19, 20). The proteins were separated by SDS-PAGE, blotted onto polyvinylidene difluoride (PVDF) membrane and probed with concanavalin A (Con A) conjugated to horseradish peroxidase (Con A-HRP) (Fig. S1). Several Con A reactive bands were observed in the J1929 membrane protein fraction within the 100-40 kDa molecular weight range, which were absent from the protein O-mannosyl transferase and polyprenol phosphate mannose synthase deficient strains DT1025 (*pmt*$^-$) and DT3017 (*ppm1*$^-$) (Fig. S1. B). The Con A reactivity was lost in the present of methyl α-D glucopyranoside, a competitive inhibitor of mannose and glucose binding. These results demonstrate the presence of a glycoproteome in *S. coelicolor*, that requires the activities of Pmt and Ppm1.

To facilitate the characterisation of the glycoproteome, lectin affinity chromatography was used to enrich for the *S. coelicolor* membrane glycoproteins. In order to maximise the number of glycoproteins isolated and to account for any growth-stage specific changes to the glycoproteome, glycoproteins were enriched from J1929 membrane protein fractions isolated after 20, 35, 43 and 60 hours of growth (Fig. S2). The total, unbound and enriched protein fractions were separated by SDS-PAGE, blotted onto a PVDF membrane and probed

with Con A-HRP (Fig. 1). Over the four time points, changes were observed in the abundance and numbers of proteins enriched after lectin affinity chromatography as shown by Coomassie staining (Fig. 1, lanes 4, 7, 10 and 14), suggesting that there may be growth-stage specific changes to the membrane glycoproteome in *S. coelicolor*. The Con A reactivity profiles of the enriched fractions, which also changed throughout the time course, are consistent with this observation (Fig. 1, lanes 17, 20, 23 and 26). The greatest number of strongly Con A reactive bands were observed in membrane protein fractions enriched after 35 and 43 hours of growth, suggesting that these fractions might yield the most glycoproteins. The unbound fractions from the Con A columns also yielded some cross-reactivity with Con A-HRP but mostly to proteins that were abundant in the Coomassie stained gels, suggesting non-specific Con A reactivity. Taken together, these results show that glycoproteins are expressed throughout the *S. coelicolor* growth cycle and that the glycoproteome varies according to the growth stage.

S. coelicolor glycoproteome characterisation using mass spectrometry.

In order to identify the *S. coelicolor* glycoproteins isolated from the membrane proteome after lectin affinity chromatography (Fig. 1) and characterise the sites of modification, liquid chromatography (LC) coupled to tandem mass spectrometry (MS/MS) was carried out. Since the previously characterised *S. coelicolor* glycoprotein PstS was shown to be modified with a trihexose (15) and numerous glycoproteins with short mannose modifications have been previously described in the closely related *M. tuberculosis* (10, 13, 21), we focussed on short hexose modifications in our analyses. To enable a comprehensive analysis of the *S.*

coelicolor glycoproteome, several different peptide fragmentation techniques were employed to facilitate both glycopeptide characterisation and glycosylation site assignment.

The fractions enriched in *S. coelicolor* glycoproteins after 20, 35, 43 and 60 hours of growth were each subjected to in-gel tryptic digestion after SDS-PAGE and analysed by liquid chromatography coupled to electrospray ionisation collision-induced dissociation tandem mass spectrometry (LC-ESI-CID-MS/MS). A total of 24 different *S. coelicolor* glycopeptides were identified over the four time points (Dataset S1), mapping to fifteen new *S. coelicolor* glycoproteins. The spectra of the glycopeptides obtained by CID fragmentation were dominated by product ions formed due to the preferential cleavage of glycosidic bonds. In these cases, the glycopeptide was identified when the mass difference between the peptide backbone identified from the MS/MS spectra and the precursor ion was equivalent to a hexose (162 Da) or multiples thereof. For example, the glycopeptide N-SATAASPSAEASGEAGGTGK-C belonging to SCO4847 was shown to be modified with nine hexose residues (Fig. 2A). The triply charged precursor ion at *m/z* 1055.76 is consistent with a glycopeptide mass of 3164.28 Da. The predicted mass of unmodified N-SATAASPSAEASGEAGGTGK-C is 1705.77 Da, which is a difference of 9 hexose residues (1458.47 Da) from the mass of the glycosylated peptide. The spectrum is dominated by the *y*-ion series that validate the sequence of the peptide backbone. While two ions were observed with the glycan intact (y_{14}+ 2Hex, M_R+ 9Hex), these were not enough to assign the glycosylation sites in the glycopeptide. Since the unambiguous assignment of the glycosylated amino acid residue relies on the observation of peptide product ions containing at least one hexose residue, in many cases it was not possible to map the glycosylation sites in the glycopeptides identified using CID fragmentation.

To widen *S. coelicolor* glycoproteome characterisation and to enable glycosylation site assignments to be made, enriched membrane glycoproteins isolated after 43 hours of growth were further analysed by mass spectrometry using complementary fragmentation techniques; higher energy collision dissociation (HCD) and electron transfer dissociation (ETD). HCD fragmentation is a higher energy form of CID available on Orbitrap mass spectrometers and produces similar fragmentation patterns to CID fragmentation (*y*- and *b*-ions). In contrast, ETD fragmentation favours cleavage of the peptide backbone (*c*- and *z*-type ions) leaving the glycan structure intact, thus facilitating glycosylation site localisation (22). The combined data acquisitions using the HCD and ETD fragmentation techniques, resulted in the identification of thirty six different *S. coelicolor* glycopeptides (Dataset S1). The spectrum with the highest confidence of a match for each glycopeptide is shown in Dataset S2. ETD fragmentation allowed for a further thirteen O-glycosylation sites to be assigned, nearly double the number of assignments made after the CID and HCD experiments combined. In total, O-glycosylation sites were assigned in approximately 30% of the glycopeptides identified in this work. While no distinct consensus sequence was identified, there was a high propensity for hydrophobic amino acids (e.g. Ala, Pro, Gly) near the glycosylation site (Fig. 2B). This feature is reminiscent of sequences surrounding O-glycosylation sites in other Actinobacteria (14, 21, 23, 24). At least 30% of the glycopeptides identified in this work were supported by multiple spectra. Hex, Hex_2 and Hex_3 modifications were all detected, as expected. Searches for Hex_4 and Hex_5 modifications revealed some hits, however upon manual inspection of these spectra it was determined that these were peptides with multiple sites modified with Hex, Hex_2 and Hex_3.

In total, thirty-seven new *S. coelicolor* glycoproteins were identified (Table 1). Additionally, the data acquired using ETD fragmentation enabled the further characterisation of the previously identified *S. coelicolor* glycoprotein PstS (SCO4142) (15), by the assignment of two glycosylation sites (residue underlined) in glycopeptides N- DGIKTVDVK-C and N-QTPGAISYFELSYAKDGIK-C (Dataset S1). Indeed, PstS is one of the most heavily glycosylated proteins identified in this work with at least three further glycosylation sites that could not be defined here (Fig. S3). Two of these glycopeptides overlapped with the synthetic peptides that were shown previously to be glycosylated in a cell free assay (15).

Database searches were carried out in order to classify the glycoproteins as either lipoproteins, membrane proteins or secreted proteins. Proteins were functionally annotated using the *Streptomyces* genome database (StrepDB; strepdb.streptomyces.org.uk/) and the Conserved Domain Database (CDD) (http://www.ncbi.nlm.nih.gov/Structure /cdd/wrpsb.cgi) (25). In some cases, the literature was contradictory to the results observed after the database searches. For example, SCO7218 is annotated as a putative iron transport lipoprotein in the StrepDB. However, the LipoP 1.0 server did not predict a lipoprotein signal peptide (SpII) in this protein. SCO7218 is upstream of an ABC transporter (SCO7216/SCO7217) which is consistent with the known genome architecture of solute binding lipoproteins in *S. coelicolor* (26). In these cases, the literature searches were considered to be more reliable in assigning a category to the proteins.

Protein O-glycosylation by Pmt was shown to be coupled to protein secretion via the Sec pathway in *M. tuberculosis,* suggesting that protein O-mannosylation should only affect extracellular proteins (16). Consistent with this precedent, more than a third of the newly identified *S. coelicolor* glycoproteins in this study were predicted lipoproteins and other

secreted proteins (Fig. 2C). The lipoproteins included SCO3357 (CseA) that is proposed to dampen the cell envelope stress response by the two component sensor regulators CseB and CseC which activate the expression of the SigE-encoding gene *sco3356* (27, 28). In addition the putative lipoprotein, SCO4905 (AfsQ3) was also glycosylated and is also proposed to be a modulator of a two component sensor regulator AfsQ1/AfsQ2 (27). Many of the glyco-lipoproteins are, or are predicted to be, substrate binding proteins that interact with ABC transporters (SCO0472, SCO5776, SCO7218, SCO4885 and SCO4142). Nearly 50% of the glycoproteins identified in this study are putative membrane proteins with predicted functions including transport (SCO4141, SCO5818) and serine/threonine kinases (SCO3848), as well as many proteins of unknown function (SCO2963, SCO3891, SCO4130, SCO4548, SCO4968, SCO5204, SCO5751). Additionally, five of the glycoproteins identified here had no predicted transmembrane domains or secretory signals. Three of these, SCO5736, SCO4307 and SCO5115, are very likely to be intracellular proteins; SCO5736 is a predicted S15 ribosomal subunit, SCO4307 is a MurNAc-6-phosphate etherase (MurQ), an enzyme that acts intracellularly to recycle peptidoglycan MurNAc (29) and SCO5115 (BldKD) is a predicted intracellular ATPase subunit for an oligopeptide uptake system (30). Clearly as these three proteins go against the precedent that Pmt glycosylates only extracellular proteins, further investigations are required to validate this observation.

Nearly 25% of the glycoproteins identified here are predicted to be TAT-targeted proteins. The TAT protein transport system functions to secrete folded proteins across the cytoplasmic membrane and to insert some integral membrane proteins into the membrane (31). The pathway is well characterised in *S. coelicolor* and it is known to translocate large numbers of lipoproteins (26, 32). SCO4934, a predicted L, D transpeptidase and glycoprotein identified in this study was experimentally verified as a TAT substrate by Thompson*, et al.*

(26) after it was shown to be absent from *S. coelicolor ΔtatC* strains. In mycobacteria, the fact that protein O-glycosylation was shown to be coupled to protein translocation via the Sec pathway, suggests that protein O-glycosylation occurs on unfolded proteins (16). While protein O-mannosylation in eukaryotes is conventionally thought to be coupled to protein translocation into the ER, Pmt mediated glycosylation of misfolded proteins after they have been translocated into the ER has been demonstrated (33). The translocation of glycoproteins via the TAT pathway in *S. coelicolor* suggests that glycosylation is also possible on folded proteins. Although Pmt has not been shown definitively to be the enzyme that glycosylates proteins secreted through the TAT pathway, one could envisage that the glycosylation occurs on surface exposed regions of the protein or in flexible loops that link secondary structure elements.

Glycoproteins with functions in cell wall biogenesis.

Upon characterising the membrane glycoproteome in *S. coelicolor*, we were particularly interested in proteins that could help to explain the antibiotic hypersensitivity phenotypes observed previously in the *pmt*$^{-}$ and *ppm1*$^{-}$ *S. coelicolor* strains (6). It was hypothesised that the *S. coelicolor* glycoproteome could contain proteins that are important in cell wall biosynthesis or for maintaining membrane integrity. In this study, at least seven glycoproteins have been identified that have predicted functions in the cell wall (SCO4934, SCO4847, SCO3044, SCO3046, SCO3184, SCO4013, SCO4307). SCO4847, for example is a putative D-Ala-D-Ala carboxypeptidase and low molecular weight penicillin-binding protein. These proteins are thought to catalyse the hydrolysis of the terminal D-alanine from the peptidoglycan stem peptide (34). SCO4013 is another predicted penicillin-binding protein,

while SCO4934 is a predicted L, D transpeptidase. L, D transpeptidases catalyse an alternative type of peptidoglycan crosslinking between the third position amino acids of tetrapeptide stems, termed 3->3 crosslinking. L, D transpeptidases have been identified in *M. tuberculosis* and were shown to be important for maintaining cell shape, virulence and resistance to β-lactam antibiotics (35). SCO3044 and SCO3046 both belong to the LytR-CpsA-Psr (LCP) family of proteins, that were first shown to catalyse the ligation of wall teichoic acids (WTA) to the N-acetylmuramic acid (MurNAc) units of peptidoglycan in *Bacillus subtilis* (36). Other studies have demonstrated that LCP proteins are required to attach the capsular polysaccharide to peptidoglycan in both *Staphylococcus aureus* and *Streptococcus pneumoniae* (37, 38). Recently however, an LCP protein in *M. tuberculosis* (Lcp1) was shown to be required for cell viability and to attach arabinogalactan to peptidoglycan in a cell free assay (39).

To investigate the putative roles of glycoproteins SCO4847 and SCO4934 in cell wall biosynthesis, *sco4847* and *sco4934* were disrupted in *S. coelicolor* by allelic exchange with cosmids containing *Tn5062* in the gene of interest. The susceptibilities of the *sco4847*$^{-}$ (TK006) and *sco4934*$^{-}$ (TK008) strains to a range of antibiotics were measured (Fig. 3). Both *sco4847*$^{-}$ (TK006) and *sco4934*$^{-}$ (TK008) mutants were significantly more susceptible to β-lactam antibiotics imipenem, meropenem, ampicillin and penicillin, than the *S. coelicolor* parent strain J1929 (Fig. 3A and B). Additionally, *sco4847*$^{-}$ (TK006) mutants displayed a slight increase in sensitivity to the vancomycin compared to J1929 (Fig. 3A). Both mutants were more sensitive to the antibiotics than DT1025 (*pmt*$^{-}$), suggesting that the non-glycosylated SCO4847 and SCO4934 isoforms may still have some activity in DT1025. The increased antibiotic susceptibility was partially complemented upon the reintroduction of the wild type copies of *sco4847* and *sco4934*, respectively. Neither of the mutants displayed

any change in susceptibility to rifampicin, bacitracin or teicoplanin (Dataset S3), suggesting that the mutants were only affected by antibiotics that targeted peptidoglycan crosslinking. To further investigate the roles of SCO4847 and SCO4934 in cell wall biosynthesis, the susceptibility of the *sco4847*$^{-}$ (TK006) and *sco4934*$^{-}$ (TK008) mutants to lysozyme was tested. The *sco4847*$^{-}$ (TK006) mutant was more sensitive to lysozyme treatment than J1929 and DT1025 (*pmt*$^{-}$), and a wild type level of lysozyme sensitivity was restored in the complemented strain (TK013) (Fig. 3C). No change in lysozyme sensitivity was observed in the *sco4934*$^{-}$ (TK008) mutant (Fig. S4). Neither of the mutants displayed any changes in colony morphology, sporulation or ϕC31*cΔ25* phage sensitivity (Data not shown). The increase in susceptibility to cell-wall targeting antibiotics in the glycoprotein-deficient mutants suggests that both proteins are required for maintaining normal cell wall integrity in *S. coelicolor*. The lack of sensitivity to lysozyme observed in the *sco4934*$^{-}$ mutant may be due to the compensatory actions of other L, D transpeptidases in the cell. A BLAST search of the SCO4934 protein sequence against the StrepDB revealed at least three other putative L, D transpeptidases in the *S. coelicolor* genome (SCO3194, SCO5458 and SCO5457). The increased lysozyme susceptibility observed in the *sco4847*$^{-}$ (TK006) mutant might suggest that SCO4847 has a very specific role in in cell wall biosynthesis *S. coelicolor* or may be required during a specific growth stage.

Conclusions

In this study, we have combined biochemical and MS-based approaches to isolate and characterise the membrane O-glycoproteome in *S. coelicolor*. Collectively we have identified thrity-seven new *S. coelicolor* glycoproteins, as well as further characterised the previously

identified glycoprotein, PstS (15). As in *M. tuberculosis* (12, 14), *S. coelicolor* glycosylates a large number of proteins with a wide range of biological functions, including solute binding, polysaccharide hydrolases, ABC transporters and cell wall biosynthesis. Glycosylation sites were found to be modified with up to three hexose residues, which is consistent with what has been seen previously in other Actinobacteria (10, 13, 14). The identification of glycoproteins with putative roles in cell wall biogenesis supports our hypothesis that glycoproteins in *S. coelicolor* may be required for maintaining cell wall integrity. Upon further investigation of two of these glycoproteins, a putative D-Ala-D-Ala carboxypeptidase (SCO4847) and an L, D transpeptidase (SCO4934), through the generation of null mutants we were able to reproduce the antibiotic susceptibility phenotype observed previously in the *S. coelicolor pmt*$^{-}$ mutants (6). Additionally, the *sco4847*$^{-}$ mutants displayed an increased susceptibility to lysozyme treatment. These findings strongly suggest that both glycoproteins are required for maintaining cell wall integrity and that glycosylation could be affecting enzyme function.

Materials and Methods

Bacterial strains, plasmids and growth conditions. Bacterial strains, plasmids, cosmids and primers used in this work are listed in Table S1. *Escherichia coli* (*E. coli*) strains were grown in LB or on LB agar. *Streptomyces coelicolor* A3(2) strains were maintained on solid Soya Flour Mannitol (SFM) media from which spores were harvested and kept frozen in 20% glycerol at -38 ^{o}C (40). For the preparation of mycelium from liquid cultures, pre-germinated spores (40) were inoculated into F134 medium (19) to an OD_{450} of 0.03 – 0.05 and grown at 30 ^{o}C with shaking (180 rpm) for up to 60 h. *E. coli* DH5α was used as a cloning host and

plasmids/cosmids were introduced into *S. coelicolor* by conjugation from the donor *E. coli* strain ET12567(pUZ8002) (40, 41). Apramycin (cosmids) or Hygromycin (complementation plasmids) was used to select for exconjugates, and nalidixic acid was used to prevent growth of the *E. coli* donors. *S. coelicolor* strains containing a Tn*5062* insertion in the desired gene in the chromosome were obtained by screening exconjugants for those that had undergone double-crossovers with the incoming cosmids and were apramycin-resistant, kanamycin-sensitive. Tn*5062* insertion mutants and complemented strains were validated by PCR and Southern blotting.

Construction of the complementation plasmids. For the construction of the sco4934 complementation plasmid pTAK32, the sco4934 coding sequence was amplified by PCR from *S. coelicolor* J1929 genomic DNA using primers TK101 and TK102 (Table S1) and cloned into NdeI digested pIJ10257. For the construction of the sco4847 complementation plasmid pTAK30, the sco4847 coding sequence could not be amplified by PCR from *S. coelicolor* J1929 genomic DNA as it contained several sequence repeats. To simplify the template for PCR, the cosmid St5G8 was restricted with BamHI, separated by agarose gel electrophoresis and a 2270 bp product containing the sco4847 coding sequence was excised and gel extracted. The purified DNA was used as a template for the amplification of sco4847 by PCR with primers TK97 and TK98 (Table S1). The resulting PCR product was cloned into NdeI digested pIJ10257. All plasmids were validated by DNA sequencing.

Antibiotic disc diffusion assays. Antibiotic disc diffusion assays were performed as described previously (6). Briefly, Difco nutrient agar plates were overlaid with soft nutrient

agar (2.5 mL) containing ~ 10^7 *S. coelicolor* spores. Sterile filter discs (5 mm width) were placed on the surface of the soft agar and 5 µl of antibiotic stock solution was allowed to absorb to the disc. Plates were incubated at 30 °C for 2 days and zones of inhibition (measured in mm) were recorded.

Lysozyme sensitivity assays. Lysozyme sensitivity assays were performed by plating 5 µL of a dilution series of *S. coelicolor* spores (10^8 to 10^4 spores/mL in ddH_2O) onto Difco nutrient agar plates with and without lysozyme (0.25 mg/mL) and incubated at 30 °C for 60 h.

Preparation of *S. coelicolor* membrane proteins. *S. coelicolor* membrane proteins were isolated as previously described (15). Briefly, the mycelium from liquid cultures was harvested by centrifugation (5 min, 3500 *g,* 4°C) and washed in 20 mM Tris-HCl buffer (pH 8, 4°C). Mycelial pellets were re-suspended in twice the pellet volume of lysis buffer at 4°C (20 mM Tris-HCl pH 8, 4 mM $MgCl_2$, protease inhibitor tablet according to volume (Roche) and 1 unit mL^{-1} Benzonase (Sigma)). The mycelium was lysed using a manual French Press (Thermo Fisher Scientific) at 25 kPsi. Cell debris was removed by centrifugation (30 min, 5525 *g* followed by 30 min at 12,000–15,000 *g*, 4 °C). Membranes in the supernatant were pelleted by ultracentrifugation (1 h, 100,000 *g*, 4 °C). Membrane pellets were solubilised overnight on ice in 1% (w/v) dodecyl-β-D maltoside (Sigma) in 20 mM Tris-HCl buffer (pH 8).

Sodium dodecyl sulfate Polyacrylamide gel electrophoresis (SDS-PAGE) and lectin western blotting. Protein concentrations were determined using the Pierce Coomassie (Bradford)

assay kit (Thermo Fisher Scientific). Proteins were prepared by boiling in 1 x RunBlue LDS Sample Buffer (Expedeon) with β-mercaptoethanol (5 % (v/v)) and separated in RunBlue SDS Protein Gels 4 - 12% (Expedeon). For protein staining, gels were soaked in InstantBlue Protein Stain (Expedeon) as per manufacturer's instructions. For glycoprotein detection, proteins were transferred to PVDF membranes by semi-dry western transfer (42). Non-specific binding to the membranes was blocked by incubation in TBS (50 mM Tris-HCl, 150 mM NaCl, pH 7.5) + 2 % (v/v) Tween 20 for 30 min, before washing the membranes 2 x 5 min in TBS. Membranes were incubated for 2 h in TBS + 0.05 % (v/v) Tween 20, 1 mM $MgCl_2$, 1 mM $MnCl_2$ and 1 mM $CaCl_2$ with 5 µg. mL^{-1} ConA-HRP conjugate (Sigma). For the inhibition of glycoprotein binding, membranes were incubated for 2 h in TBS + 0.05 % (v/v) Tween 20, 1 mM $MgCl_2$, 1 mM $MnCl_2$ and 1 mM $CaCl_2$ with 5 µg. mL^{-1} ConA-HRP conjugate and 200 mM methyl α-D-glucopyranoside. The membranes were washed for 2 x 10 min in TBS + 0.05 % (v/v) Tween 20 and 1 x 5 min in TBS. Chemiluminescent detection solution was prepared by adding 5 mL of 100 mM Tris-HCl pH 8.5 buffer with 0.2 mM p-coumaric acid (Sigma) and 1.25 mM Luminol to 15 µL of 3 % (v/v) hydrogen peroxide solution. Under dark room conditions the membranes were incubated in chemiluminescent detection solution for 1 min. After exposure to the blot, X-ray film (GE Healthcare Life Sciences) was incubated for 3 – 5 min in Developer solution (Kodak) and 3 min in Fixer solution (Kodak).

Lectin affinity chromatography. Lectin affinity chromatography was performed on the AKTA Pure chromatography system (GE Healthcare) using a column of agarose bound Concanavalin A (Vector Laboratories). Prior to sample loading, the column was washed in lectin buffer (20 mM Tris-HCl pH 7.5, 400 mM NaCl, 5 mM $MgCl_2$, 5 mM $MnCl_2$ and 5 mM

409 $CaCl_2$) and then equilibrated in 5 x CV of binding buffer (20 mM Tris-HCl, pH 7.5, 0.4 M NaCl
410 and 0.1 % (w/v) n-dodecyl β-D-maltoside). Samples were loaded onto the column at a flow
411 rate of 5 mL. min^{-1}, the column was washed with 16 x CV of binding buffer and glycoproteins
412 were eluted in 4 x CV of a 200 mM methyl α-D-glucopyranoside solution. Glycoprotein
413 fractions were concentrated using 9 kDa MWCO Amicon Ultra Centrifugal Filters (Merck)
414 and stored in 50 % (w/v) glycerol at -80 °C.

415

416 **Glycoproteomics.** For detailed methods, please see the supplementary material.
417 Glycoproteins were in-gel digested with trypsin before LC-MS/MS acquisition over 180 min
418 using multiple fragmentation strategies. CID fragmentation acquisitions were performed
419 using a Waters nanoAcquity UPLC interfaced to a Bruker maXis HD mass spectrometer as
420 previously described (43). HCD, ETD and mixed fragmentation acquisitions were performed
421 using a Thermo UltiMate 3000 RSLCnano HPLC and Orbitrap Fusion hybrid mass
422 spectrometer. Four MS^2 strategies were employed: ETD spectra acquired in the linear ion
423 trap (ETD_IT), ETD spectra acquired in the Orbitrap (ETD_OT), HCD spectra acquired in the
424 linear ion trap (HCD_IT) and HCD spectra acquired in the linear ion trap with ETD spectra
425 acquired in the Orbitrap (HCD/ETD IC). Resulting tandem mass spectral data were searched
426 against *Streptomyces coelicolor* subset of the NCBI database using Mascot. Search criteria
427 specified: Enzyme, trypsin; Fixed modifications, carbamidomethyl (C); Variable
428 modifications, oxidation (M), deamidated (NQ), $Hex_{(1-5)}$ (ST). Mass tolerance and
429 fragmentation ion types were adjusted for to match acquisition dependencies
430 (supplementary information). Peptide spectral matches were filtered to expect scores ≤0.05.
431 All glycopeptide spectra with MASCOT expect scores of 0.05 or lower were manually

validated. For glycopeptide spectra generated by CID and HCD fragmentation, glycosylation sites were only assigned in cases where only a single glycosylated residue was possible within the glycopeptide. For the site localisations of glycopeptides identified in the ETD_IT and ETD_OT acquisitions, an MD-score cut off of 10 was applied. In matches were the MD-score was greater than 10, the spectra were manually validated to confirm the site localisation. All proteomics data is available through MassIVE, data set MSV000083115.

Acknowledgements

We are grateful to Professor Anne Dell FRS and Dr Paul Hitchen (Imperial College, London) and to Professor Jane Thomas-Oates (University of York) for technical advice and insights. This work was funded by the Biotechnology and Biological Sciences Research Council (project grant BB/J016691 to MCMS) and TK received a studentship stipend by the University of York. The York Centre of Excellence in Mass Spectrometry was created thanks to a major capital investment through Science City York, supported by Yorkshire Forward with funds from the Northern Way Initiative, and subsequent support from EPSRC (EP/K039660/1; EP/M028127/1).

References

1. Lommel M & Strahl S (2009) Protein O-mannosylation: conserved from bacteria to humans. *Glycobiology* 19(8):816-828.
2. Dell A, Galadari A, Sastre F, & Hitchen P (2010) Similarities and differences in the glycosylation mechanisms in prokaryotes and eukaryotes. *Int J Microbiol* 2010:148178.
3. Eichler J (2013) Extreme sweetness: protein glycosylation in archaea. *Nat Rev Microbiol* 11(3):151-156.
4. Iwashkiw JA, Vozza NF, Kinsella RL, & Feldman MF (2013) Pour some sugar on it: the expanding world of bacterial protein O-linked glycosylation. *Mol Microbiol* 89(1):14-28.
5. Szymanski CM & Wren BW (2005) Protein glycosylation in bacterial mucosal pathogens. *Nat Rev Microbiol* 3(3):225-237.
6. Howlett R*, et al.* (2018) Streptomyces coelicolor strains lacking polyprenol phosphate mannose synthase and protein O-mannosyl transferase are hyper-susceptible to multiple antibiotics. *Microbiology* 164(3):369-382.
7. Liu CF*, et al.* (2013) Bacterial protein-O-mannosylating enzyme is crucial for virulence of Mycobacterium tuberculosis. *Proceedings of the National Academy of Sciences of the United States of America* 110(16):6560-6565.
8. Mahne M, Tauch A, Puhler A, & Kalinowski J (2006) The Corynebacterium glutamicum gene pmt encoding a glycosyltransferase related to eukaryotic protein-

476 O-mannosyltransferases is essential for glycosylation of the resuscitation promoting
477 factor (Rpf2) and other secreted proteins. *FEMS Microbiol Lett* 259(2):226-233.
478 9. Cowlishaw DA & Smith MC (2001) Glycosylation of a Streptomyces coelicolor A3(2)
479 cell envelope protein is required for infection by bacteriophage phi C31. *Mol*
480 *Microbiol* 41(3):601-610.
481 10. Dobos KM, Khoo KH, Swiderek KM, Brennan PJ, & Belisle JT (1996) Definition of the
482 full extent of glycosylation of the 45-kilodalton glycoprotein of Mycobacterium
483 tuberculosis. *J Bacteriol* 178(9):2498-2506.
484 11. Espitia C & Mancilla R (1989) Identification, isolation and partial characterization of
485 Mycobacterium tuberculosis glycoprotein antigens. *Clin Exp Immunol* 77(3):378-383.
486 12. Gonzalez-Zamorano M*, et al.* (2009) Mycobacterium tuberculosis glycoproteomics
487 based on ConA-lectin affinity capture of mannosylated proteins. *J Proteome Res*
488 8(2):721-733.
489 13. Sartain MJ & Belisle JT (2009) N-Terminal clustering of the O-glycosylation sites in
490 the Mycobacterium tuberculosis lipoprotein SodC. *Glycobiology* 19(1):38-51.
491 14. Smith GT, Sweredoski MJ, & Hess S (2014) O-linked glycosylation sites profiling in
492 Mycobacterium tuberculosis culture filtrate proteins. *J Proteomics* 97:296-306.
493 15. Wehmeier S*, et al.* (2009) Glycosylation of the phosphate binding protein, PstS, in
494 Streptomyces coelicolor by a pathway that resembles protein O-mannosylation in
495 eukaryotes. *Mol Microbiol* 71(2):421-433.
496 16. VanderVen BC, Harder JD, Crick DC, & Belisle JT (2005) Export-mediated assembly of
497 mycobacterial glycoproteins parallels eukaryotic pathways. *Science* 309(5736):941-
498 943.

17. Gurcha SS*, et al.* (2002) Ppm1, a novel polyprenol monophosphomannose synthase from Mycobacterium tuberculosis. *Biochem J* 365(Pt 2):441-450.

18. Howlett R, Anttonen K, Read N, & Smith MCM (2018) Disruption of the GDP-mannose synthesis pathway in Streptomyces coelicolor results in antibiotic hyper-susceptible phenotypes. *Microbiology* 164(4):614-624.

19. Nieselt K*, et al.* (2010) The dynamic architecture of the metabolic switch in Streptomyces coelicolor. *BMC Genomics* 11:10.

20. Thomas L*, et al.* (2012) Metabolic switches and adaptations deduced from the proteomes of Streptomyces coelicolor wild type and phoP mutant grown in batch culture. *Molecular & Cellular Proteomics* 11(2):M111. 013797.

21. Michell SL*, et al.* (2003) The MPB83 antigen from Mycobacterium bovis contains O-linked mannose and (1-->3)-mannobiose moieties. *J Biol Chem* 278(18):16423-16432.

22. Huang T-Y & McLuckey SA (2010) Gas-phase chemistry of multiply charged bioions in analytical mass spectrometry. *Annual Review of Analytical Chemistry* 3:365-385.

23. Dobos KM, Swiderek K, Khoo KH, Brennan PJ, & Belisle JT (1995) Evidence for glycosylation sites on the 45-kilodalton glycoprotein of Mycobacterium tuberculosis. *Infect Immun* 63(8):2846-2853.

24. Herrmann J, O'Gaora P, Gallagher A, Thole J, & Young D (1996) Bacterial glycoproteins: a link between glycosylation and proteolytic cleavage of a 19 kDa antigen from Mycobacterium tuberculosis. *The EMBO journal* 15(14):3547-3554.

25. Marchler-Bauer A*, et al.* (2014) CDD: NCBI's conserved domain database. *Nucleic acids research* 43(D1):D222-D226.

26. Thompson BJ*, et al.* (2010) Investigating lipoprotein biogenesis and function in the model Gram-positive bacterium Streptomyces coelicolor. *Molecular microbiology* 77(4):943-957.

27. Hutchings MI, Hong HJ, & Buttner MJ (2006) The vancomycin resistance VanRS two-component signal transduction system of Streptomyces coelicolor. *Mol Microbiol* 59(3):923-935.

28. Paget MSB, Chamberlin L, Atrih A, Foster SJ, & Buttner MJ (1999) Evidence that the extracytoplasmic function sigma factor sigmaE is required for normal cell wall structure in Streptomyces coelicolor A3(2). *Journal of Bacteriology* 181(1):204-211.

29. Borisova M*, et al.* (2016) Peptidoglycan Recycling in Gram-Positive Bacteria Is Crucial for Survival in Stationary Phase. *MBio* 7(5).

30. Nodwell JR, McGovern K, & Losick R (1996) An oligopeptide permease responsible for the import of an extracellular signal governing aerial mycelium formation in Streptomyces coelicolor. *Mol Microbiol* 22(5):881-893.

31. Berks BC, Palmer T, & Sargent F (2003) The Tat protein translocation pathway and its role in microbial physiology.

32. Widdick DA*, et al.* (2006) The twin-arginine translocation pathway is a major route of protein export in Streptomyces coelicolor. *Proc Natl Acad Sci U S A* 103(47):17927-17932.

33. Harty C, Strahl S, & Romisch K (2001) O-mannosylation protects mutant alpha-factor precursor from endoplasmic reticulum-associated degradation. *Mol Biol Cell* 12(4):1093-1101.

34. Pratt R (2008) Substrate specificity of bacterial DD-peptidases (penicillin-binding proteins). *Cellular and Molecular Life Sciences* 65(14):2138-2155.

35. Schoonmaker MK, Bishai WR, & Lamichhane G (2014) Nonclassical transpeptidases of Mycobacterium tuberculosis alter cell size, morphology, the cytosolic matrix, protein localization, virulence, and resistance to β-lactams. *Journal of bacteriology* 196(7):1394-1402.

36. Kawai Y*, et al.* (2011) A widespread family of bacterial cell wall assembly proteins. *The EMBO journal* 30(24):4931-4941.

37. Eberhardt A*, et al.* (2012) Attachment of capsular polysaccharide to the cell wall in Streptococcus pneumoniae. *Microbial drug resistance* 18(3):240-255.

38. Chan YG-Y, Kim HK, Schneewind O, & Missiakas D (2014) The capsular polysaccharide of Staphylococcus aureus is attached to peptidoglycan by the LytR-CpsA-Psr (LCP) family of enzymes. *Journal of Biological Chemistry* 289(22):15680-15690.

39. Harrison J*, et al.* (2016) Lcp1 is a phosphotransferase responsible for ligating arabinogalactan to peptidoglycan in Mycobacterium tuberculosis. *MBio* 7(4):e00972-00916.

40. Kieser T, Bibb MJ, Buttner MJ, Chater KF, & Hopwood DA (2000) *Practical Streptomyces Genetics* (The John Innes Foundation, Norwich).

41. MacNeil DJ (1988) Characterization of a unique methyl-specific restriction system in Streptomyces avermitilis. *J Bacteriol* 170(12):5607-5612.

42. Kurien BT & Scofield RH (2006) Western blotting. *Methods* 38(4):283-293.

43. Dowle AA, Wilson J, & Thomas JR (2016) Comparing the Diagnostic Classification Accuracy of iTRAQ, Peak-Area, Spectral-Counting, and emPAI Methods for Relative Quantification in Expression Proteomics. *J Proteome Res* 15(10):3550-3562.

568

569

570 **Legends to Figures**

571

572 **Fig. 1 Glycoprotein enrichment time course by Con A affinity chromatography.** Total
573 membrane (T), unbound membrane (UB) and eluted (E) protein fractions were separated by
574 SDS-PAGE and stained with protein stain (lanes 1 - 14) or probed with Con A-HRP after
575 western blotting (lanes 15 - 26).

576

577 **Fig. 2 Characterisation of enriched glycoproteins by mass spectrometry.** (A) CID spectrum
578 of the glycopeptide SATAASPSAEASGEAGGTGK-9Hex from SCO4847, isolated after 35 h of
579 growth. Precursor *m/z* 1055.7991; charge: 2+; RT: 25.7 min; e-value: 0.0003. (B) *S. coelicolor*
580 O-glycosylation site motif (C) Subcellular localisation of *S. coelicolor* glycoproteins.

581

582 **Fig. 3 Antibiotic sensitivities of glycoprotein deficient mutants.** (A) and (B) Diameters of
583 growth inhibition zones from disc diffusion assays for the *S. coelicolor* glycoprotein deficient
584 mutants, TK006 (*sco4847::*Tn*5062*) (A) and TK008 (*sco4934::*Tn*5062*) (B) and respective
585 complement strains TK013 (*sco4847::*Tn*5062,* pTAK30) and TK010
586 (*sco4934::T*n*5062,*pTAK32), against the parent strain J1929 and the glycosylation deficient
587 strain DT1025 (*pmt*$^{-}$). Mean of three biological replicates is shown except for TK006, where
588 the mean of two biological replicates and three technical replicates is shown. Error bars
589 indicate SEM. * indicates $p < 0.05$ that the difference between the glycoprotein deficient

590 mutant and the parent strain J1929 has occurred by chance. Only a selection of antibiotic
591 concentrations (vancomycin: 40 µg, imipenem: 4 µg, meropenem: 4 µg, penicillin: 100 µg,
592 ampicillin: 200 µg) are shown here; the full set is in Dataset S3. (C) Lysozyme sensitivity of
593 TK006 (*sco4847::*Tn*5062*) and complement strain TK013 (*sco4847::*Tn*5062,* pTAK30)
594 compared to the parent strain J1929, DT1025 (*pmt*$^{-}$) and DT3017 (*ppm1*$^{-}$). Images
595 representative of two biological replicates and two technical replicates.

596

597

Table 1. *S. coelicolor* glycoproteins identified in this work.

Protein	Function	#TMHMM [1]	SignalP 4.1 [2]	TatP 1.0 [3]	LipoP 1.0 [4]	Classification
SCO0472	Putative secreted protein	-	Y - 0.548	Y - 0.381	SpII - 22.2623	Lipoprotein
SCO0996	Putative metal-binding lipoprotein	-	Y - 0.526	N	SpI - 11.5964	Lipoprotein
SCO1714	Putative secreted protein	1	Y - 0.498	N	SpII - 12.878	Lipoprotein
SCO2838	Putative secreted endoglucanase.	-	Y - 0.639	Y - 0.377	SpII - 32.6736	Lipoprotein
SCO3357	Hypothetical protein	-	N	Y - 0.492	SpII - 17.3077	Lipoprotein
SCO4142	PstS, substrate binding domain of ABC-type phosphate transporter	-	Y - 0.595	N	SpII - 26.7983	Lipoprotein
SCO4739	Putative lipoprotein	-	Y - 0.579	N	SpII - 20.7928	Lipoprotein
SCO4885	Putative nucleoside-binding lipoprotein	-	N	N	SpII - 23.8395	Lipoprotein
SCO4905	Putative lipoprotein	-	Y - 0.574	N	SpII - 13.7291	Lipoprotein
SCO4934	Putative L, D transpeptidase	-	Y - 0.571	Y - 0.483	SpII - 24.1553	Lipoprotein
SCO5646	Putative thiamine-binding lipoprotein	-	N	Y - 0.468	SpII - 13.5061	Lipoprotein
SCO7218	Putative iron transport lipoprotein	-	Y - 0.632	N	SpI - 14.1761	Lipoprotein
SCO2096	Transglutaminase/Protease like membrane protein	6	Y - 0.529	N	SpII - 8.2333	membrane
SCO2035	Putative disulphide oxidoreductase	1	N	N	N	membrane
SCO2156	Putative cytochrome c oxidase subunit II	3	N	N	N	membrane
SCO2963	Putative membrane protein	1	N	N	N	membrane
SCO3044	Putative cell envelope-associated transcriptional attenuator LytR-CpsA-Psr	1	N	N	N	membrane
SCO3046	Putative cell envelope-associated transcriptional attenuator LytR-CpsA-Psr	1	N	N	N	membrane
SCO3184	Putative penicillin acylase	1	N	Y - 0.366	N	membrane
SCO3848	Putative serine/threonine protein kinase	1	N	N	N	membrane
SCO3891	Putative membrane protein	1	N	N	N	membrane
SCO4013	Putative secreted penicillin-binding protein FtsI	1	N	N	N	membrane
SCO4130	Putative integral membrane protein	1	N	N	N	membrane
SCO4141	Phosphate ABC transport system permease protein	5	N	N	N	membrane
SCO4256	Putative hydrolytic protein	1	N	N	N	membrane

SCO4548	Putative integral membrane protein	3	N	Y - 0.479	N	membrane
SCO4968	Putative membrane protein	1	N	N	N	membrane
SCO5204	Integral membrane protein	7	N	N	N	membrane
SCO5751	Putative membrane protein	1	N	N	N	membrane
SCO5818	Putative ABC-type Na+ transport system	5	N	N	N	membrane
SCO3540	Proteinase (putative secreted protein)	1	Y - 0.627	Y - 0.700	SpI - 18.2099	secreted
SCO4847	DacC, putative D-alanyl-D-alanine carboxypeptidase	1	Y - 0.711	Y - 0.427	SpI - 27.3476	secreted
SCO5776	Glutamate binding protein	-	Y - 0.618	N	SpI - 21.8509	secreted
SCO3353	Hypothetical protein	-	N	N	N	Other
SCO4307	MurQ, N-acetylmuramic acid-6-phosphate etherase	-	N	N	N	Other
SCO5115	BldKD, putative ABC transporter intracellular ATPase subunit	-	N	N	N	Other
SCO5736	30S ribosomal protein S15	-	N	N	N	Other
SCO6558	Putative oxidoreductase	-	N	N	N	Other

[1] The number of transmembrane helices predicted by the TMHMM 2.0 server (http://www.cbs.dtu.dk/services/TMHMM/).

[2] SignalP 4.1 software predicts the presence of a signal peptide (http://www.cbs.dtu.dk/services/SignalP/). D-score is a score used to discriminate signal peptides from non-signal peptides. Scores > 0.450 indicate a signal peptide.

[3] TatP 1.0 predicts the presence of twin arginine (TAT) signal peptides. D-sore > 0.36 predicts the presence of a TAT pathway signal.

[4] LipoP 1.0 software produces predictions of lipoproteins (http://www.cbs.dtu.dk/services/LipoP/). SpI denotes SEC signal peptide; SpII denotes lipoprotein

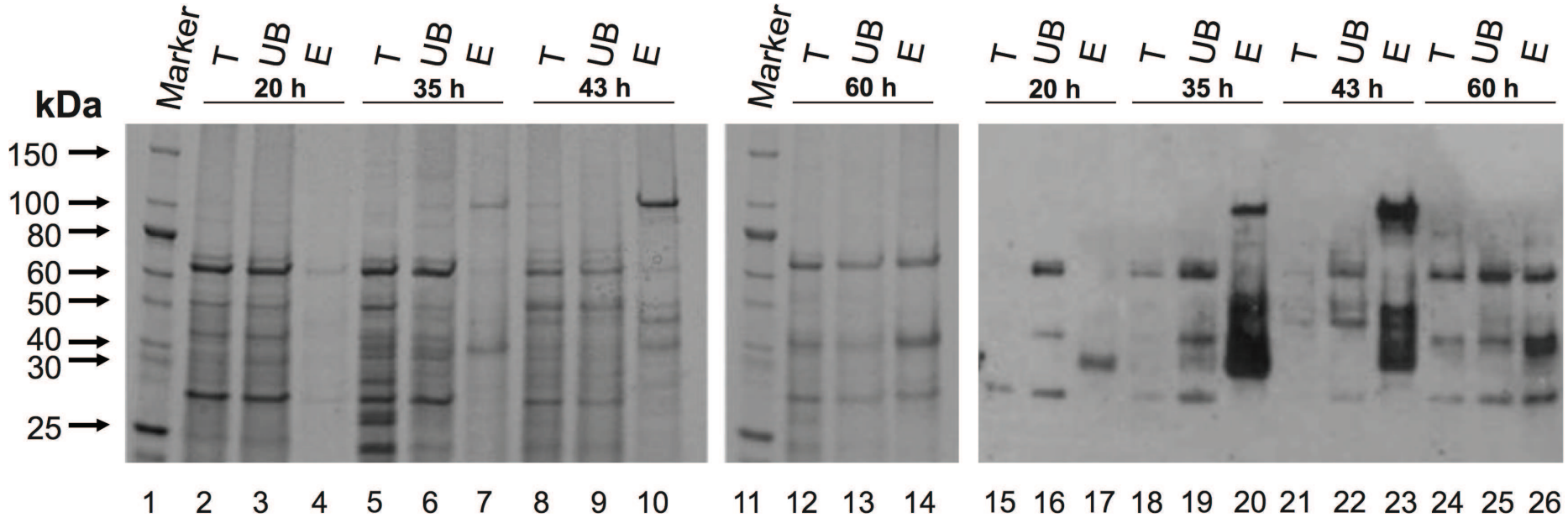
kDa
150
100
80
60
50
40
30
25
Marker
T
UB
E
20 h
35 h
43 h
Marker
T
UB
E
60 h
T
UB
E
20 h
35 h
43 h
60 h
1 2 3 4 5 6 7 8 9 10 11 12 13 14 15 16 17 18 19 20 21 22 23 24 25 26

Figure 1

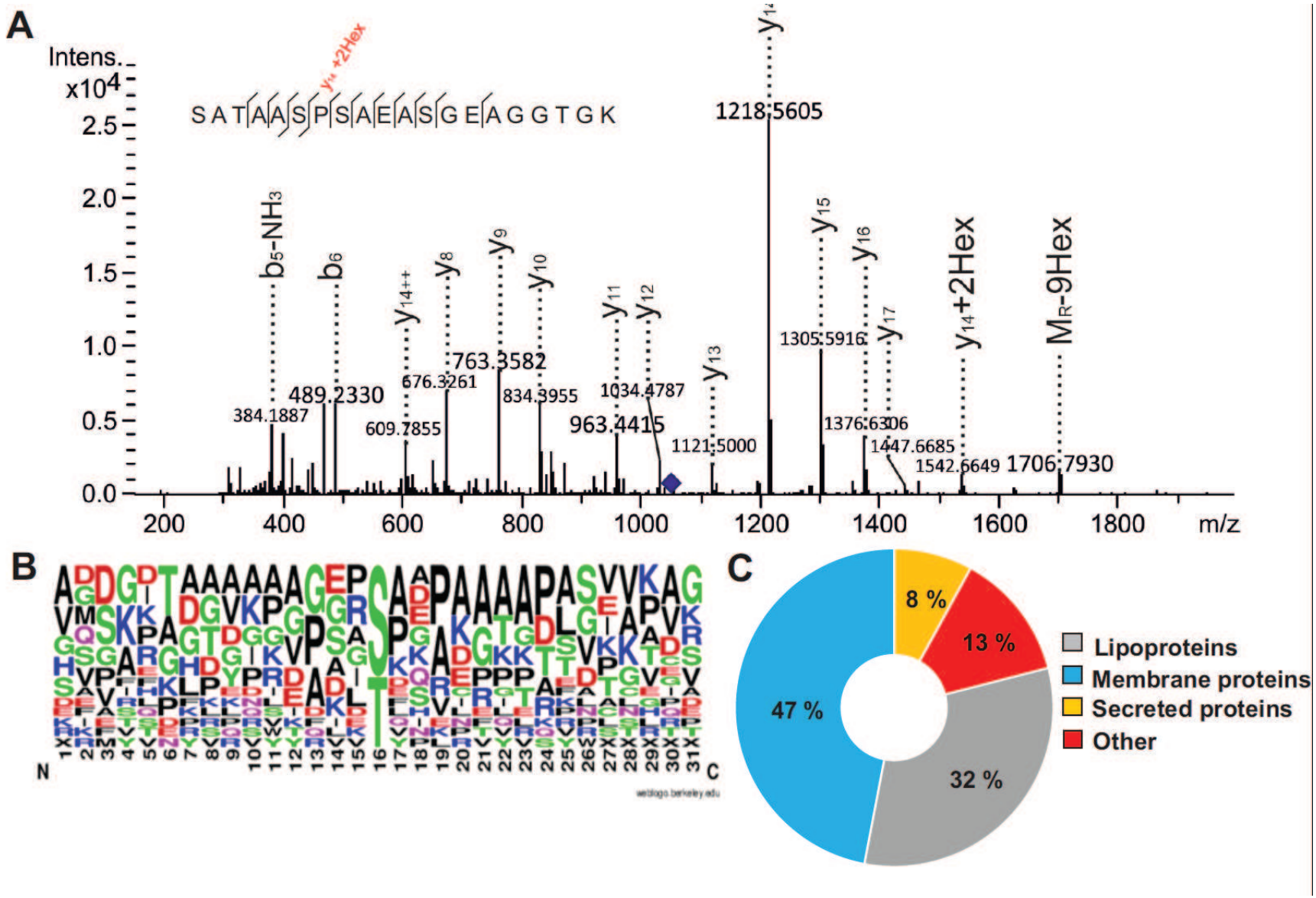
A
Intens.
x10^4
2.5
2.0
1.5
1.0
0.5
0.0
S A T A A S P S A E A S G E A G G T G K
y14 +2Hex
b5-NH3
b6
y14++
y8
y9
y10
y11
y12
y13
y15
y16
y17
y14+2Hex
MR-9Hex
1218.5605
1305.5916
763.3582
676.3261
489.2330
384.1887
834.3955
1034.4787
963.4415
609.7855
1121.5000
1376.6306
1447.6685
1542.6649
1706.7930
200
400
600
800
1000
1200
1400
1600
1800
m/z
B
N
C
weblogo.berkeley.edu
C
8 %
13 %
47 %
32 %
Lipoproteins
Membrane proteins
Secreted proteins
Other

Figure 2

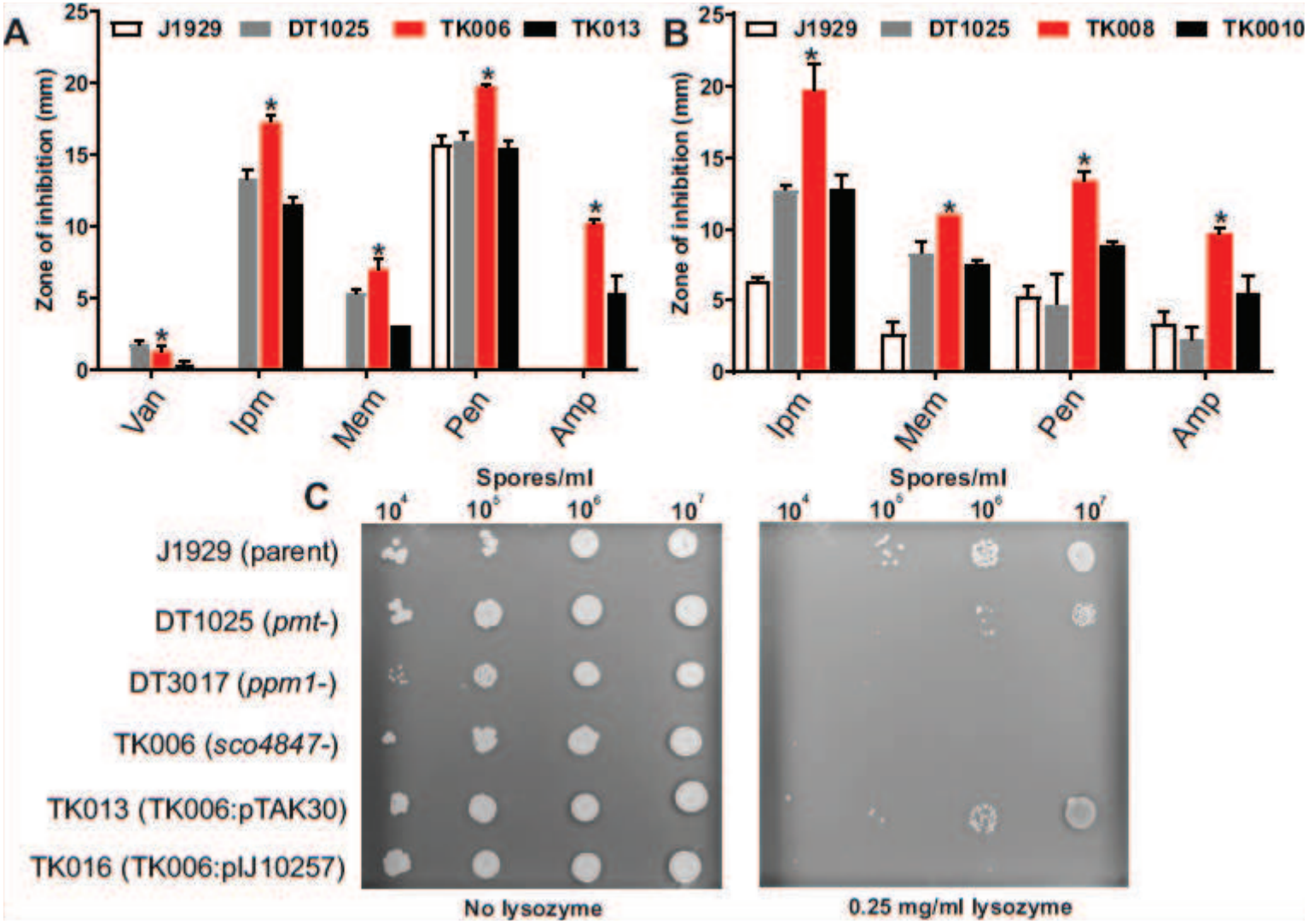
A
J1929
DT1025
TK006
TK013
Zone of inhibition (mm)
Van
Ipm
Mem
Pen
Amp
B
J1929
DT1025
TK008
TK0010
Zone of inhibition (mm)
Ipm
Mem
Pen
Amp
C
Spores/ml
10^4
10^5
10^6
10^7
J1929 (parent)
DT1025 (pmt-)
DT3017 (ppm1-)
TK006 (sco4847-)
TK013 (TK006:pTAK30)
TK016 (TK006:pIJ10257)
No lysozyme
Spores/ml
10^4
10^5
10^6
10^7
0.25 mg/ml lysozyme

Figure 3

Table S1. Bacterial strains, cosmids, plasmids and primers used in this work

***Streptomyces* Strain**	**Genotype**	**Source**
S. coelicolor J1929	*pglY* mutant	(11)
S. coelicolor DT1025	*pmt* mutant	(12)
S. coelicolor DT3017	*ppm1* mutant	(13)
S. coelicolor TK006	*sco4847* mutant	This work
S. coelicolor TK008	*sco4934* mutant	This work
S. coelicolor TK010	TK008: pTAK32	This work
S. coelicolor TK013	TK006: pTAK30	This work

***E.coli* Strain**	**Genotype**	**Source**
DH5α	*F– Φ80lacZΔM15 (Δ(lacZYA-argF) U169 recA1 endA1 hsdR17 (rK–, mK+) phoA supE44 λ– thi-1 gyrA96 relA*	Invitrogen
ET12567 [pUZ8002]	*ET12567 - dam-13::Tn9, dcm-6, hsdM, hsdS; pUZ8002 – tra, neo, RP4*	(14)

Cosmid	**Description**	**Source**
2SCK31.2.F11	*sco4909-sco4945*, Tn*5062* in *sco4934* at nt 5369107	(15)
5G8.1.A11	*sco4820-sco4860*, Tn*5062* in *sco4847* at nt 5279744	(15)

Plasmid name	**Description**	**Source**
pIJ10257	attP-int-derived integration vector for the conjugal transfer of DNA from *E. coli* to *Streptomyces spp.* Contains Hyg^R, oriT and *ermE*p* promoter.	(16)
pGEM7	Cloning vector; fi oriC, SP6 and T7 RNA polymerase promoters , multiple cloning site, Amp^R, *lacZ* for blue/white screening	Promega
pTAK30	*sco4847* in pIJ10257	This work
pTAK32	*sco4934* in pIJ10257	This work

Primer	**Sequence**	**Description**
TK97	ACAGGAGGCCCCATATGGTGCCCGCTCCCAAGAAG	Forward primer - cloning *sco4847* into pIJ10257
TK98	ACTCGAGATCTCATATGGGCAGCAAGGCGCAGGAA	Reverse primer - cloning *sco4847* into pIJ10257
TK101	ACAGGAGGCCCCATATGATGACGGACGGTAAGCGG	Forward primer - cloning *sco4934* into pIJ10257
TK102	ACTCGAGATCTCATATGTCAGACCGCCGAACCCGC	Reverse primer - cloning *sco4934* into pIJ10257

Supplemental methods

Mass spectrometry analysis of glycoproteins.

In-gel digestion of glycoproteins. After the separation of glycoproteins for 7 min in NuPAGE™ 10 % Bis-Tris precast gels, the gels were stained with InstantBlue Protein Stain and the protein stained regions were cut into ~1 mm pieces for processing. Gel pieces were destained by washing with 200 µL of 50 % (v/v) aqueous acetonitrile containing 25 mM $(NH_4)HCO_3$(2 x 20 min), then once with 200 µL of acetonitrile (5 min) and dried in a vacuum concentrator (20 min). The samples were reduced by adding 200 µL of 10 mM dithioerythritol (DTE) in 100 mM $(NH_4)HCO_3$ aq. and incubating 56 °C (1 h). The supernatant was discarded and the gel pieces were cooled to RT. The samples were alkylated by adding 200 µL of 50 mM iodoacetamide in 100 mM $(NH_4)HCO_3$ aq. and incubating in the dark (RT, 30 min). The supernatant was discarded and the gel pieces were washed in 200 µL of 100 mM $(NH_4)HCO$ aq. (15 min). After the supernatant was discarded, the gel pieces were washed in 50 % (v/v) aqueous acetonitrile containing 25 mM $(NH_4)HCO_3$ (15 min). The supernatant was discarded and the gel pieces were dehydrated in 200 µL of acetonitrile (5 min). The supernatant was removed and the gel pieces were dried in a vacuum concentrator (20 min). Sequencing-grade, modified porcine trypsin (Promega) 0.2 µg in 25 mM $(NH_4)HCO_3$ was added to the gel pieces, and the digest was incubated at 37°C overnight. The supernatant containing digested peptides was retained. The peptides from the residual gel were extracted by adding 200 µL of 50 % (v/v) aqueous acetonitrile for 15 min. The extracts were added to the retained supernatant and the extraction was repeated twice. The combined supernatant

was dried in a vacuum concentrator and the peptides were reconstituted in 20 µL of 0.1 % TFA in ddH_2O.

LC-ESI-CID-MS/MS analysis. Samples were loaded onto a nanoAcquity UPLC system (Waters) equipped with a nanoAcquity Symmetry C_{18}, 5 µm trap (180 µm x 20 mm Waters) and a nanoAcquity HSS T3 1.8 µm C_{18} capillary column (75 µm x 250 mm, Waters). The trap wash solvent was 0.1 % (v/v) aqueous formic acid and the trapping flow rate was 10 µL/min. The trap was washed for 5 min before switching flow to the capillary column. The separation used a gradient elution of two solvents (solvent A: 0.1 % (v/v) formic acid; solvent B: acetonitrile containing 0.1% (v/v) formic acid). The flow rate for the capillary column was 300 nL/min. Column temperature was 60 °C and the gradient profile was liner 2 – 30 % B over 125 mins then linear 30-50 %B over 5 mins. All runs then proceeded to wash with 95 % solvent B for 2.5 min. The column was returned to initial conditions and re-equilibrated for 25 min before subsequent injections. The nanoLC system was interfaced with a maXis HD LC-MS/MS system (Bruker Daltonics) with a CaptiveSpray ionisation source (Bruker Daltonics). Positive ESI- MS & MS/MS spectra were acquired using AutoMSMS mode. Instrument control, data acquisition and processing were performed using Compass 1.7 software (microTOF control, Hystar and DataAnalysis, Bruker Daltonics). Instrument settings were: ion spray voltage: 1,450 V, dry gas: 3 L/min, dry gas temperature 150 °C, ion acquisition range: *m/z* 150-2,000, quadrupole low mass: 300 *m/*z, transfer time: 120 ms, collision RF: 1,400 Vpp, MS spectra rate: 5 Hz, cycle time: 3 s, and MS/MS spectra rate: 5 Hz at 2,500 cts to 20 Hz at 250,000 Hz. The collision energy and isolation width settings were

automatically calculated using the AutoMSMS fragmentation table, absolute threshold 200 counts, preferred charge states: 2 – 4, singly charged ions excluded. A single MS/MS spectrum was acquired for each precursor and former target ions were excluded for 0.8 min unless the precursor intensity increased fourfold. Tandem mass spectral data were searched against a subset of the NCBInr database containing only *Streptomyces coelicolor* entries (8,578 sequences; 2,791,553 residues) using a locally-running copy of the Mascot program (Matrix Science Ltd., version 2.5), through the Bruker ProteinScape interface (version 2.1). Search criteria specified: Enzyme, trypsin; Peptide tolerance, 10 ppm; MS/MS tolerance, 0.1 Da; Instrument, ESI-QUAD-TOF; Fixed modifications, carbamidomethyl (C); Variable modifications, oxidation (M) and deamidated (NQ). Samples included the variable modifications Hex_1 to Hex_5 (ST). Results were filtered to accept only peptides with an expect score of 0.05 or lower.

HCD/ETD mass spectrometry analysis. Samples were loaded onto an UltiMate 3000 RSLCnano HPLC system (Thermo) equipped with a PepMap 100 Å C_{18}, 5 μm trap column (300 μm x 5 mm Thermo) and an Acclaim PepMap RSLC, 2 μm, 100 Å, C_{18} RSLC nanocapillary column (75 μm x 150 mm, Thermo). The trap wash solvent was 0.05% (v/v) aqueous trifluoroacetic acid and the trapping flow rate was 15 μL/min. The trap was washed for 3 min before switching flow to the capillary column. The separation used gradient elution of two solvents (solvent A: aqueous 1% (v/v) formic acid; solvent B: aqueous 80% (v/v) acetonitrile containing 1% (v/v) formic acid). The flow rate for the capillary column was 300 nL/min and the column temperature was 50°C. The linear multi-step gradient profile was: 3-10% B over 8 mins, 10-35% B over 125 mins, 35-65%

B over 50 mins, 65-99% B over 7 mins and then proceeded to wash with 99% solvent B for 4 min. The column was returned to initial conditions and re-equilibrated for 15 min before subsequent injections. The nanoLC system was interfaced with an Orbitrap Fusion hybrid mass spectrometer (Thermo) with a Nanospray Flex ionisation source (Thermo). Positive ESI-MS and MS^2 spectra were acquired using Xcalibur software (version 4.0, Thermo). Instrument source settings were: ion spray voltage, 2,200 V; sweep gas, 0 Arb; ion transfer tube temperature; 275°C. MS^1 spectra were acquired in the Orbitrap with: 120,000 resolution, scan range: *m/z* 375-1,500; AGC target, $4e^5$; max fill time, 100 ms; data type, profile. Four distinct MS^2 strategies were employed as detailed below:

ETD_IT. MS^2 spectra were acquired in the linear ion trap specifying: quadrupole isolation, isolation window, *m/z* 1.6; activation type, ETD; reaction time, 50 ms; reagent target, 1e6; maximum ETD reagent inject time, 200 ms; scan range, normal; scan rate, rapid; first mass, *m/z* 110; AGC target, $5e^3$; max injection time, 100 ms; data type, centroid. Data dependent acquisition was performed in top speed mode using a 1 s cycle, selecting the most intense precursors with charge states 3-8. Dynamic exclusion was performed for 50 s post precursor selection and a minimum threshold for fragmentation was set at $5e^4$.

EDT_OT. MS^2 spectra were acquired in the Orbitrap specifying: quadrupole isolation, isolation window, *m/z* 1.6; activation type, ETD; reaction time, 50 ms; reagent target, 1e6; maximum ETD reagent inject time, 200 ms; scan range, normal; Orbitrap resolution, 30,000; first mass, *m/z* 110; AGC target, $5e^3$; max injection time, 100 ms; data type, centroid. Data dependent acquisition was performed in top speed mode using a 3 s cycle,

selecting most the intense precursors. Dynamic exclusion was performed for 50 s post precursor selection and a minimum threshold for fragmentation was set at $5e^4$.

HCD_IT. MS^2 spectra were acquired in the linear ion trap specifying: quadrupole isolation, isolation window, *m/z* 1.6; activation type, HCD; collision energy, 32%; scan range, normal; scan rate, rapid; first mass, *m/z* 110; AGC target, $5e^3$; max injection time, 100 ms; data type, centroid. Data dependent acquisition was performed in top speed mode using a 3 s cycle, with most intense precursors selected. Dynamic exclusion was performed for 50 s post precursor selection and a minimum threshold for fragmentation was set at $5e^3$.

HCD/ETD_IC. Precursors were sequentially selected and fragmented by both HCD and ETD. HCD spectra were acquired in the linear ion trap specifying quadrupole isolation, isolation window, *m/z* 1.6; activation type, HCD; collision energy, 30%; scan range, normal; scan rate, rapid; first mass, *m/z* 110; AGC target, $1e^4$; max injection time, 60 ms; data type, centroid. ETD spectra were acquired in the Orbitrap specifying: quadrupole isolation, isolation window, *m/z* 1.6; activation type, ETD; EThdD SA collision energy (15%), maximum ETD reagent inject time, 120 ms; scan range, normal; Orbitrap resolution, 60,000; first mass, *m/z* 120; AGC target, $5e^4$; max injection time, 200 ms; data type, centroid. Data dependent acquisition was performed in top N mode using a 20 precursor cycle for charge states 3-8. Highest charge state then most intense were set as selection priorities. Dynamic exclusion was performed for 50 s post precursor selection and a minimum threshold for fragmentation was set at $5e^3$.

Peak lists were generated in MGF format using Mascot Distiller (version 5, Matrix Science), stipulating a minimum signal to noise ratio of 2 and correlation (Rho) of 0.6. MGF files were searched against the *Streptomyces coelicolor* subset of the NCBInr database (8,578 sequences; 2,791,553 residues) using a locally-running copy of the Mascot search program (Matrix Science Ltd., version 2.5.1). Search criteria specified: Enzyme, trypsin; Fixed modifications, carbamidomethyl (C); Variable modifications, Hex (S,T), Hex_2 (S,T), Hex_3(S,T) and oxidation (M); Peptide tolerance, 10 ppm. MS/MS tolerance was set to 0.5 Da for linear ion trap data and 0.05 Da for Orbitrap data. Instrument type was set at ESI-TRAP, ETD-TRAP or CID + ETD as appropriate. Results were filtered to accept only peptides with expect scores of 0.05 or lower.

Bioinformatic tools for the prediction of subcellular localisation of glycoproteins. Predicted transmembrane domains were identified using TMHMM server 2.0 (1) . Predicted lipoproteins were identified using the LipoP 1.0 server (2). Signal peptides were predicted using SignalP 4.1 Server and the TatP 1.0 server (3, 4).

References for supplemental methods:

1. Krogh A, Larsson B, Von Heijne G, & Sonnhammer EL (2001) Predicting transmembrane protein topology with a hidden Markov model: application to complete genomes. *Journal of molecular biology* 305(3):567-580.
2. Juncker AS*, et al.* (2003) Prediction of lipoprotein signal peptides in Gram-negative bacteria. *Protein Science* 12(8):1652-1662.
3. Bendtsen JD, Nielsen H, Widdick D, Palmer T, & Brunak S (2005) Prediction of twin-arginine signal peptides. *BMC bioinformatics* 6(1):167.
4. Petersen TN, Brunak S, von Heijne G, & Nielsen H (2011) SignalP 4.0: discriminating signal peptides from transmembrane regions. *Nature methods* 8(10):785.

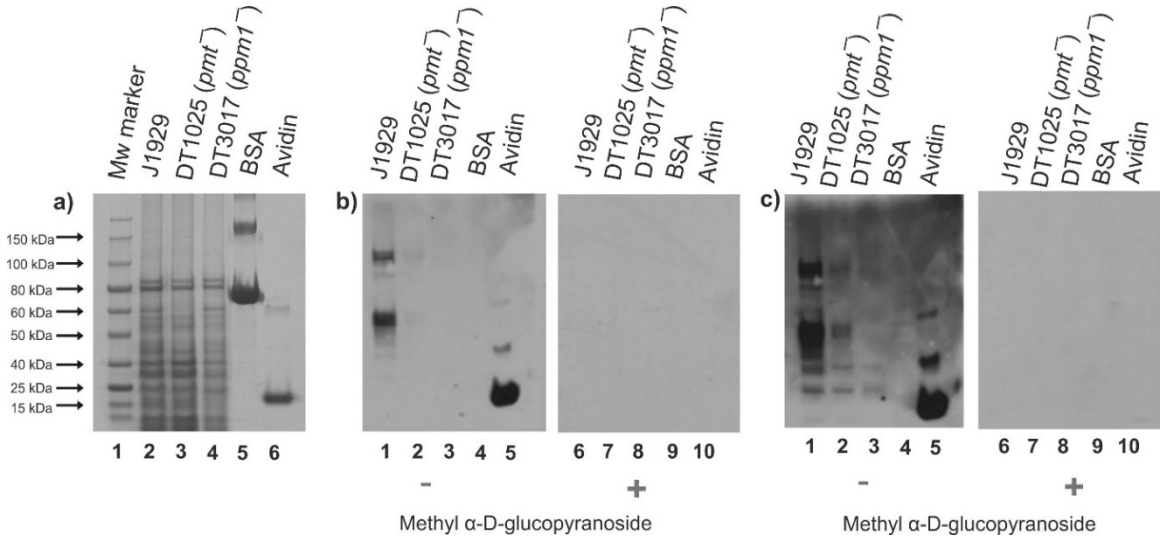

Fig. S1. Detection of glycosylated proteins in the membrane proteome of S. coelicolor J1929 using Con A-HRP**.** *S. coelicolor* J1929 and derivatives DT1025 (pmt¯) and DT3017 (ppm1¯) were grown in liquid culture for 25 h and the total membrane protein was isolated. Proteins were separated by SDS-PAGE and either stained with InstantBlue protein stain (a), or blotted onto PVDF membranes (b and c) and probed with Con A-HRP in the presence (lanes 1 - 5) and absence (lanes 6 - 10) of methyl α-D glucopyranoside. Protein loading was 17 µg for gels stained with InstantBlue protein stain and 5 µg for western blots probed with Con A-HRP. For the western blots probed with Con A-HRP, a 2 min (b) and 8 min (c) exposure to the membrane is shown. Bovine serum albumin (BSA) was a negative control and Avidin was a positive control for the Con A-HRP reactivity. The protein marker was the Broad range 10 – 250 kDa Mw marker (NEB).

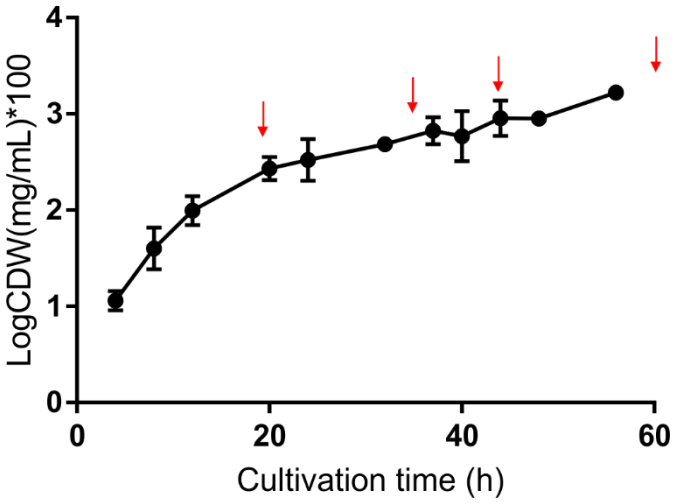

Fig S2. Growth of S. coelicolor J1929 in liquid F134 medium. S. coelicolor J1929 spores were germinated for 6 h and the cultures were grown for 56 h in F134 medium. Measurements of cell dry weight (CDW) were taken to monitor growth at regular intervals. The time points selected to harvest the cultures for glycoprotein isolation are indicated by red arrows. Error bars represent the standard error of the mean of three biological replicates.

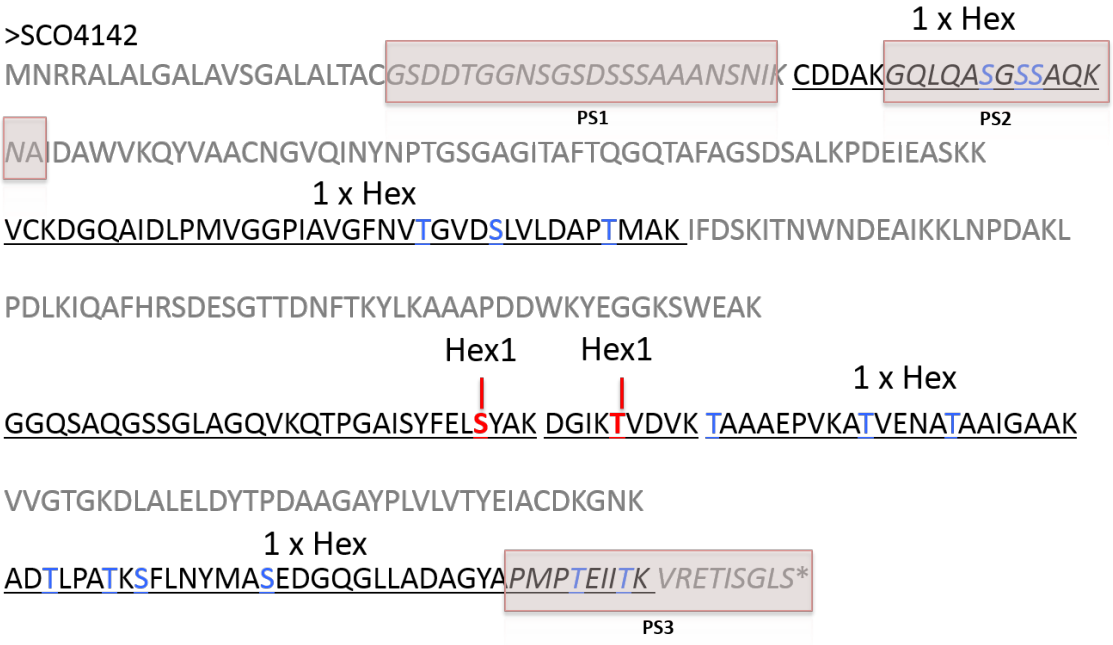

Fig S3. PstS glycopeptides overlap with synthetic peptides previously shown to be glycosylated in a cell free assay. Synthetic peptides PS1, PS2 and PS3 (shown in pink box) were previously tested in a cell free assay glycosylation assay. PS2 and PS3 were shown to be glycosylated. Glycopeptides identified by mass spectrometry are underlined, with validated glycosylation sites in shown in red. In glycopeptides where the glycosylation site was not validated, potential glycosylation sites are shown in blue.

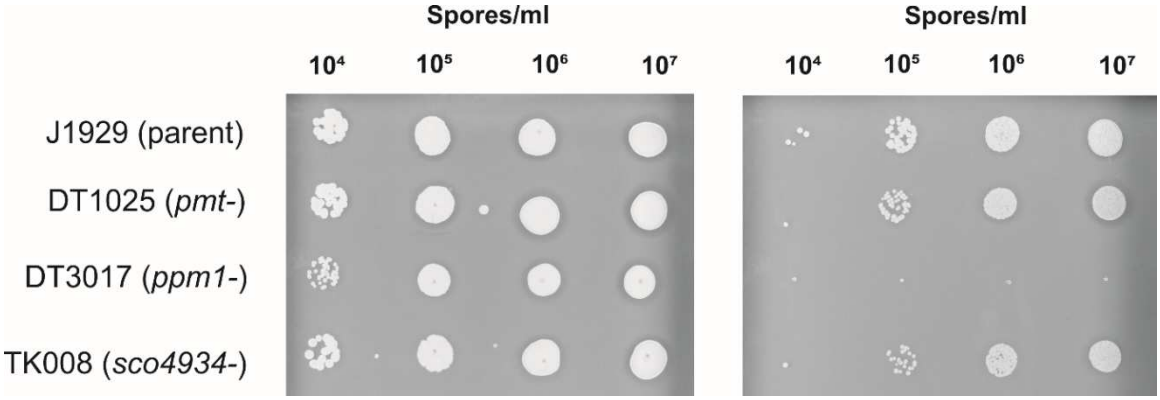

Fig S4. Lysozyme sensitivity of TK008 (sco4934^{-}) compared to the parent strain J1929, DT1025 (pmt^{-}) and DT3017 (ppm1^{-}). Spores were adjusted to 10^8 spores/mL and a ten-fold serial dilution was carried out to get 10^4 spores/mL. 5 µL of each spore stock was plated onto DNA without lysozyme (left-hand panel) and with 0.25 mg/mL of lysozyme (right-hand panel). Images are representative of three biological replicates.

SCO Number	Expect score[1]	Peptide sequence	# Hex[2]	Site allocation	MD-score[3]	Method	Time point	Precursor ion *m/z*	Charge	Scan	Retention time (min)
SCO0472	0.00021	GGGSTPSATPAASVQDPLVATFDGGLYILDGK	9	-	-	CID	35	1507.67	3	-	136.5
SCO0472	0.01	GGGSTPSATPAASVQDPLVATFDGGLYILDGK	9	-	-	CID	35	1507.67	3	-	136.5
SCO0996	0.00003	ATAPSAEGFPVTIDNCGVK	3	-	-	CID	20	1210.56	2	-	75.7
SCO0996	0.00082	ATAPSAEGFPVTIDNCGVK	2	-	-	HCD_IT	43	753.3517	3	46383	N/A
SCO0996	0.021	ATAPSAEGFPVTIDNCGVK	3	-	-	HCD_IT	43	1210.55	2	45042	N/A
SCO1714	0.019	TVTEPAADR	3	-	-	CID	35	723.318	2	-	25.9
SCO2035	0.0066	DDGSESAGPVVAPSGAQGK	2	-	-	HCD_IT	43	1026.959	2	14239	N/A
SCO2096	0.0059	KLDACPNESAVAVPVTGDDGPK	3	-	-	HCD_IT	43	909.4205	3	26945	N/A
SCO2156	0.0015	EGTFLGKCAELCGVDHSR	1	-	-	HCD_IT	43	733.3296	3	25242	N/A
SCO2838	0.002	AAGAGITQQPK	2	T7	Only possible site	ETD_IT	43	683.3412	2	2576	-
SCO2963	0.0065	GRGSSDADR	1	-	-	ETD_IT	43	541.7381	2	8834	-
SCO3044	0.000032	GDAGQPSDEPAADSEIGVLVQNATR	3	-	-	HCD_IT	43	995.119	3	63502	-
SCO3044	0.0064	GDAGQPSDEPAADSEIGVLVQNATR	3	-	-	HCD_IT	43	995.1174	3	63661	-
SCO3046	0.0000031	VAKPTPNAAGQTPLNILVIGSDAR	2	T5	32	ETD_OT	43	909.8197	3	Sum of 2 scans in range 22872 to 22874	-
SCO3046	0.000086	VAKPTPNAAGQTPLNILVIGSDAR	2	-	-	HCD_IT	43	909.8185	3	56534	-
SCO3184	0.000011	ATVETAAPDRGDGYGVALR	1	-	4.1	ETD_OT	43	694.3423	3	9131	-
SCO3184	0.00026	ATVETAAPDRGDGYGVALR	1	-	8.4	ETD_IT	43	694.3432	3	10892	-
SCO3184	0.0016	ATVETAAPDRGDGYGVALR	1	-	2.1	ETD_OT	43	694.3431	3	Sum of 2 scans in range 10601 to 10603	-
SCO3184	0.0014	KATVETAAPDRGDGYGVALR	1	-	-	HCD_IT	43	737.0407	3	Sum of scans in range 16301 to 16323	-
SCO3184	0.045	KATVETAAPDRGDGYGVALR	1	-	-	HCD_IT	43	737.0419	3	16390	-
SCO3353	0.000016	KPSAPECGTPPAGSAK	2	T9	35.2	ETD_OT	43	626.9599	3	2027	-
SCO3353	0.00055	KPSAPECGTPPAGSAK	2	-	-	HCD_IT	43	939.9368	2	4189	-
SCO3353	0.00071	KPSAPECGTPPAGSAK	3	-	-	HCD_IT	43	680.9775	3	4050	-
SCO3353	0.00078	KPSAPECGTPPAGSAK	2	T9	28.2	ETD_IT	43	626.9593	3	2303	-
SCO3353	0.0015	KPSAPECGTPPAGSAK	3	T9	15.5	ETD_OT	43	680.9777	3	1965	-
SCO3353	0.0016	KPSAPECGTPPAGSAK	3	T9	23.5	ETD_IT	43	680.9773	3	2241	-
SCO3357	0.029	ASPSKAPDRVDAVR	6	-	-	ETD_IT	43	814.373	3	2155	-
SCO3357	0.00076	DEGPAHADAVGGAGSASPAPAAK	6	S15 S17	Manual assignment	ETD_OT	43	992.7591	3	Sum of 2 scans in range 2970 to 2972	-
SCO3357	0.013	DEGPAHADAVGGAGSASPAPAAK	6	-	-	CID	43	992.761	3	-	35.9
SCO3540	0.000055	ATPAELSPYYEQK	2	-	-	CID	35	910.927	2	-	53.2
SCO3540	0.019	ATPAELSPYYEQK	2	T2	Manual assignment	CID	43	910.921	2	-	56.4
SCO4130	0.000065	TSATAPSGTRPVQSGFAHDAQGAQSAAANYAVALGSDGMFDK	2	-	-	HCD_IT	43	1109.511	4	58511	-
SCO4130	0.00036	TSATAPSGTRPVQSGFAHDAQGAQSAAANYAVALGSDGMFDK	2	-	4.7	HCD_IT	43	1109.514	4	Sum of 2 scans in range 23637to 23639	-
SCO4130	0.0098	TSATAPSGTRPVQSGFAHDAQGAQSAAANYAVALGSDGMFDK	2	-	-	HCD_IT	43	1113.511	4	Sum of 2 scans in range 21239 to 21241	-
SCO4141	0.00021	TPQPPATEDTRPGR	1	T1	27.8	ETD_OT	43	562.2769	3	Sum of 2 scans in range 2571 to 2584	-
SCO4141	0.0041	TPQPPATEDTRPGR	1	T1	13	ETD_OT	43	562.2767	3	2323	-
SCO4141	0.0061	TPQPPATEDTRPGR	1	T1	21.7	ETD_IT	43	562.2783	3	Sum of 2 scans in range 2611 to 2665	-
SCO4141	0.037	TPQPPATEDTRPGR	1	-	-	HCD_IT	43	842.9104	2	5650	-
SCO4141	0.04	TPQPPATEDTRPGR	1	-	-	CID	60	562.28	3	-	31.2
SCO4142	0.00078	ADTLPATKSFLNYMASEDGQGLLADAGYAPMPTEIITK	1	-	-	HCD_IT	43	1388.343	3	91188	-
SCO4142	0.048	CDDAKGQLQASGSSAQK	1	-	-	HCD_IT	43	956.9326	2	4208	-
SCO4142	0.0081	DGIKTVDVK	1	T5	Only possible site	ETD_OT	43	379.5407	3	3598	-
SCO4142	0.000036	GGQSAQGSSGLAGQVKQTPGAISYFELSYAK	1	-	-	HCD_IT	43	1083.868	3	58627	-
SCO4142	0.0028	QTPGAISYFELSYAKDGIK	1	S12	24.8	ETD_IT	43	750.7115	3	24203	-
SCO4142	0.0019	TAAAEPVKATVENATAAIGAAK	1	-	-	HCD_IT	43	739.7253	3	42536	-
SCO4142	0.017	TAAAEPVKATVENATAAIGAAK	1	-	0.8	ETD_IT	43	739.7249	3	Sum of 2 scans in range 18332 to 18361	-
SCO4142	0.014	VCKDGQAIDLPMVGGPIAVGFNVTGVDSLVLDAPTMAK	1	-	-	HCD_IT	43	1345.343	3	92043	-
SCO4256	0.018	GGGGGGGGESKKPKPPVR	3	S10	Only possible site	ETD_OT	43	527.7643	4	Sum of 2 scans in range 1711 to 1712	-
SCO4307	0.006	LIYAGAGTAGR	1	T8	Only possible site	ETD_IT	43	404.5446	3	6751	-
SCO4548	0.00042	TTSSSSSTAPSAPSAPR	1	-	-	HCD_IT	43	877.4079	2	6204	-
SCO4739	0.000000011	TEQSASAGGAEESAPAGK	3	-	-	CID	20	1067.46	2	-	25.7
SCO4739	0.0000041	TEQSASAGGAEESAPAGK	4	-	-	CID	20	1148.48	2	-	25.1
SCO4739	0.00025	TEQSASAGGAEESAPAGK	6	-	-	CID	20	874.023	3	-	24.3
SCO4739	0.00034	TEQSASAGGAEESAPAGK	9	-	-	CID	20	1036.08	3	-	23.6
SCO4739	0.0011	TEQSASAGGAEESAPAGK	8	-	-	CID	20	982.061	3	-	23.7
SCO4739	0.0018	TEQSASAGGAEESAPAGK	8	-	-	CID	20	982.06	3	-	23.8
SCO4739	0.0022	TEQSASAGGAEESAPAGK	8	-	-	CID	20	982.061	3	-	23.9
SCO4739	0.0025	TEQSASAGGAEESAPAGK	5	-	-	CID	20	1229.5	2	-	24.8
SCO4739	0.0041	TEQSASAGGAEESAPAGK	8	-	-	CID	60	982.063	3	-	23.8
SCO4739	0.0045	TEQSASAGGAEESAPAGK	8	-	-	CID	35	982.063	3	-	23.3
SCO4739	0.0087	TEQSASAGGAEESAPAGK	9	-	-	CID	35	1036.08	3	-	23.1
SCO4739	0.012	TEQSASAGGAEESAPAGK	7	-	-	CID	20	928.04	3	-	24.1
SCO4739	0.029	TEQSASAGGAEESAPAGK	7	-	-	CID	20	928.045	3	-	24.3
SCO4739	0.031	TEQSASAGGAEESAPAGK	8	-	-	CID	35	982.063	3	-	23.4
SCO4739	0.034	TEQSASAGGAEESAPAGK	8	-	-	CID	20	982.063	3	-	23.8
SCO4847	0.0003	SATAASPSAEASGEAGGTGK	9	-	-	CID	35	1055.76	3	-	59.5
SCO4847	0.00083	SATAASPSAEASGEAGGTGK	9	-	-	CID	20	1055.76	3	-	59.5
SCO4885	0.00000081	SDQAPEPGFADSPYITVTFR	1	-	-	HCD_IT	43	1180.552	2	71923	-

SCO4905	0.0091	ATEVPTDYGPAPSR	3	-	-	CID	60	973.935	2	-	46.7
SCO4905	0.000000016	ATPGLPAQVFLLCGSSLVAVDR	3	-	-	CID	20	919.788	3	-	121.6
SCO4905	0.000072	ATPGLPAQVFLLCGSSLVAVDR	2	-	-	HCD_IT	43	865.7785	3	88724	-
SCO4905	0.00019	ATPGLPAQVFLLCGSSLVAVDR	2	-	-	CID	20	865.783	3	-	122.5
SCO4905	0.024	ATPGLPAQVFLLCGSSLVAVDR	3	-	-	HCD_IT	43	919.7954	3	88232	-
SCO4934	0.00019	TSQAEVDEAAAK	2	-	-	CID	35	772.341	2	-	27.4
SCO4934	0.00019	TSQAEVDEAAAK	2	-	-	CID	60	772.35	2	-	27.7
SCO4934	0.00024	TSQAEVDEAAAK	3	-	-	CID	35	853.368	2	-	27
SCO4934	0.0036	TSQAEVDEAAAK	3	-	-	CID	43	853.373	2	-	30.1
SCO4934	0.023	TSQAEVDEAAAK	3	-	-	CID	20	853.378	2	-	27.9
SCO4934	0.024	TSQAEVDEAAAK	3	-	-	CID	60	853.375	2	-	27.4
SCO4968	0.0000091	VDFKEPAEQDASAGPEAKPQR	1	S12	Only possible site	ETD_OT	43	811.3916	3	Sum of 2 scans in range 6230 to 6232	-
SCO4968	0.032	VDFKEPAEQDASAGPEAKPQR	1	S12	Only possible site	HCD_IT	43	811.3906	3	13570	-
SCO5115	0.0089	AVDGLSFDLER	1	S6	Only possible site	CID	60	692.336	2	-	103.6
SCO5204	0.012	QVQSQFNSEQDIAESIR	1	-	-	CID	43	1071	2	-	73.2
SCO5646	0.0059	AILTKDNPQGDVFFGVDNTLLSR	1	-	-	HCD_IT	43	894.7915	3	72287	-
SCO5736	0.0005	EGDTGSPEVQVALLSR	1	-	-	CID	20	910.45	2	-	79.3
SCO5751	0.00044	KPADPKPEPSDSAIAAAPADKVTVK	6	S10 S12	31.8	ETD_OT	43	869.6701	4	Sum of 4 scans in range 4856 to 4896	-
SCO5751	0.0029	KPADPKPEPSDSAIAAAPADKVTVK	6	S10 S12	28	ETD_OT	43	695.9383	5	4335	-
SCO5776	0.0013	SEKVDFAGPYLLAHQDVLIR	1	S1	Only possible site	HCD_IT	43	609.072	4	60208	-
SCO5818	0.041	SPHAARLAALVTK	3	S1, T12	Manual assignment	CID	60	910.982	2	-	128.8
SCO6558	0.012	IPDITLER	1	T5	Only possible site	CID	43	559.797	2	-	87.9
SCO6558	0.046	IPDITLER	1	T5	Only possible site	CID	43	559.798	2	-	85.6
SCO7218	0.00066	ASSGGHYPVTVENCGEK	3	-	7.8	ETD_OT	43	759.9905	3	Sum of 2 scans in range 3702 to 3705	-
SCO7218	0.027	ASSGGHYPVTVENCGEK	3	-	-	ETD_OT	43	759.9905	3	3332	-
SCO7218	0.0047	ASSGGHYPVTVENCGEKLTFEK	3	-	6.1	ETD_IT	43	724.83	4	11845	-

Spectra generated by LC-ESI-CID-MS/MS on the Bruker maXis HD system

Key:

Ion Type	Description
b(++)	doubly charged ion series
b(*)	b - NH_3
b(0)	b - H_2O
y(++)	doubly charged ion series
y(*)	y - NH_3
y(0)	y - H_2O

Time point	60 hr
SCO number	SCO5115
Precursor ion mass	692.336
Charge	2
Retention time	103.6
Hex on peptide	1
e-value	8.90E-03
Site allocated?	Ser43

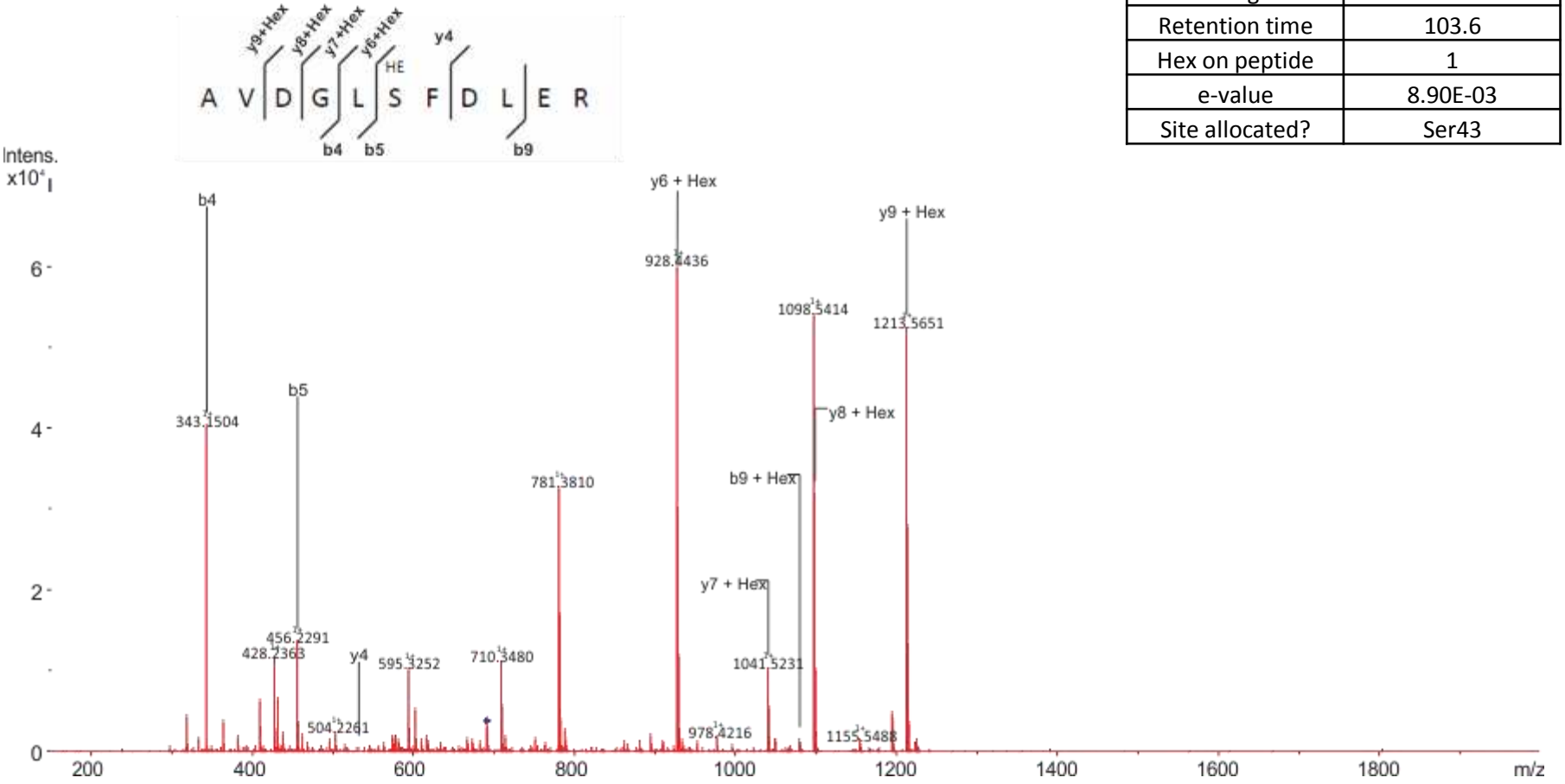

Time point	43 hr
SCO number	SCO6558
Precursor ion mass	559.797
Charge	2
Retention time	87.9
Hex on peptide	1
e-value	1.20E-02
Site allocated?	Thr104

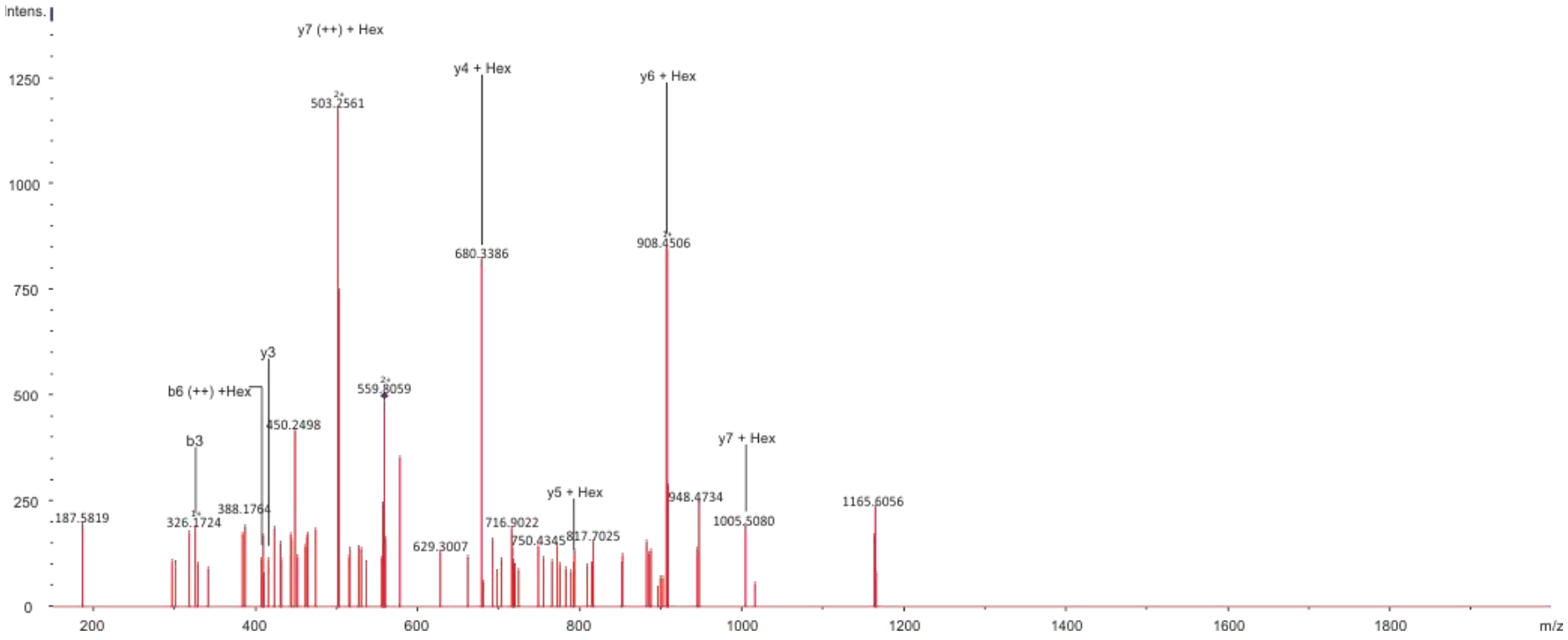

Time point	60 hr
SCO number	SCO5815
Precursor ion mass	910.981
Charge	2
Retention time	128.8
Hex on peptide	3
e-value	4.10E-02
Site allocated?	Ser228, Thr239

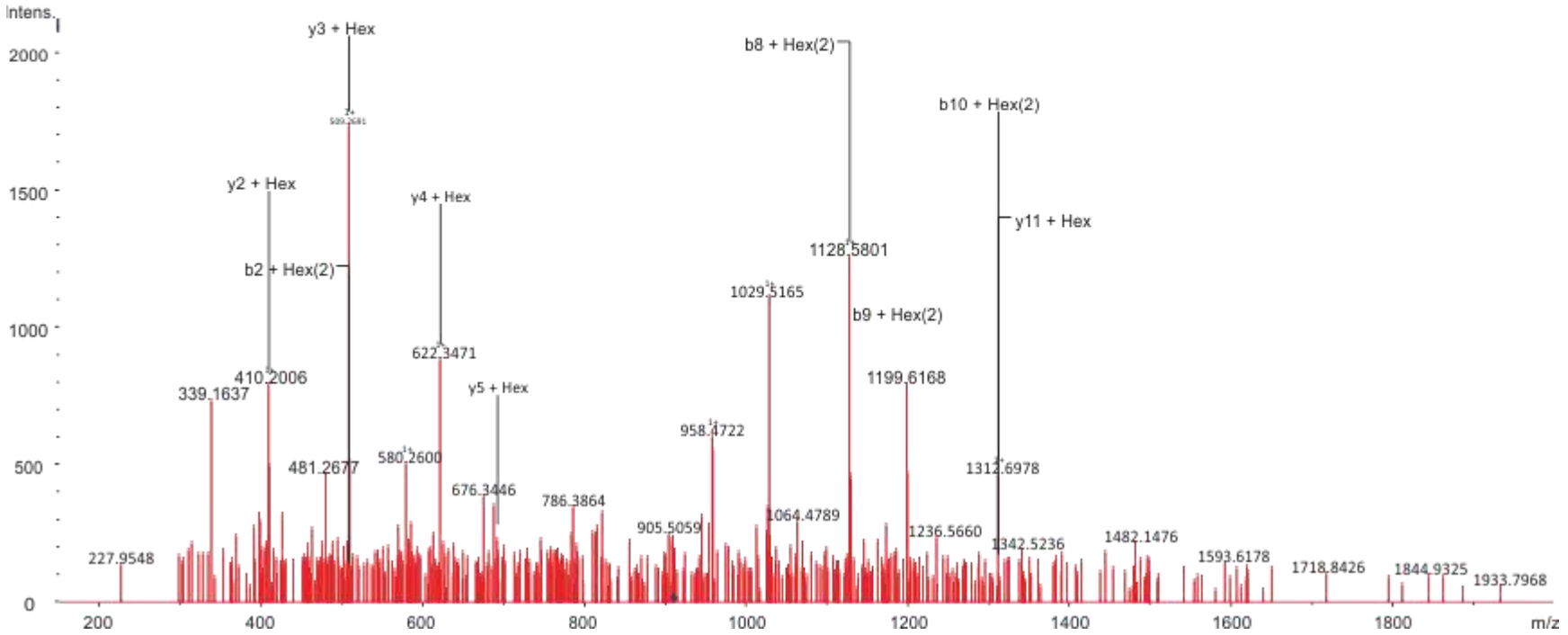

Time point	20 hr
SCO number	SCO5736
Precursor ion mass	910.450
Charge	2
Retention time	79.3
Hex on peptide	1
e-value	0.0005
Site allocated?	N

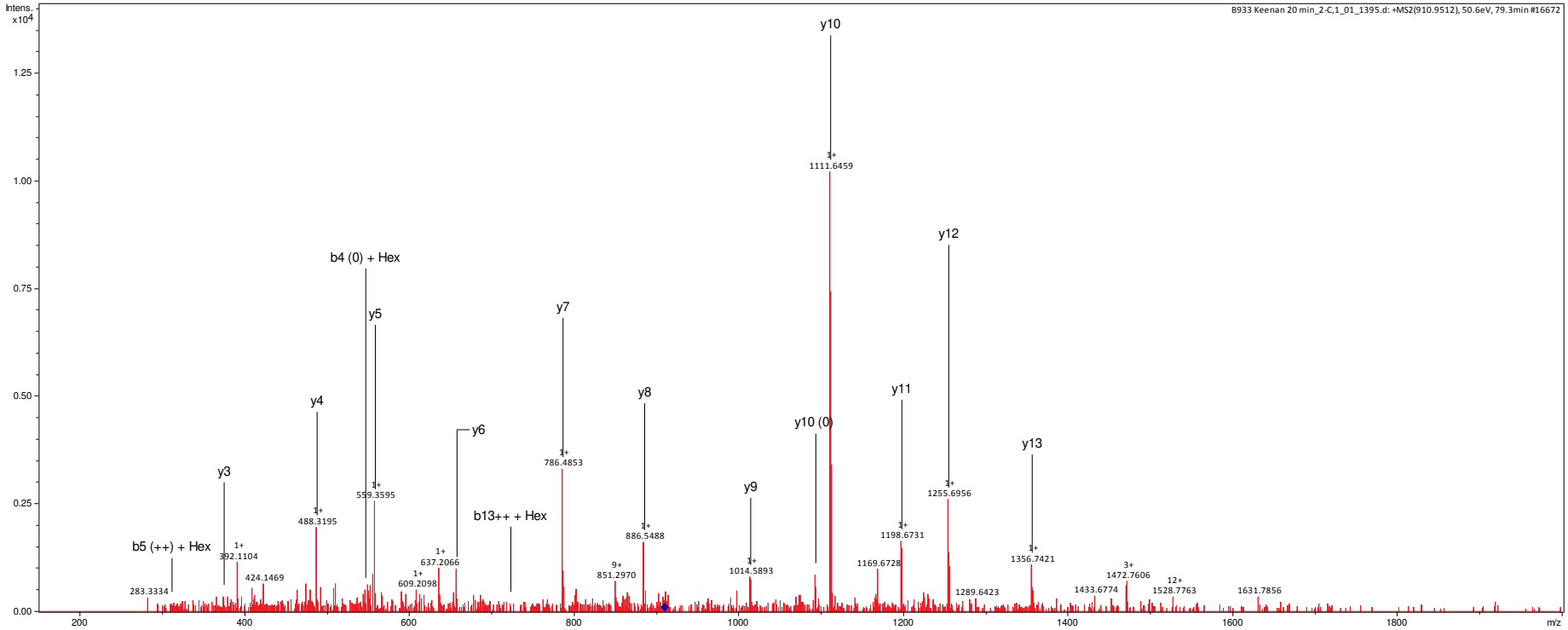

Time point	20 hr
SCO number	SCO4847
Precursor ion mass	1055.759
Charge	3
Retention time	59.5
Hex on peptide	9
e-value	0.00083
Site allocated?	N

S A T A A S P S A E A S G E A G G T G K

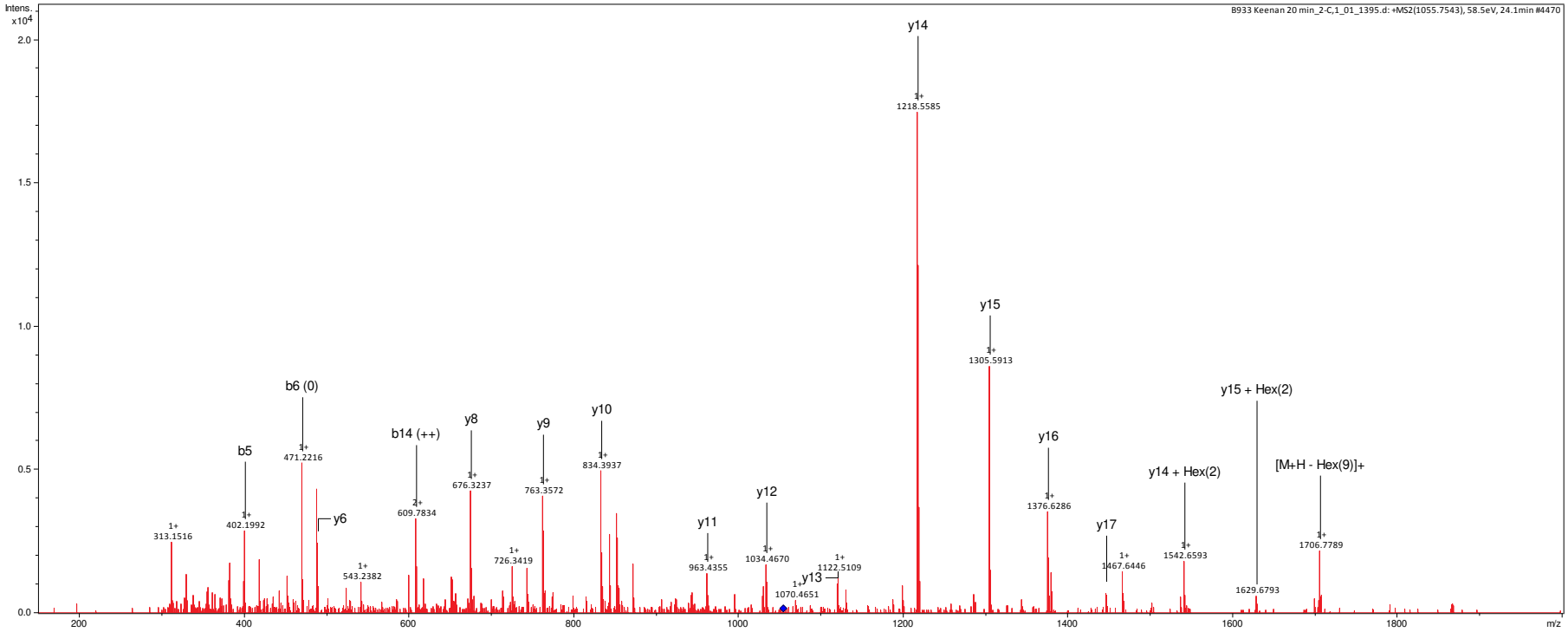

Time point	20 hr
SCO number	SCO4739
Precursor ion mass	1148.485
Charge	2
Retention time	25.1
Hex on peptide	4
e-value	0.0000041
Site allocated?	N

T E Q S A S A G G A E E S A P A G K

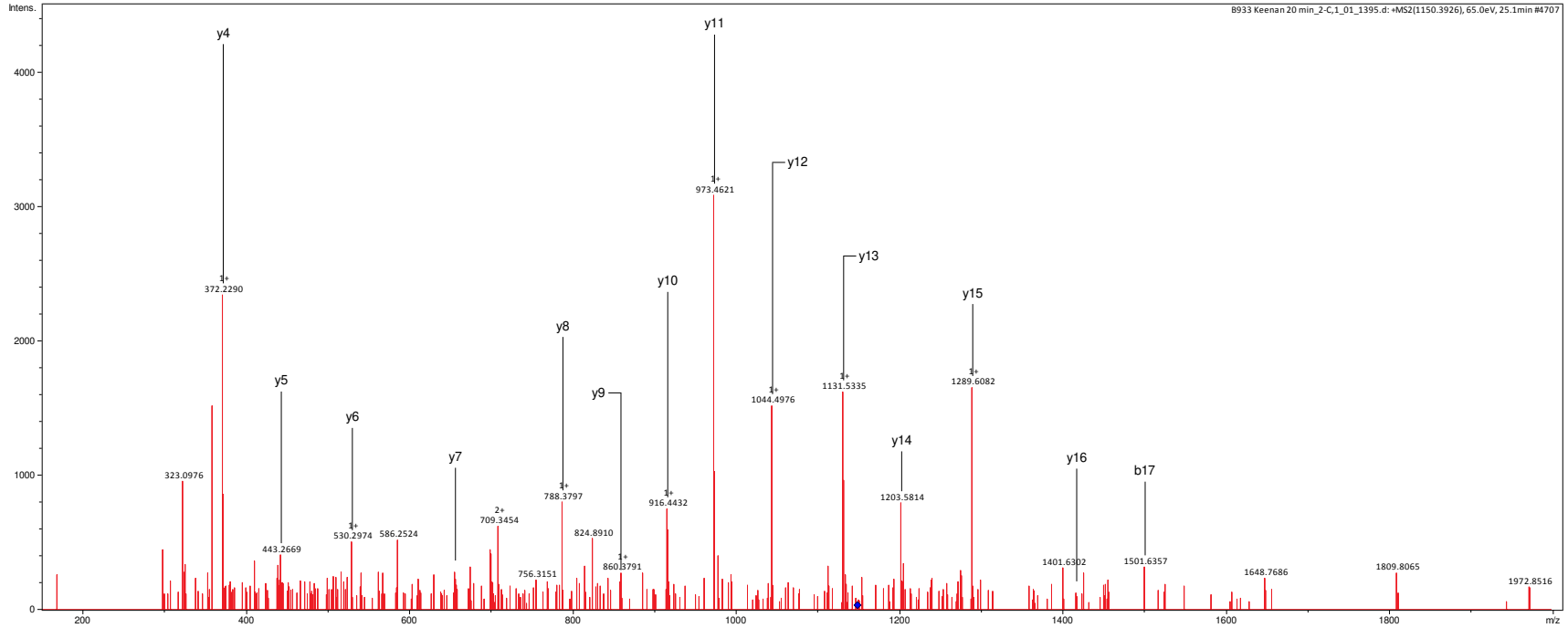

Time point	20 hr
SCO number	SCO4739
Precursor ion mass	1229.501
Charge	2
Retention time	24.8
Hex on peptide	5
e-value	0.0025
Site allocated?	N

T E Q S A S A G G A E E S A P A G K

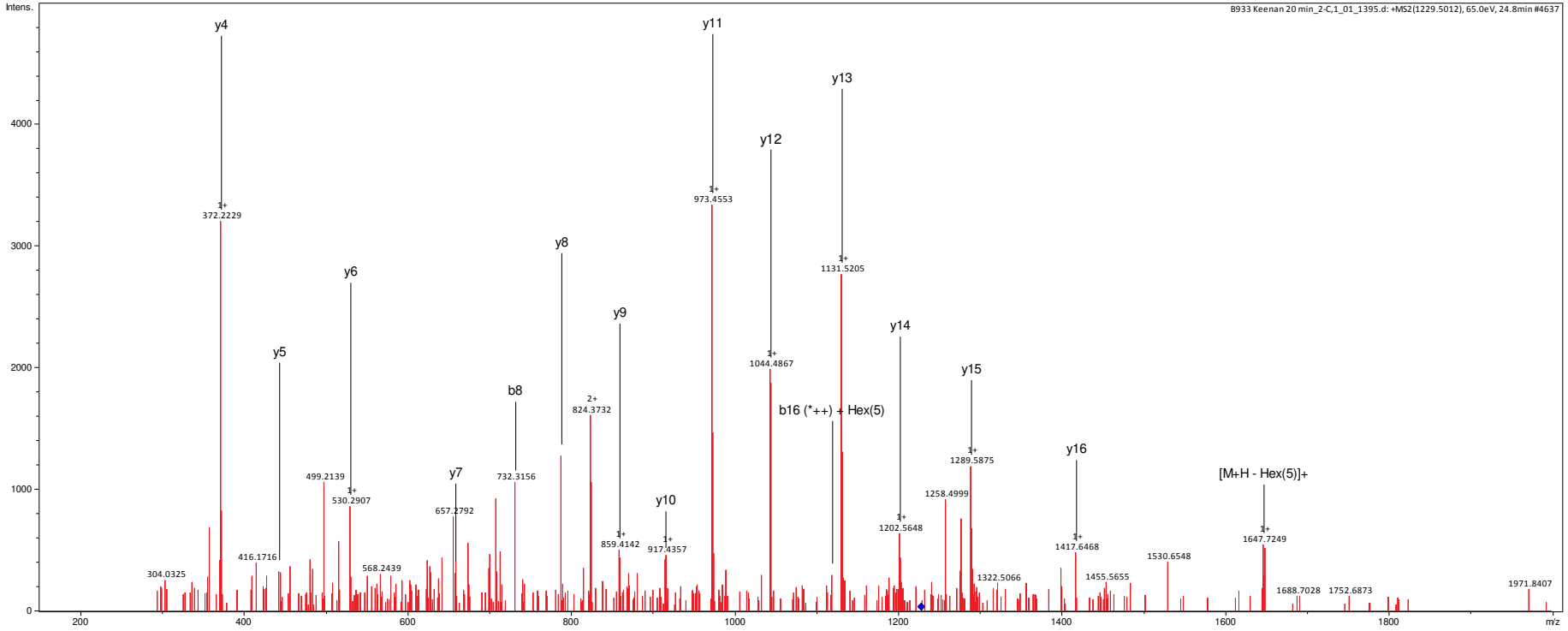

Time point	20 hr
SCO number	SCO4739
Precursor ion mass	874.023
Charge	3
Retention time	24.3
Hex on peptide	6
e-value	0.00025
Site allocated?	N

T E Q S A S A G G A E E S A P A G K

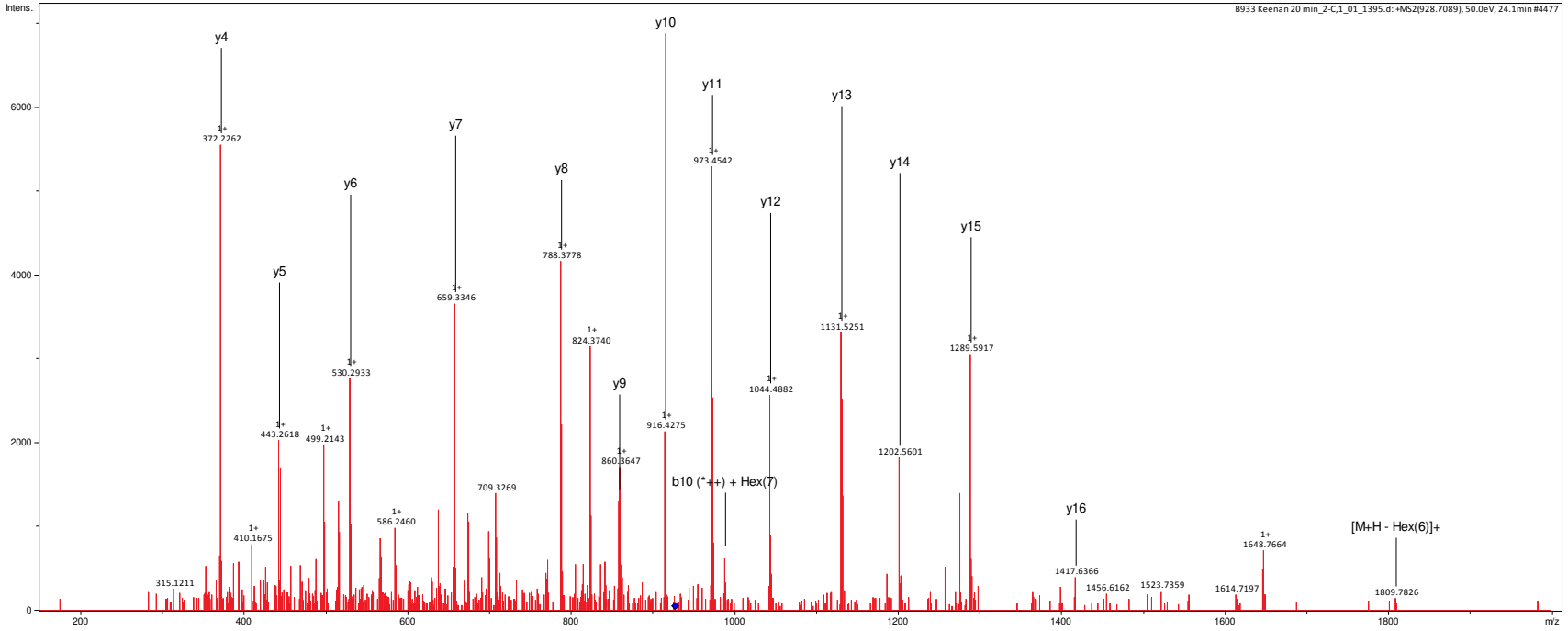

Time point	20 hr
SCO number	SCO4739
Precursor ion mass	928.040
Charge	3
Retention time	24.1
Hex on peptide	7
e-value	0.012
Site allocated?	N

T E Q S A S A G G A E E S A P A G K

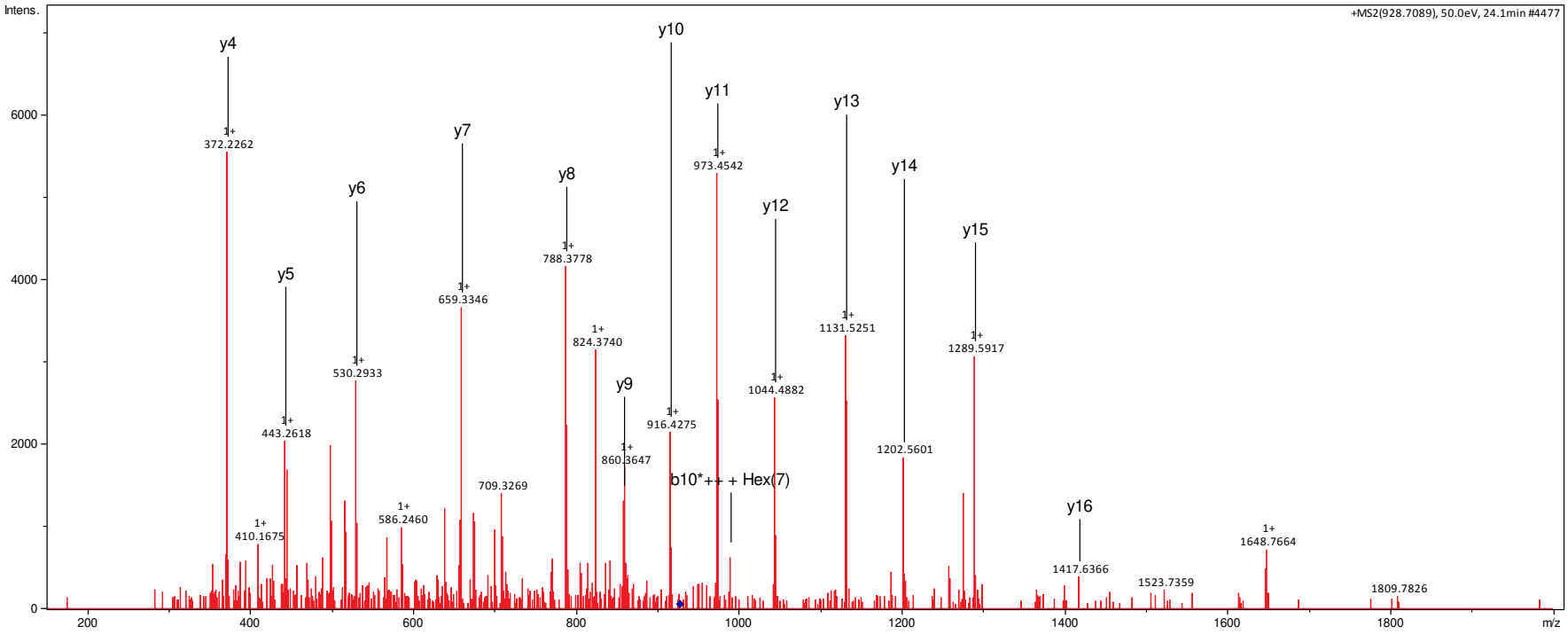

Time point	20 hr
SCO number	SCO4739
Precursor ion mass	982.060
Charge	3
Retention time	23.8
Hex on peptide	8
e-value	0.0018
Site allocated?	N

T E Q S A S A G G A E E S A P A G K

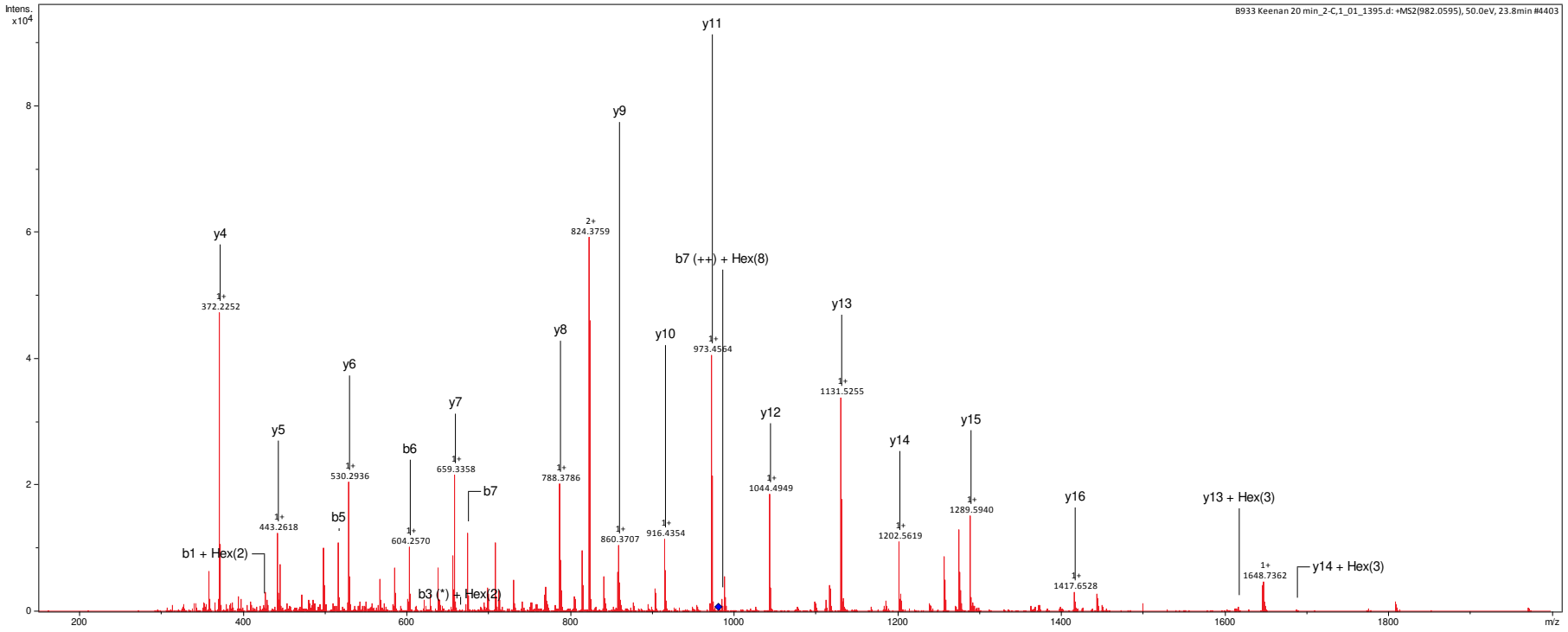

Time point	20 hr
SCO number	SCO4739
Precursor ion mass	1036.081
Charge	3
Retention time	23.6
Hex on peptide	9
e-value	0.00034
Site allocated?	N

T E Q S A S A G G A E E S A P A G K

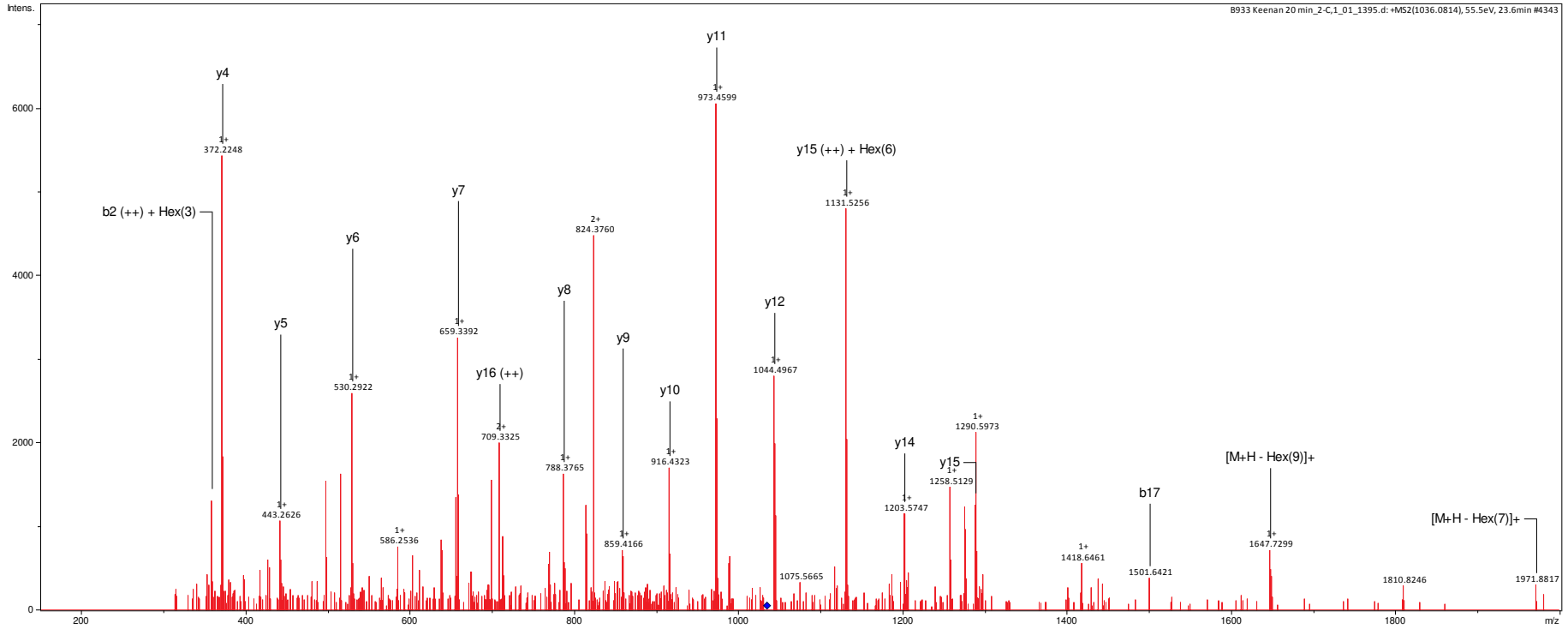

Time point	20 hr
SCO number	SCO0996
Precursor ion mass	1210.556
Charge	2
Retention time	75.7
Hex on peptide	3
e-value	0.00003
Site allocated?	N

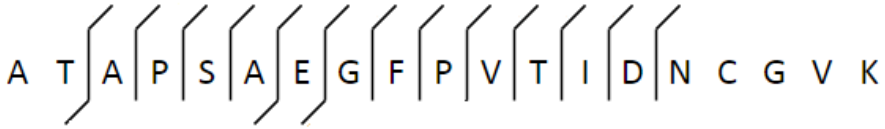

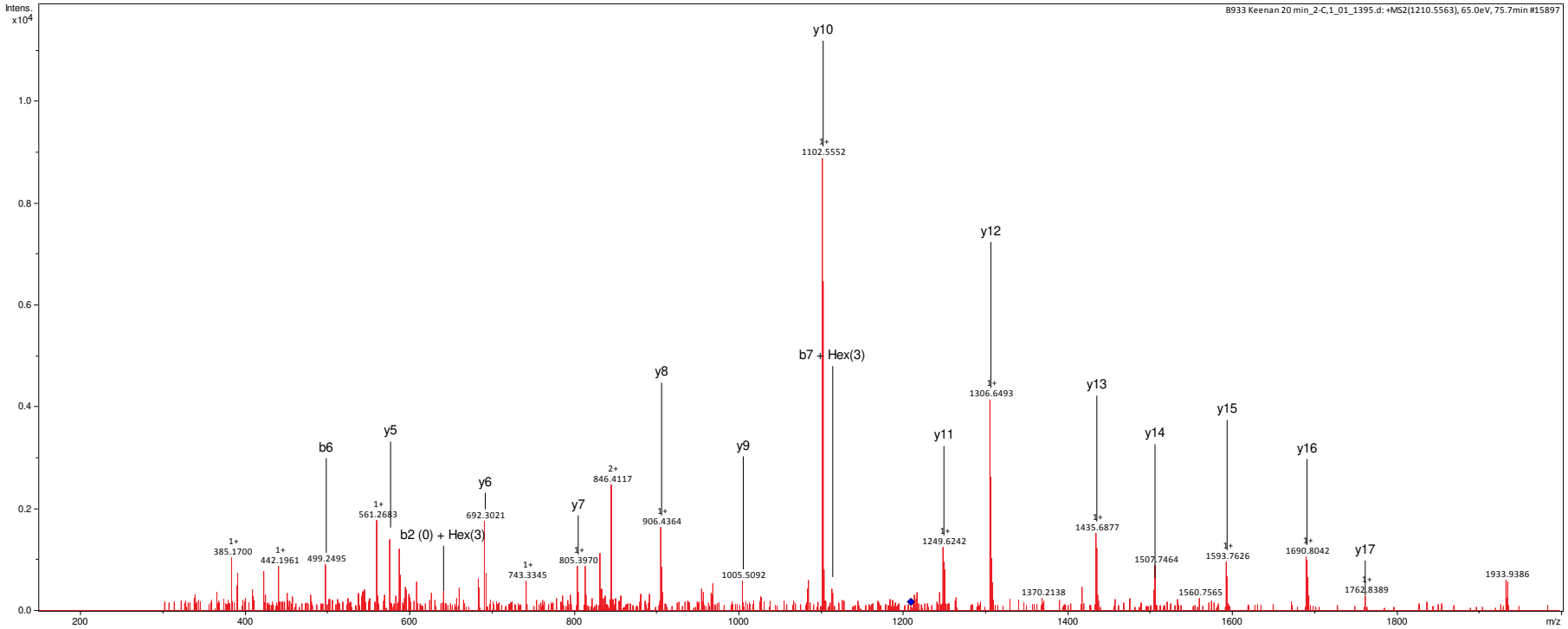

Time point	20 hr
SCO number	SCO4905
Precursor ion mass	919.788
Charge	3
Retention time	121.6
Hex on peptide	3
e-value	0.000000016
Site allocated?	N

A T P G L P A Q V F L L C G S S L V A V D R

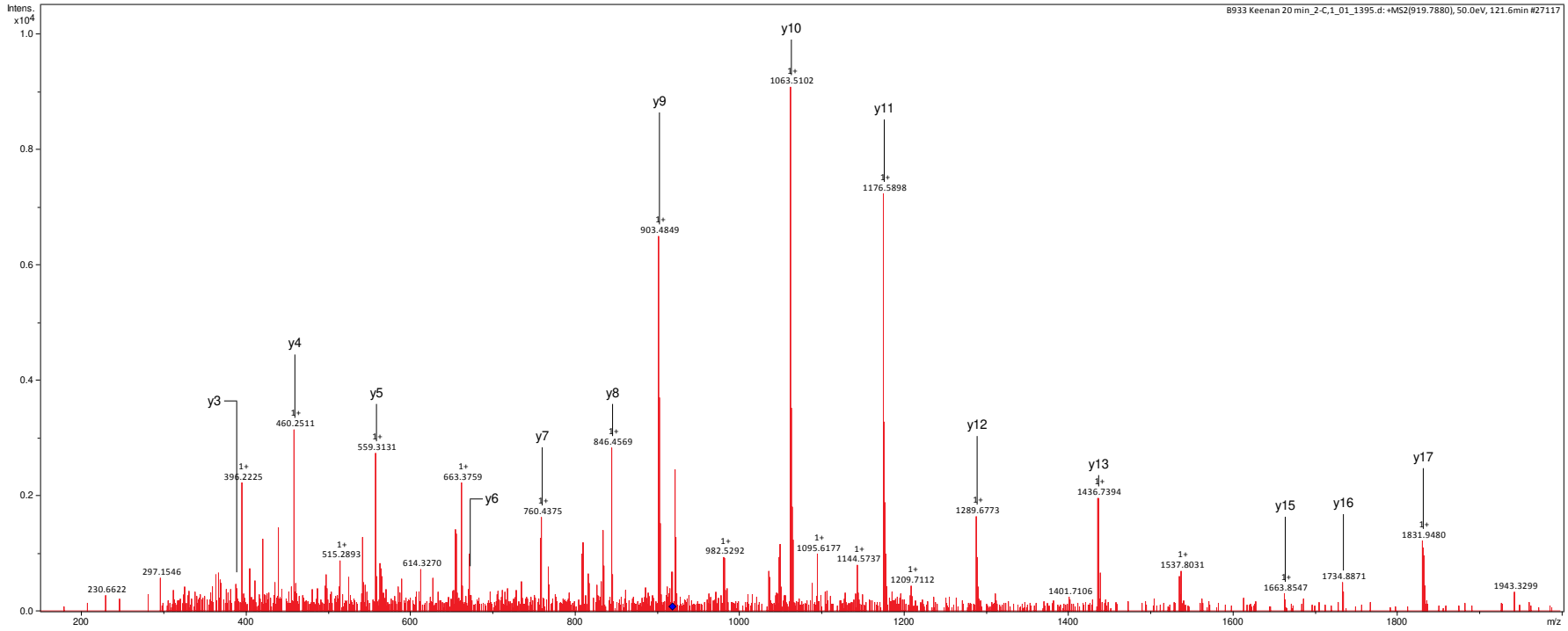

Time point	20 hr
SCO number	SCO4934
Precursor ion mass	853.378
Charge	2
Retention time	27.9
Hex on peptide	3
e-value	0.023
Site allocated?	N

T S Q A E V D E A A A K

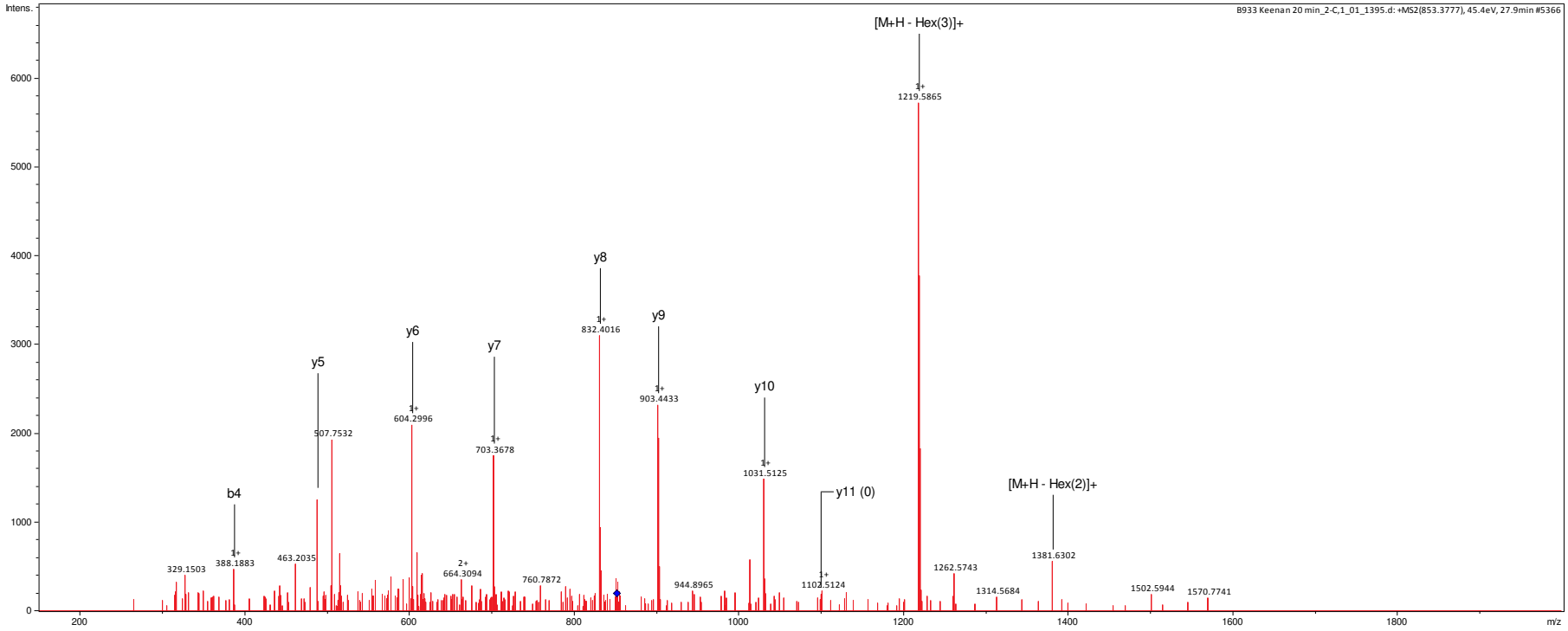

Time point	35 hr
SCO number	SCO4934
Precursor ion mass	772.341
Charge	2
Retention time	27.4
Hex on peptide	2
e-value	0.00019
Site allocated?	N

T S Q A E V D E A A A K

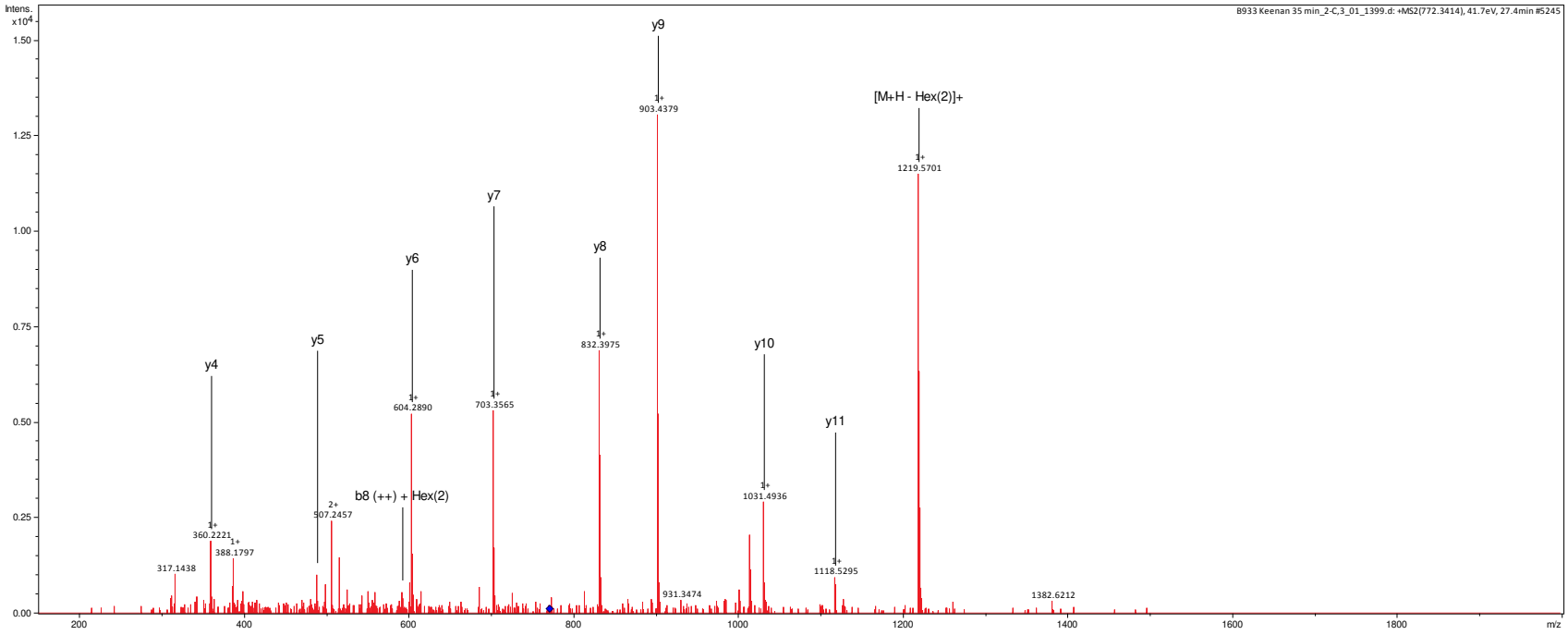

Time point	35 hr
SCO number	SCO4934
Precursor ion mass	853.368
Charge	2
Retention time	27
Hex on peptide	3
e-value	0.00024
Site allocated?	N

T S Q A E V D E A A A K

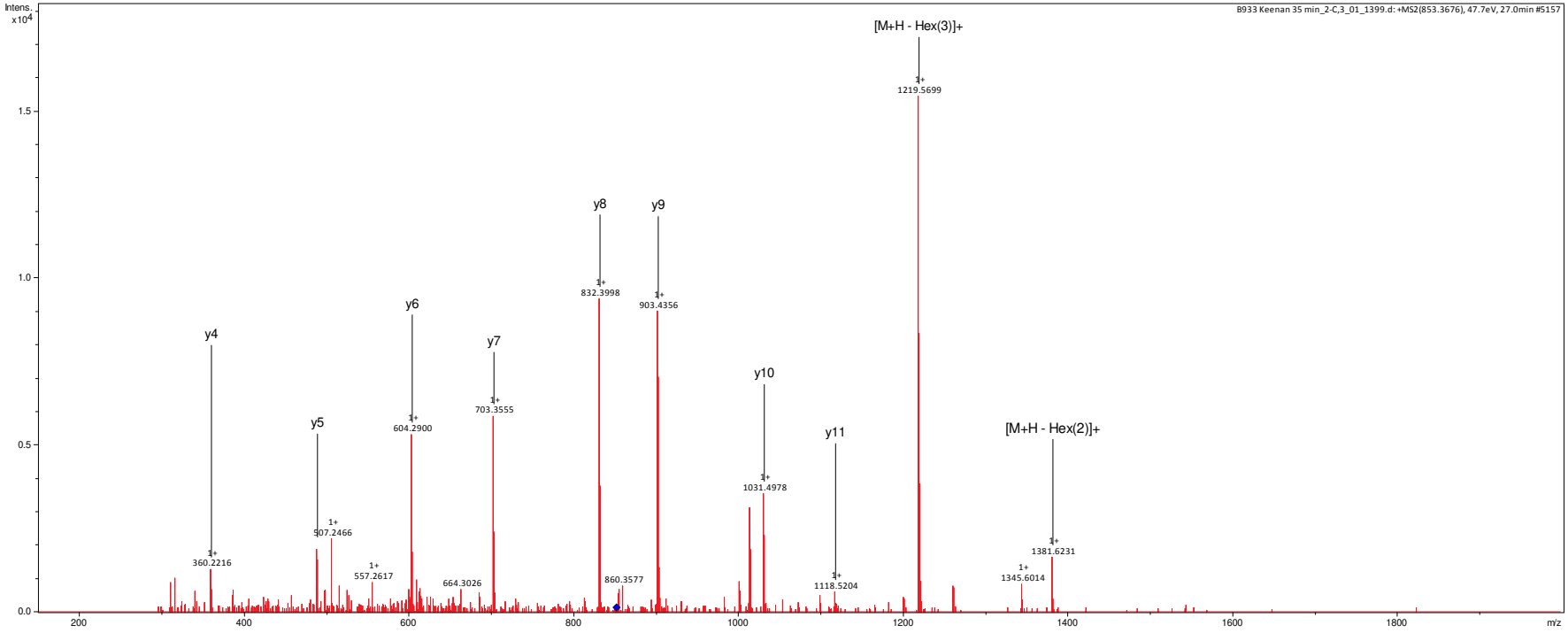

Time point	35 hr
SCO number	SCO4847
Precursor ion mass	1055.759
Charge	3
Retention time	59.5
Hex on peptide	9
e-value	0.0003
Site allocated?	N

S A T A A S P S A E A S G E A G G T G K

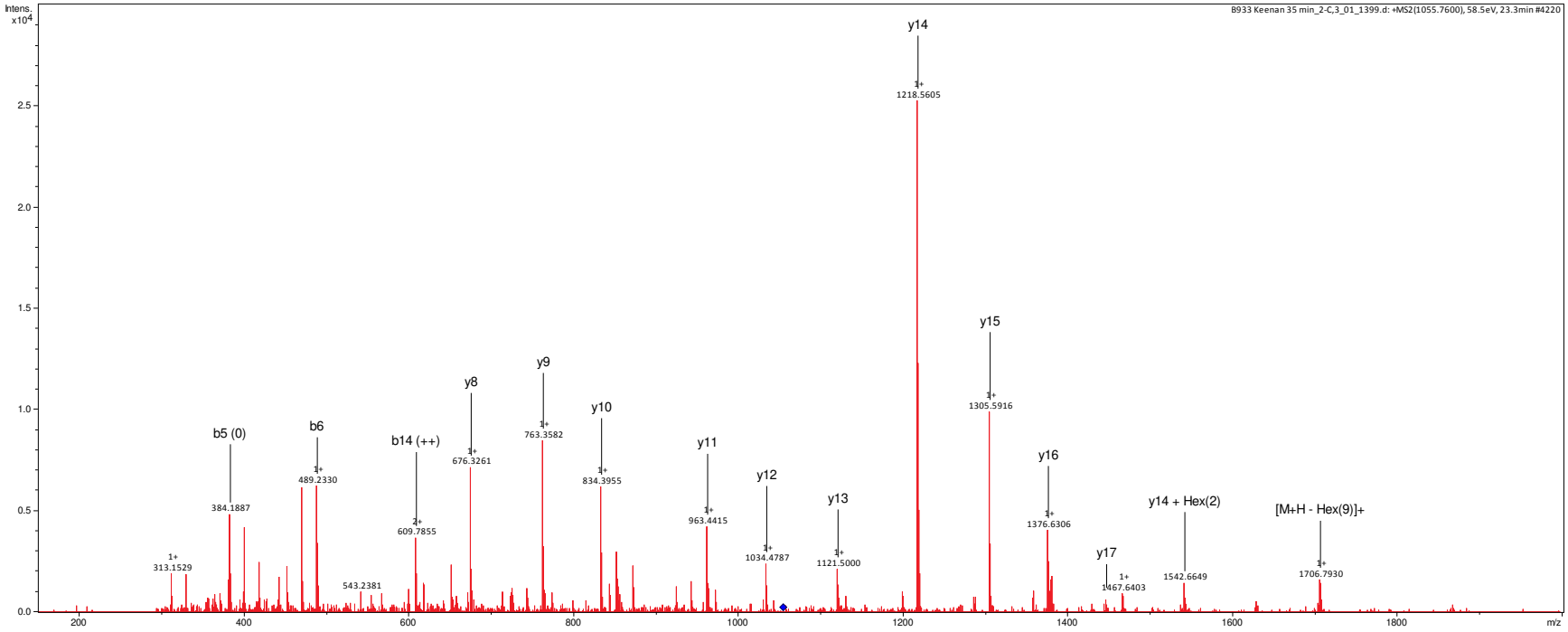

Time point	35 hr
SCO number	SCO4739
Precursor ion mass	982.063
Charge	3
Retention time	23.3
Hex on peptide	8
e-value	0.0045
Site allocated?	N

T E Q S A S A G G A E E S A P A G K

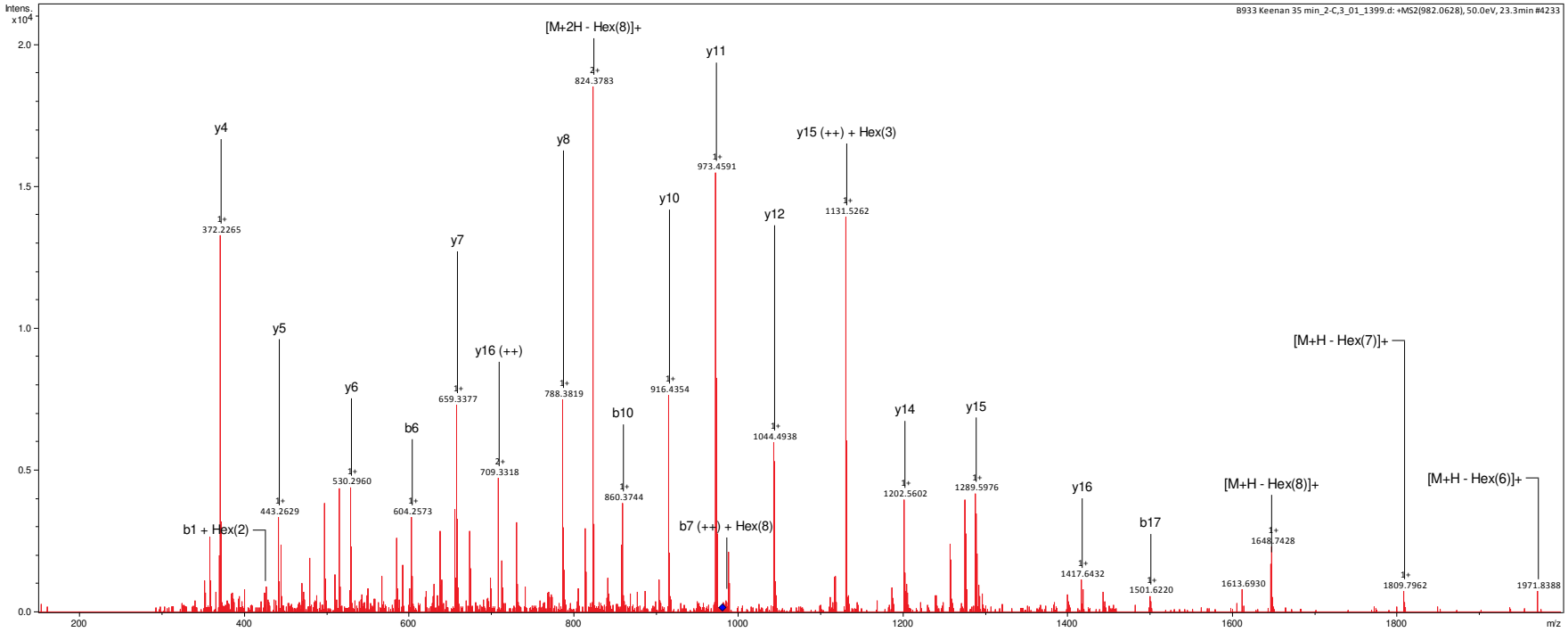

Time point	35 hr
SCO number	SCO4739
Precursor ion mass	1036.084
Charge	3
Retention time	23.1
Hex on peptide	9
e-value	0.0087
Site allocated?	N

T E Q S A S A G G A E E S A P A G K

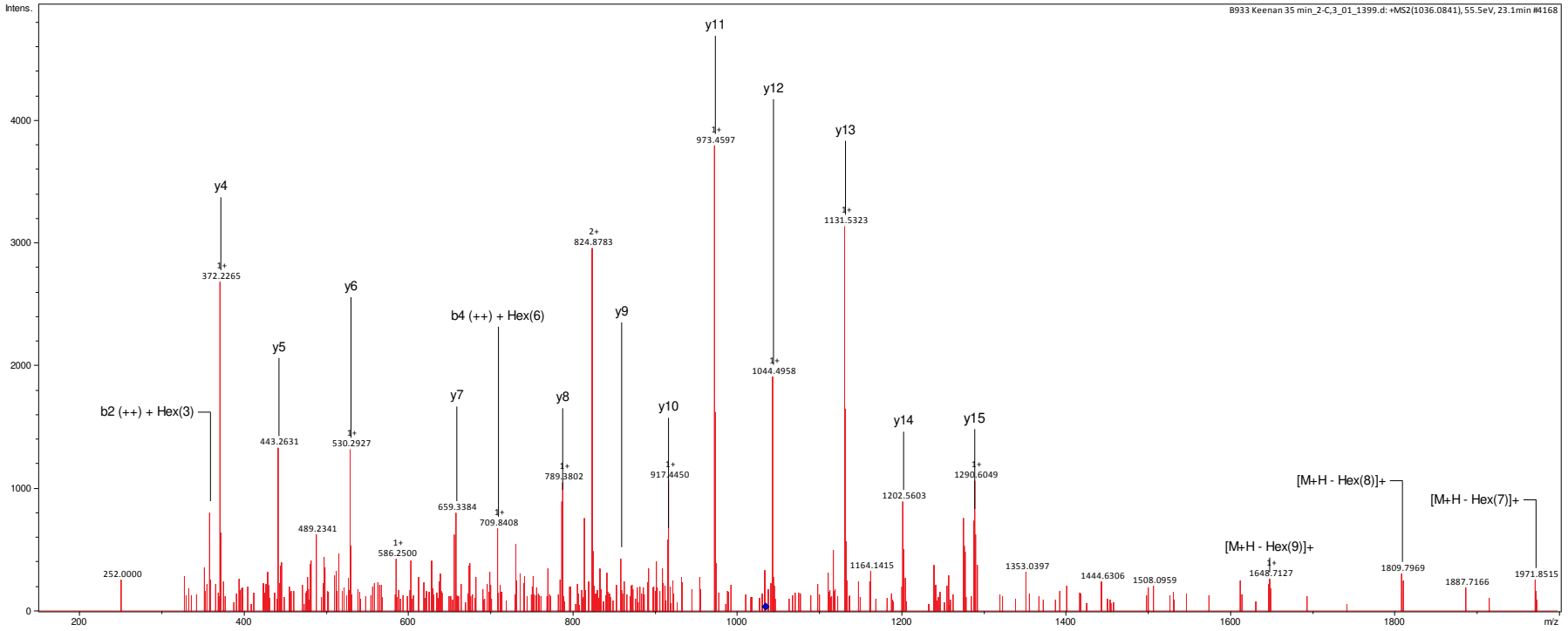

Time point	35 hr
SCO number	SCO1714
Precursor ion mass	723.318
Charge	2
Retention time	25.9
Hex on peptide	3
e-value	0.019
Site allocated?	N

T V T E P A A D R

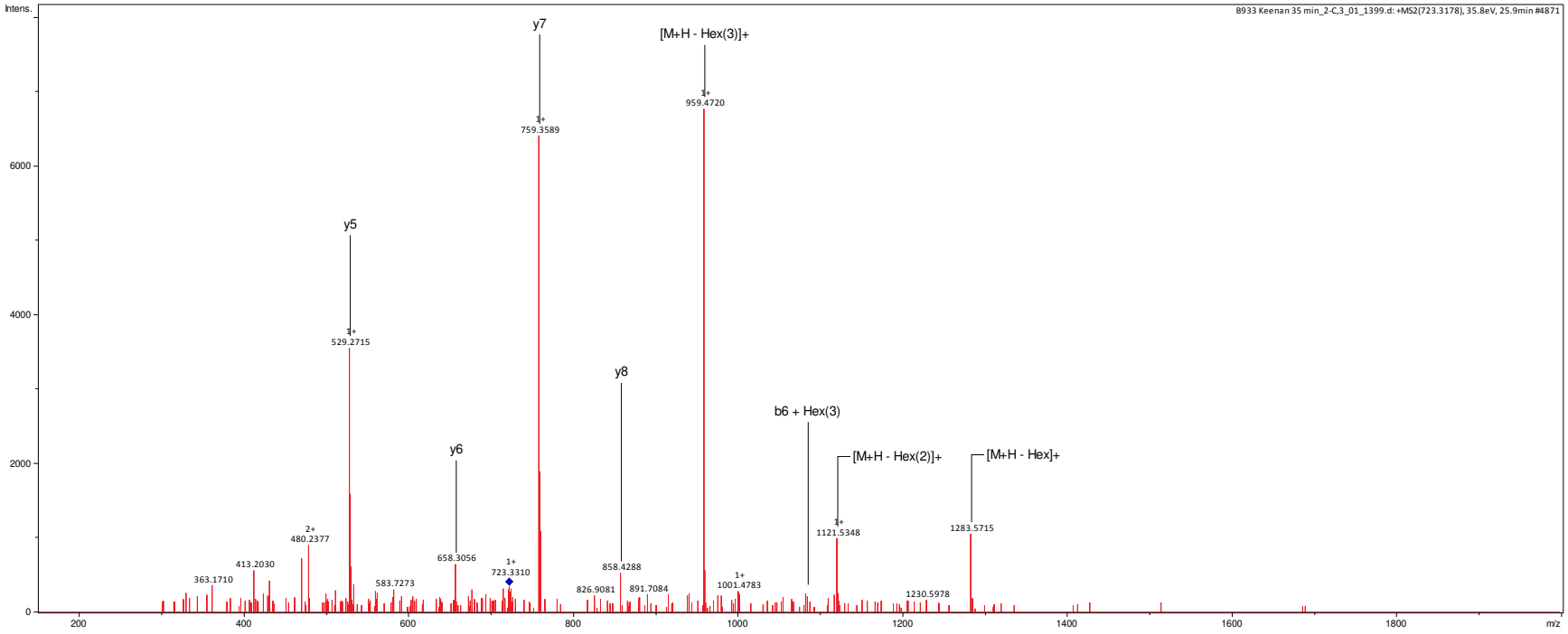

Time point	35 hr
SCO number	SCO3540
Precursor ion mass	910.927
Charge	2
Retention time	53.2
Hex on peptide	2
e-value	0.000055
Site allocated?	N

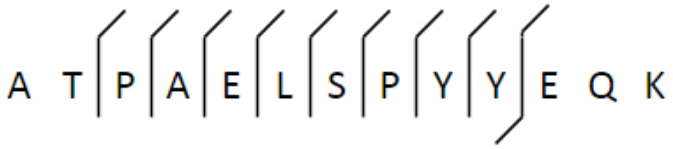

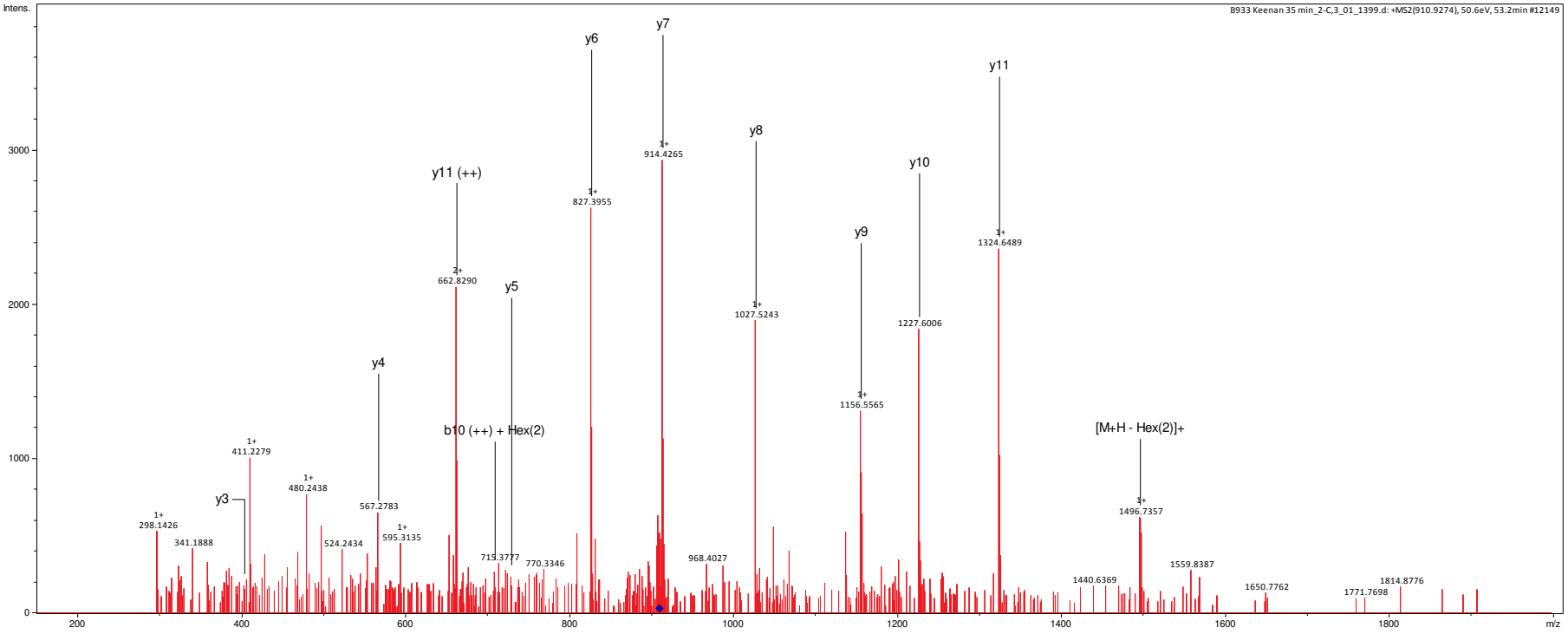

Time point	35 hr
SCO number	SCO0472
Precursor ion mass	1507.674
Charge	3
Retention time	136.5
Hex on peptide	9
e-value	0.00021
Site allocated?	N

G G G S T P S A T P A A S V Q D P L V A T F D G G L Y I L D G K

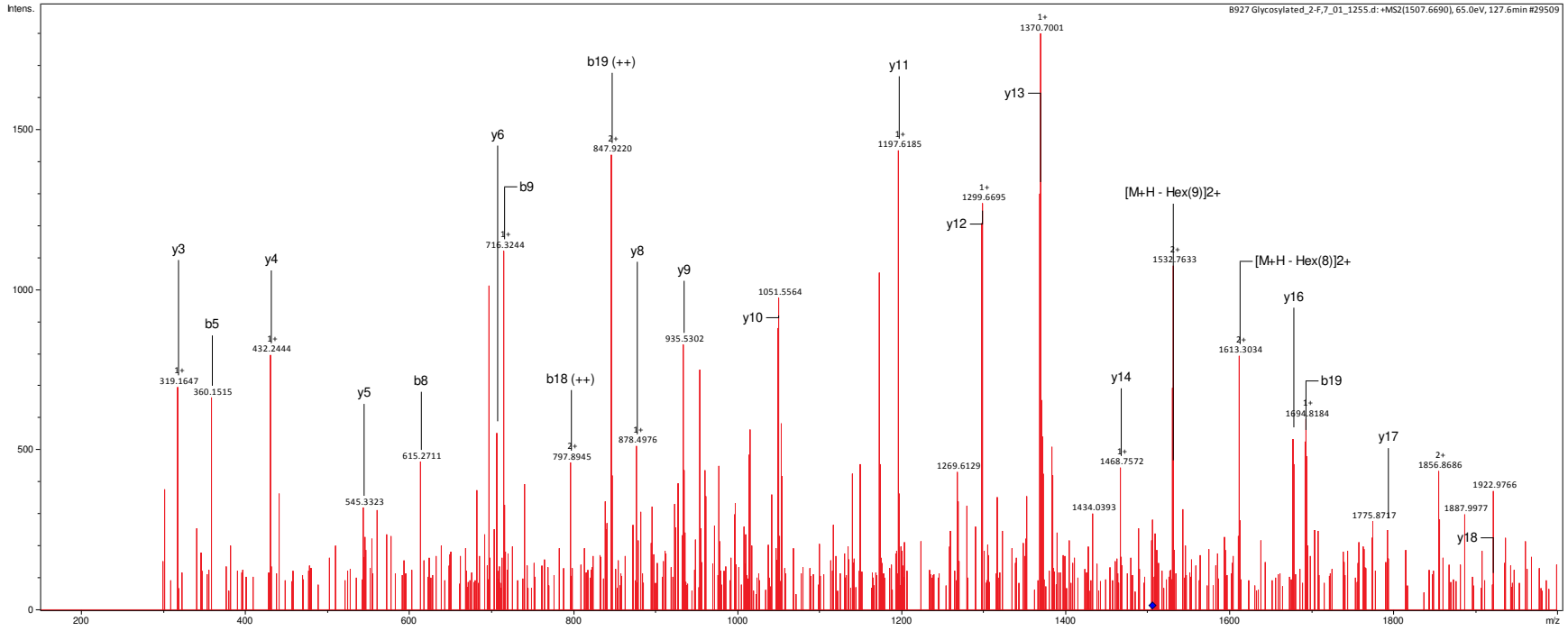

Time point	43 hr
SCO number	SCO5204
Precursor ion mass	1070.999
Charge	2
Retention time	73.2
Hex on peptide	1
e-value	0.012
Site allocated?	N

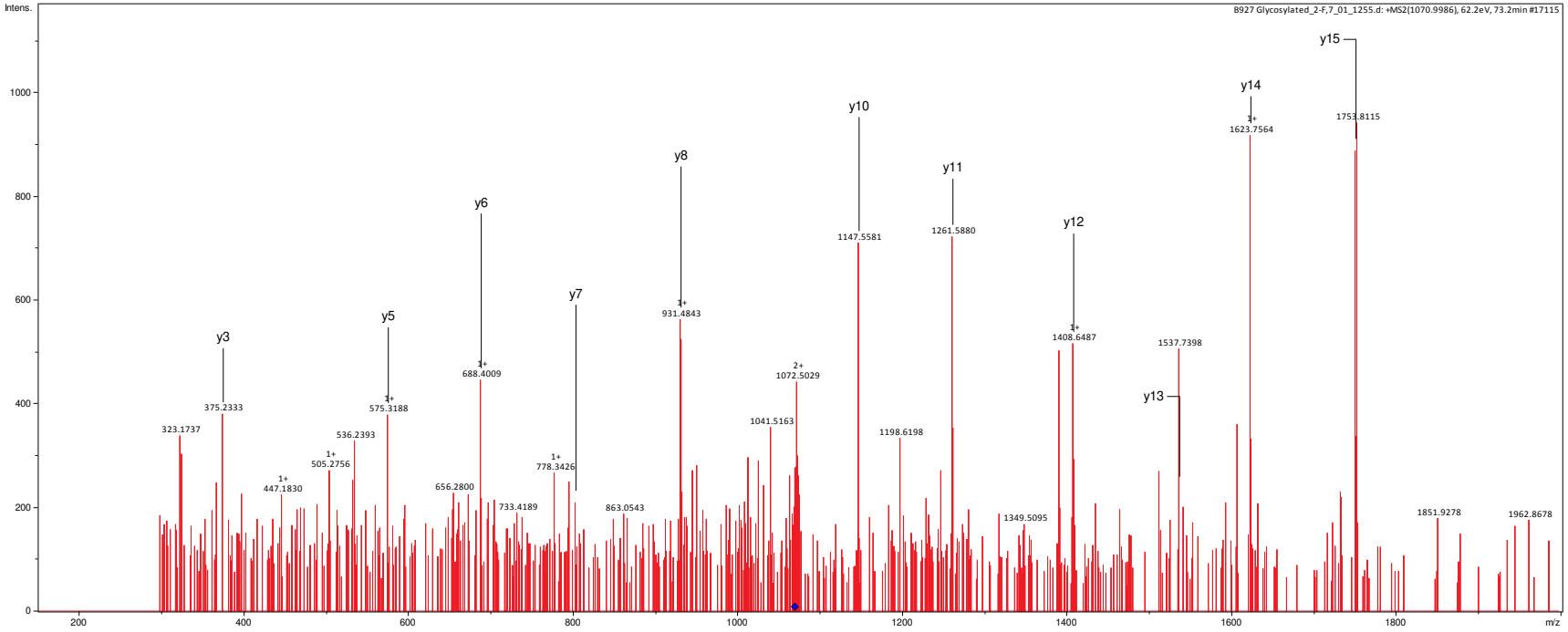

Time point	43 hr
SCO number	SCO4934
Precursor ion mass	853.373
Charge	2
Elution time	30.1
Hex on peptide	3
e-value	0.0036
Site allocated?	N

T S Q A E V D E A A A K

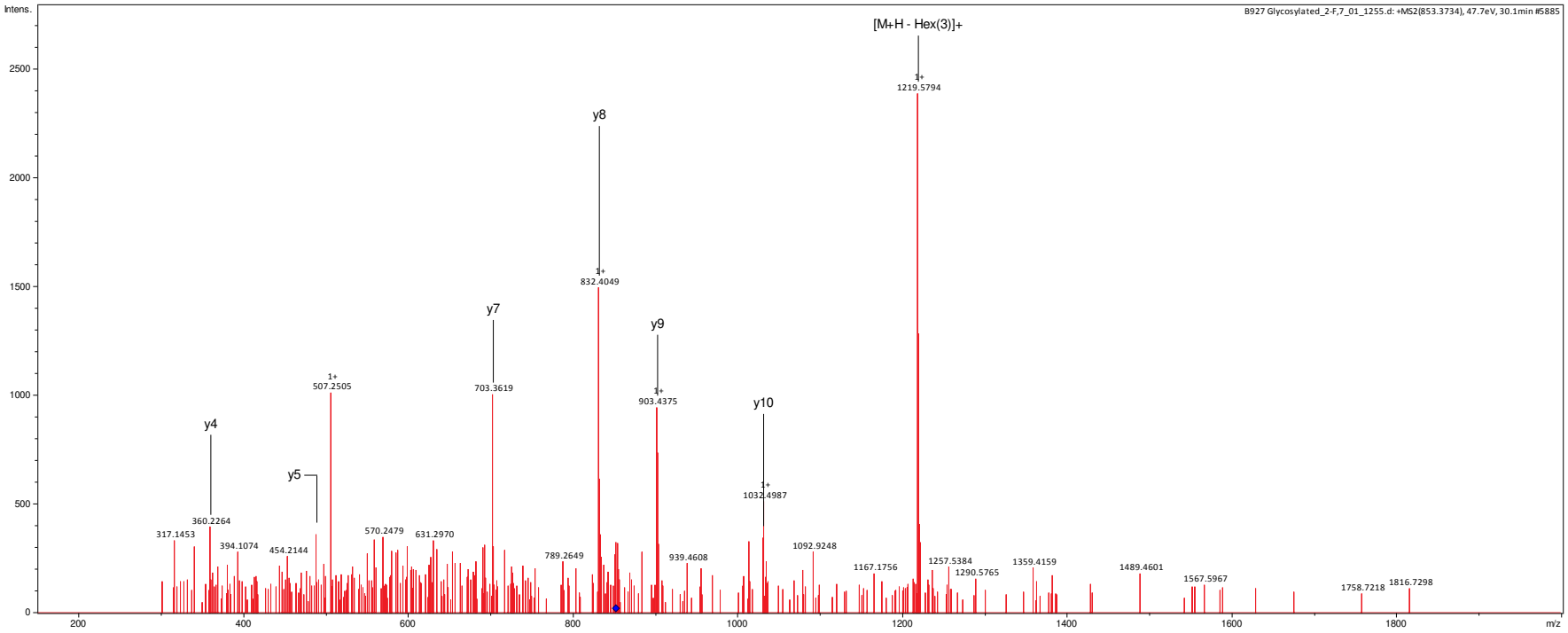

Time point	43 hr
SCO number	SCO3540
Precursor ion mass	910.921
Charge	2
Retention time	56.4
Hex on peptide	2
e-value	0.019
Site allocated?	T2

A T P A E L S P Y Y E Q K

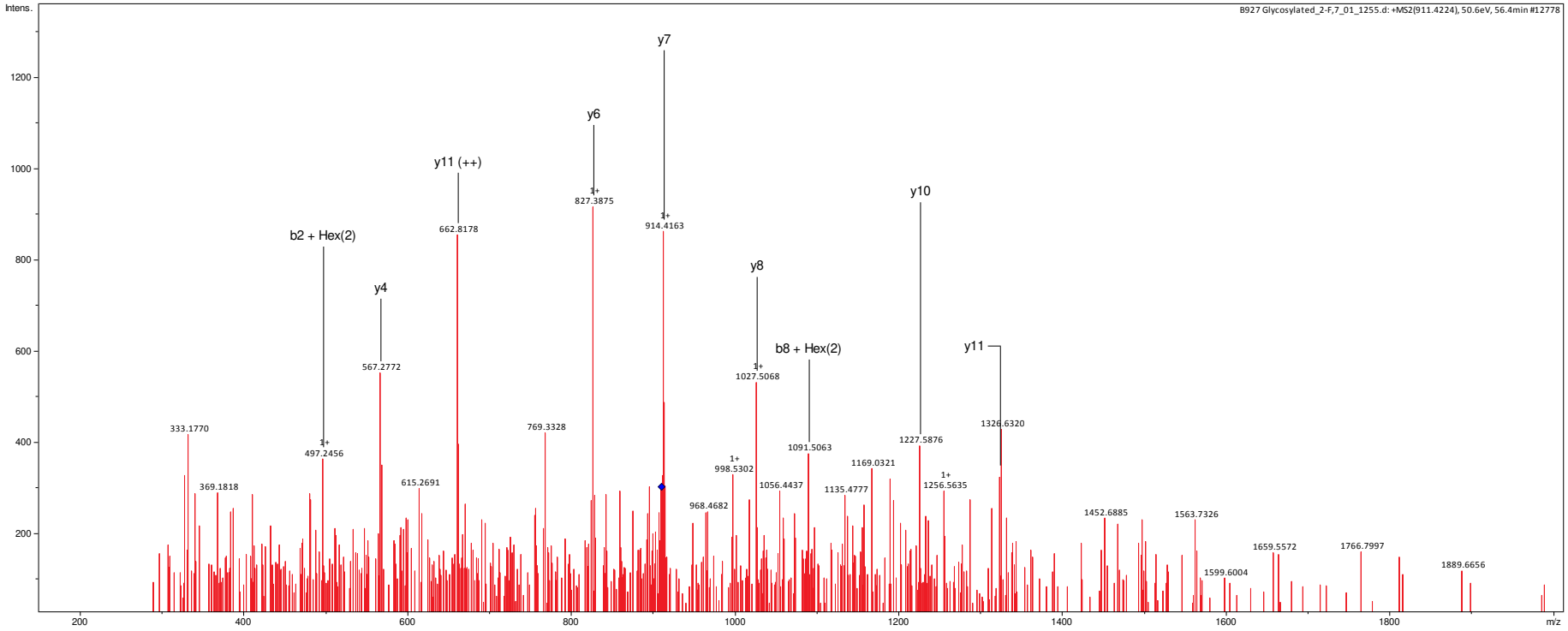

Time point	43 hr
SCO number	SCO3357
Precursor ion mass	992.761
Charge	3
Retention time	35.9
Hex on peptide	6
e-value	0.013
Site allocated?	N

D E G P A H A D A V G G A G S A S P A P A A K

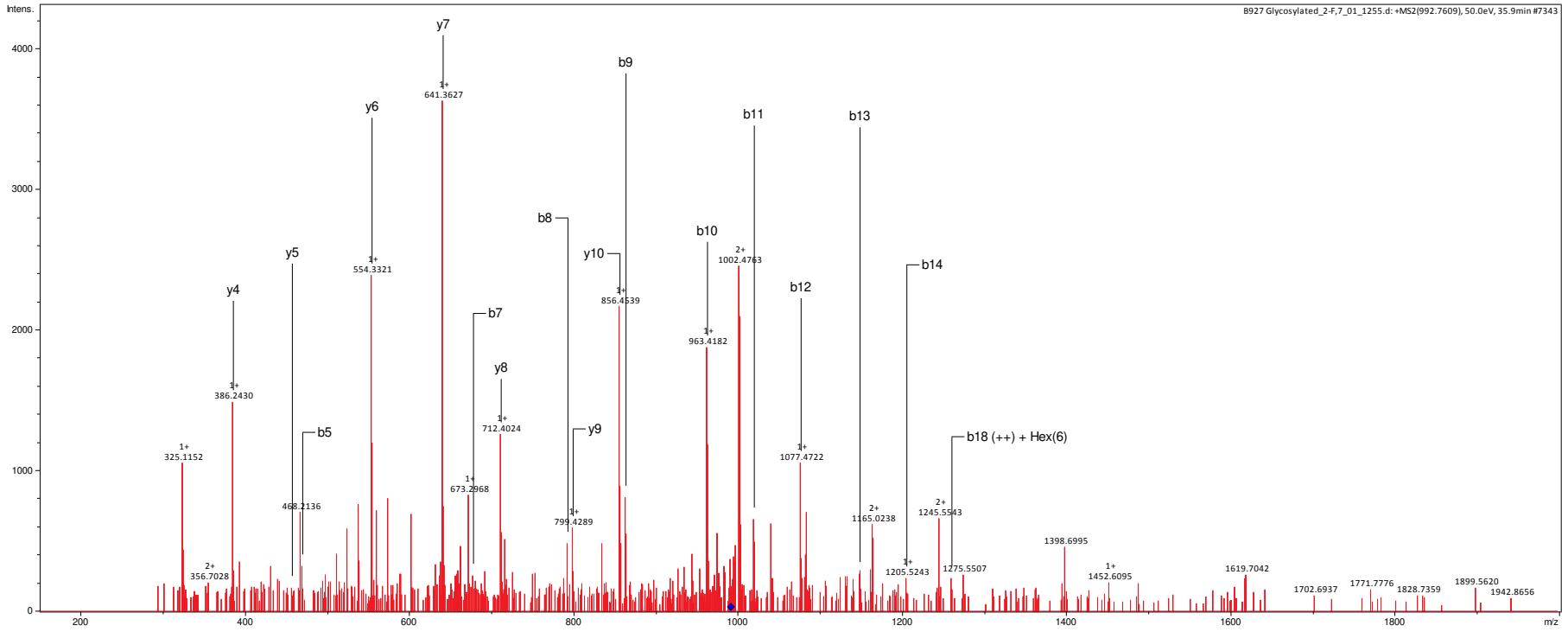

Time point	60 hr
SCO number	SCO4934
Precursor ion mass	772.350
Charge	2
Retention time	27.7
Hex on peptide	2
e-value	0.00019
Site allocated?	N

T S Q A E V D E A A A K

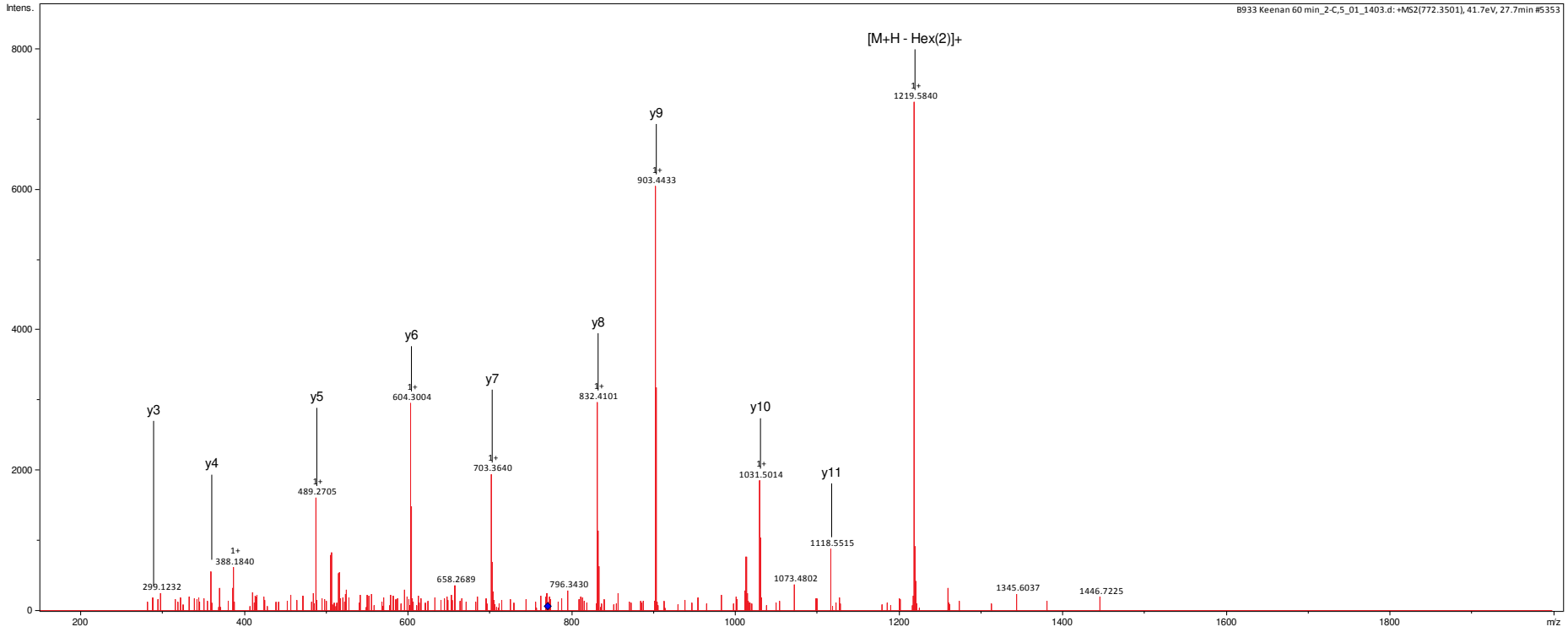

Time point	60 hr
SCO number	SCO4934
Precursor ion mass	853.375
Charge	2
Retention time	27.4
Hex on peptide	3
e-value	0.024
Site allocated?	N

T S Q A E V D E A A A K

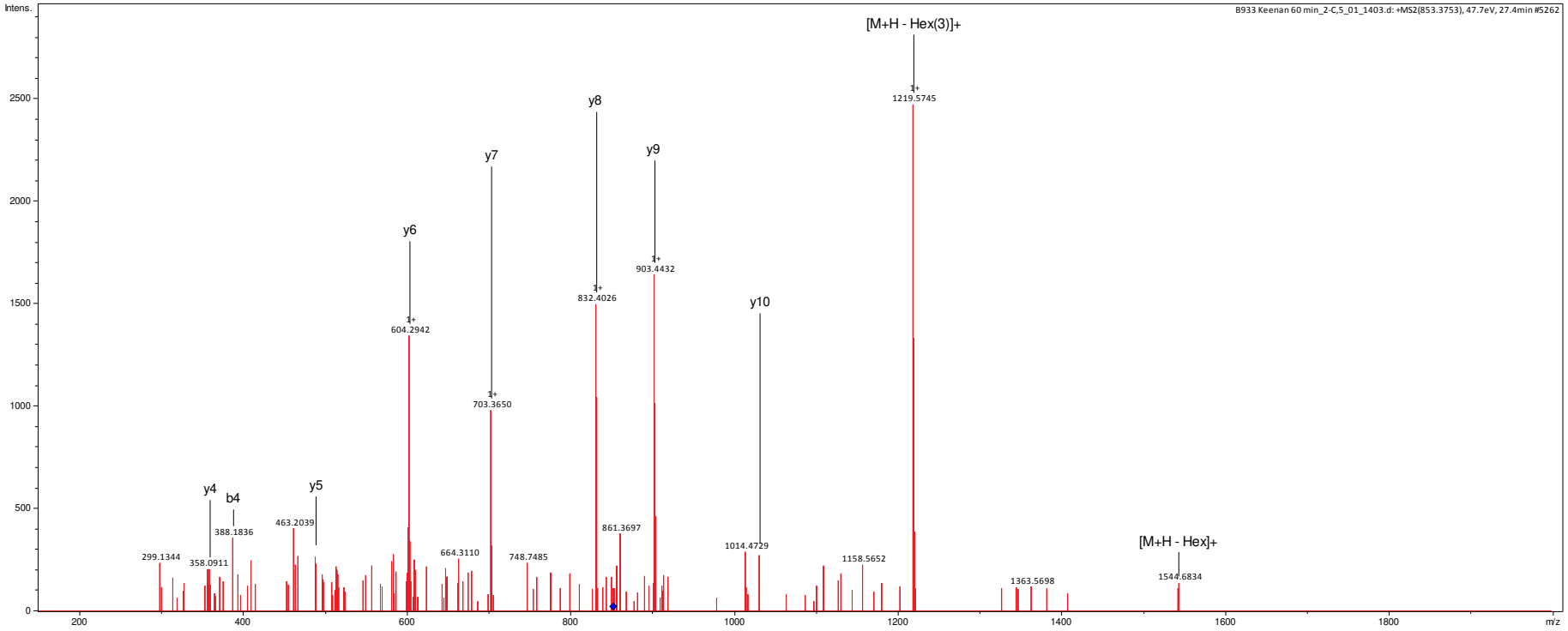

Time point	60 hr
SCO number	SCO4141
Precursor ion mass	562.279
Charge	3
Retention time	31.2
Hex on peptide	1
e-value	0.04
Site allocated?	N

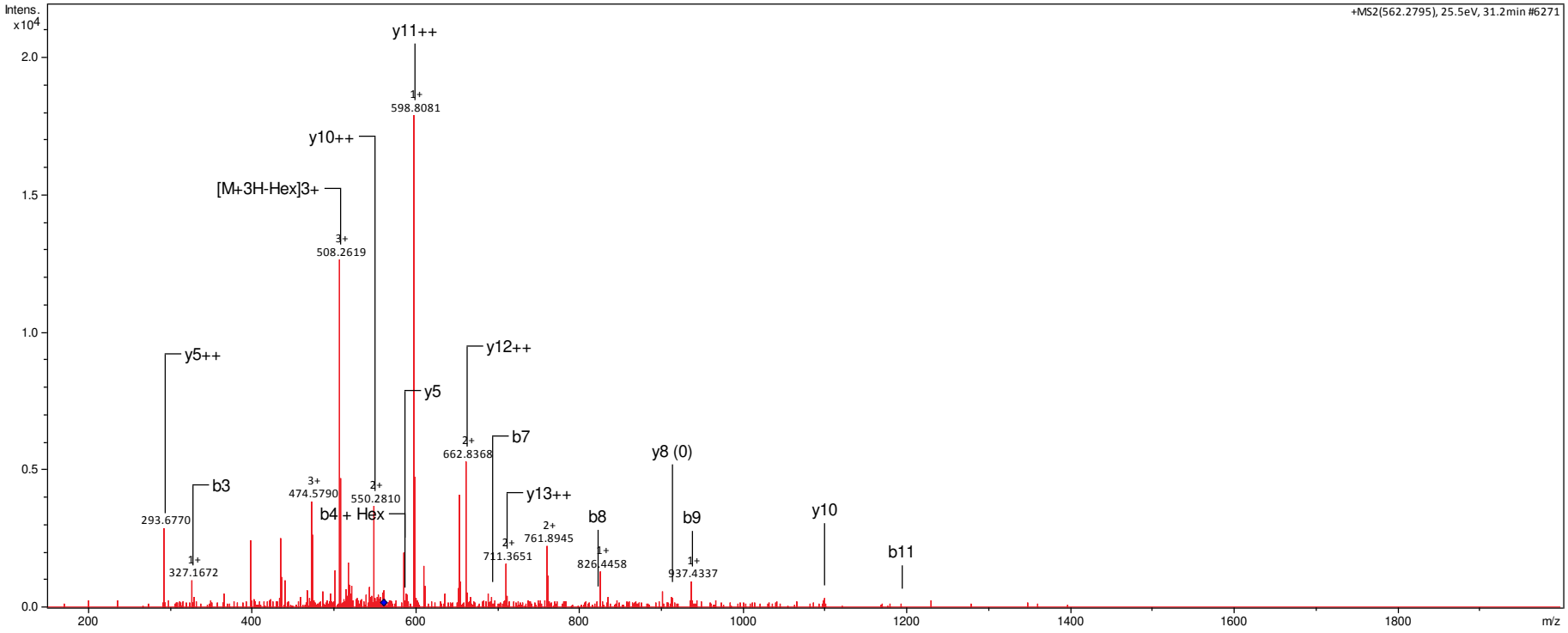

Time point	60 hr
SCO number	SCO4905
Precursor ion mass	973.935
Charge	2
Retention time	46.7
Hex on peptide	3
e-value	0.0091
Site allocated?	N

A T E V P T D Y G P A P S R

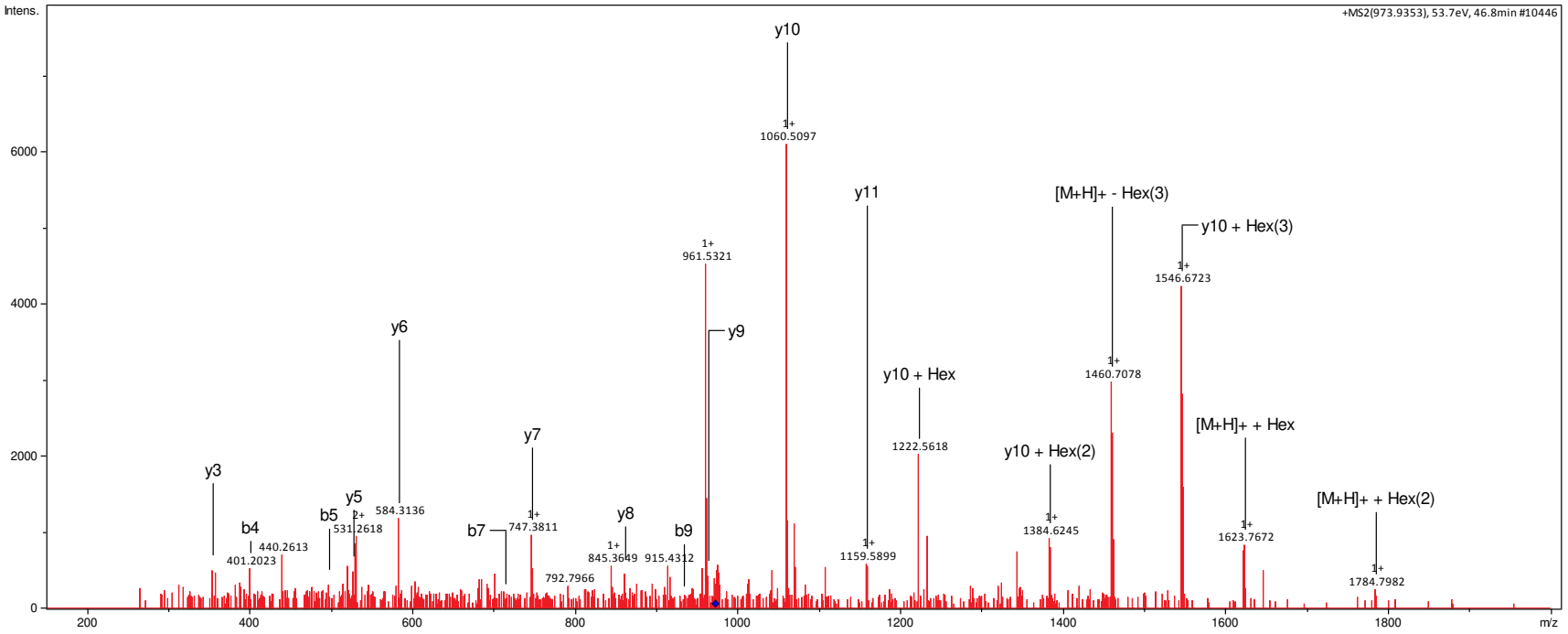

Time point	60 hr
SCO number	SCO4739
Precursor ion mass	982.063
Charge	3
Retention time	23.8
Hex on peptide	8
e-value	0.0041
Site allocated?	N

T E Q S A S A G G A E E S A P A G K

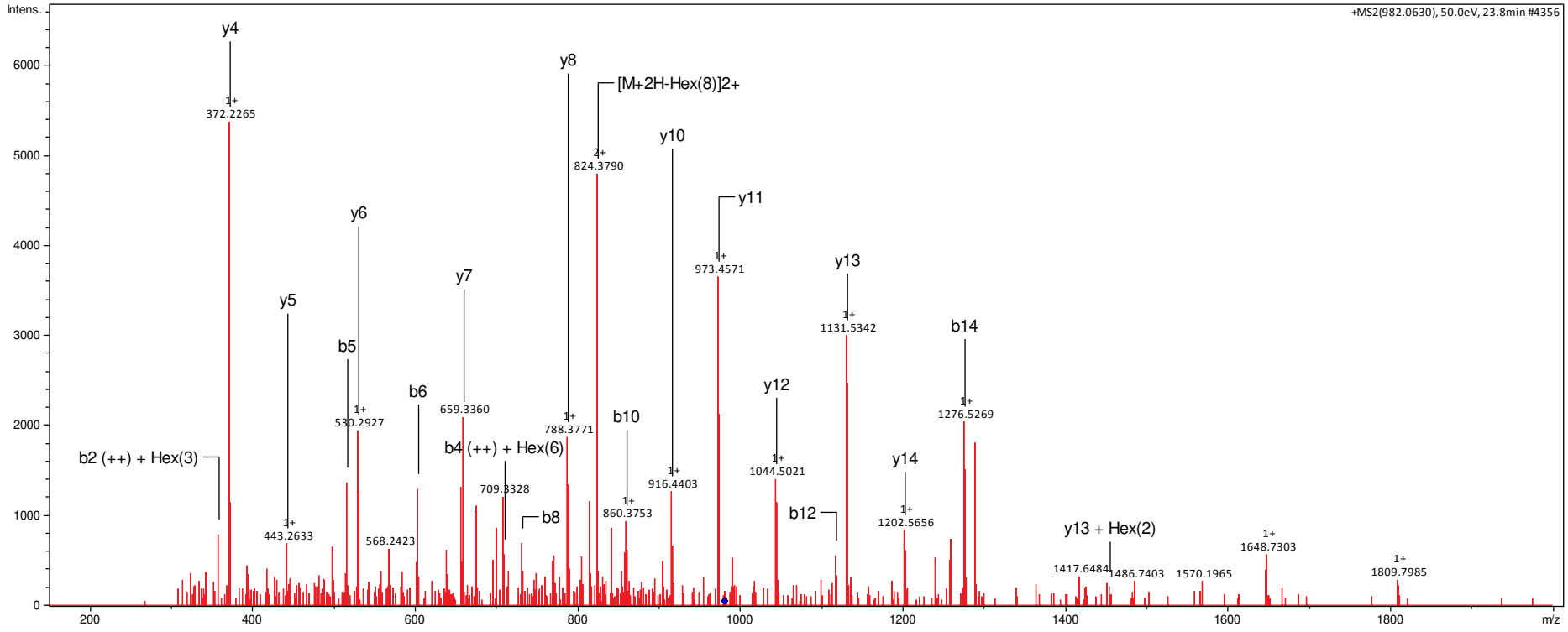

Time point	20 hr
SCO number	SCO4739
Precursor ion mass	1067.459
Charge	2
Retention time	25.7
Hex on peptide	3
e-value	1.10E-08
Site allocated?	N

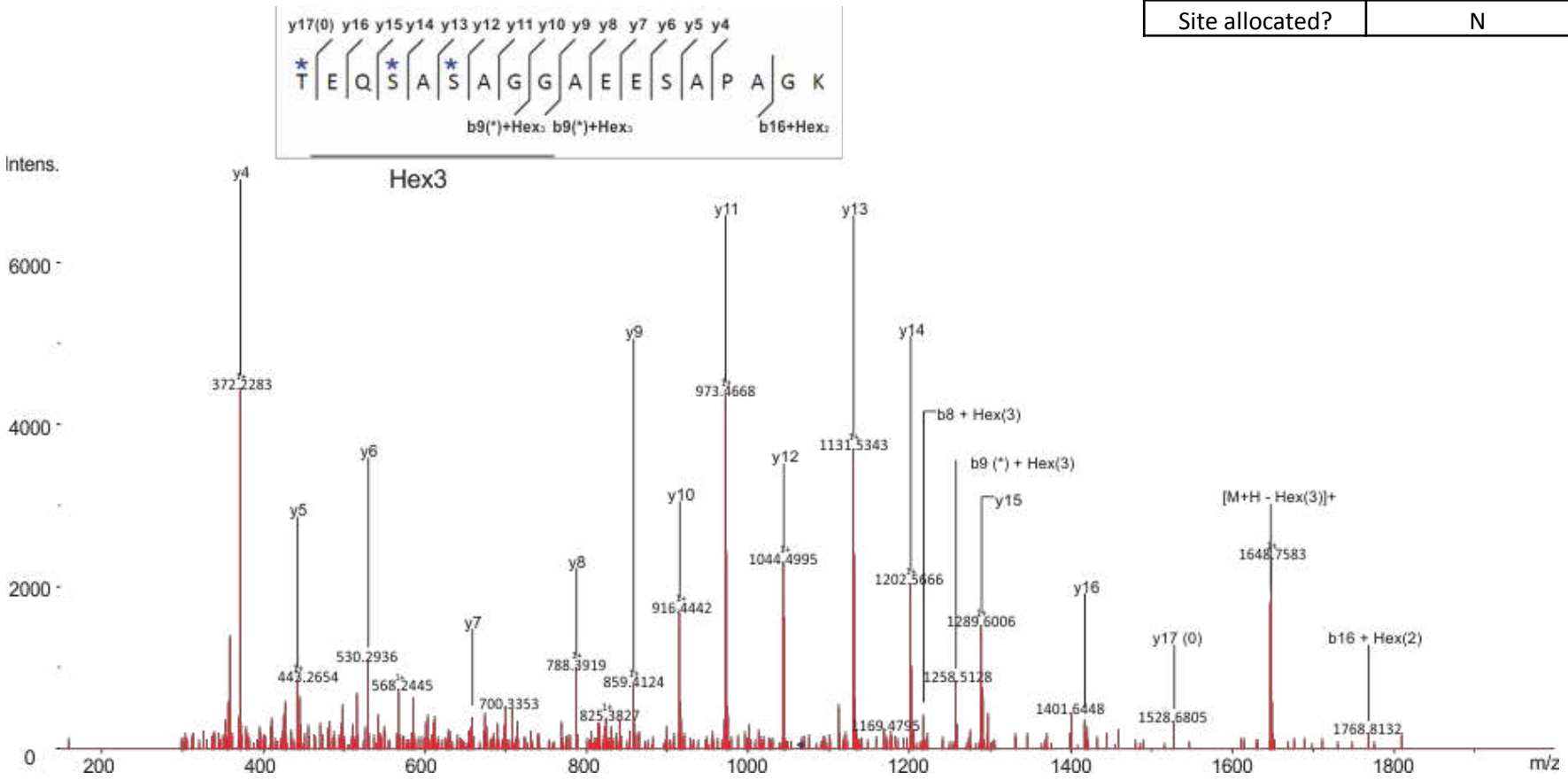

Time point	20 hr
SCO number	SCO4905
Precursor ion mass	865.783
Charge	3
Retention time	122.5
Hex on peptide	1
e-value	1.90E-04
Site allocated?	N

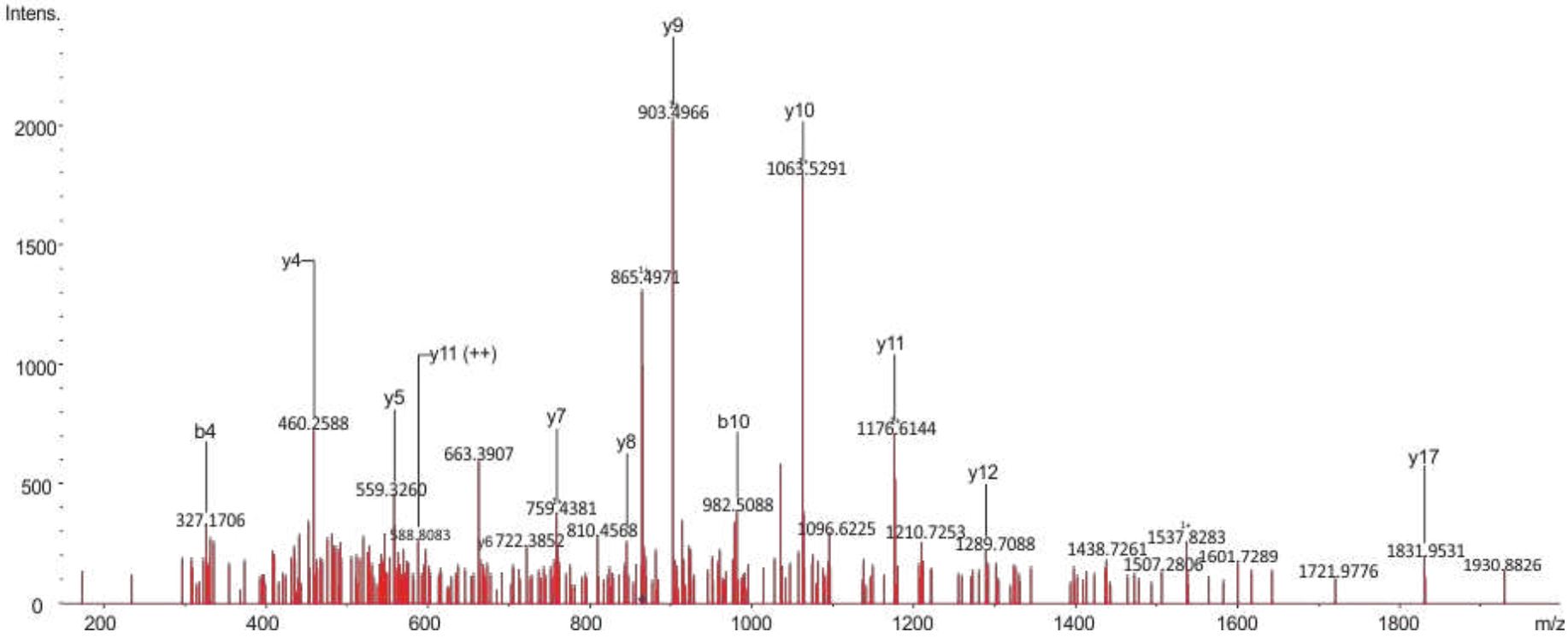

Spectra generated using HCD and ETD fragmentation techniques on the Thermo Orbitrap Fusion Tribrid mass spectrometer.

Key:

Ion Type	Description
c(++)	doubly charged series
y(++)	doubly charged series
z(+2)	z + 2
z(++)	doubly charged series
z(+2++)	z+2 doubly charged series

SCO Number	SCO4142
Precursor m/z	750.712
Charge	3
Retention time	91.5
Scan number	24203
Hex on peptide	1
e-value	0.0028
Site allocated?	Ser251
Method	ETD_IT

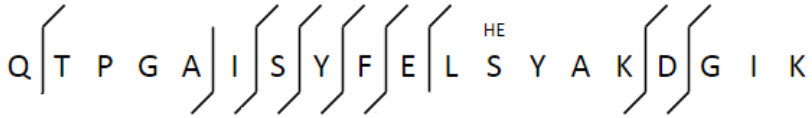

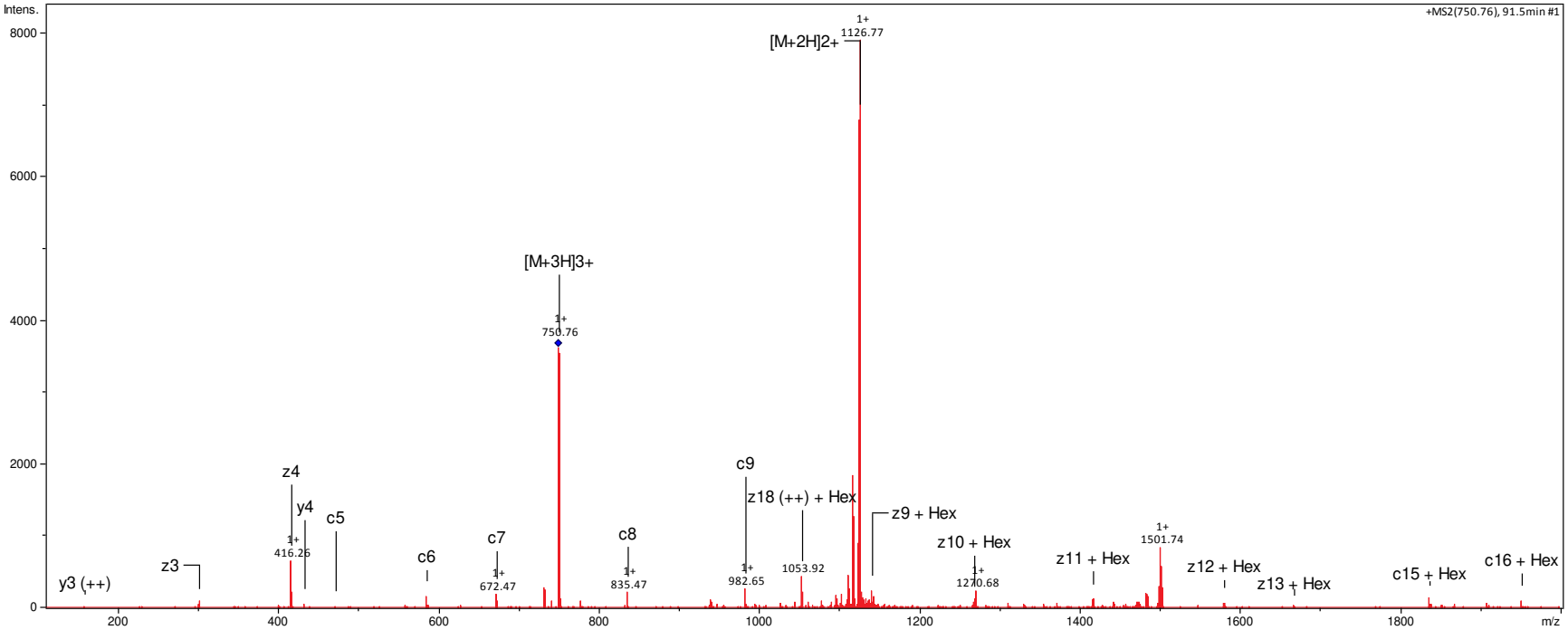

SCO Number	SCO3046
Precursor m/z	909.820
Charge	3
Retention time	89.4
Scan number	22874
Hex on peptide	2
e-value	0.0000031
Site allocated?	Thr47
Method	HCD_IT, ETD_OT

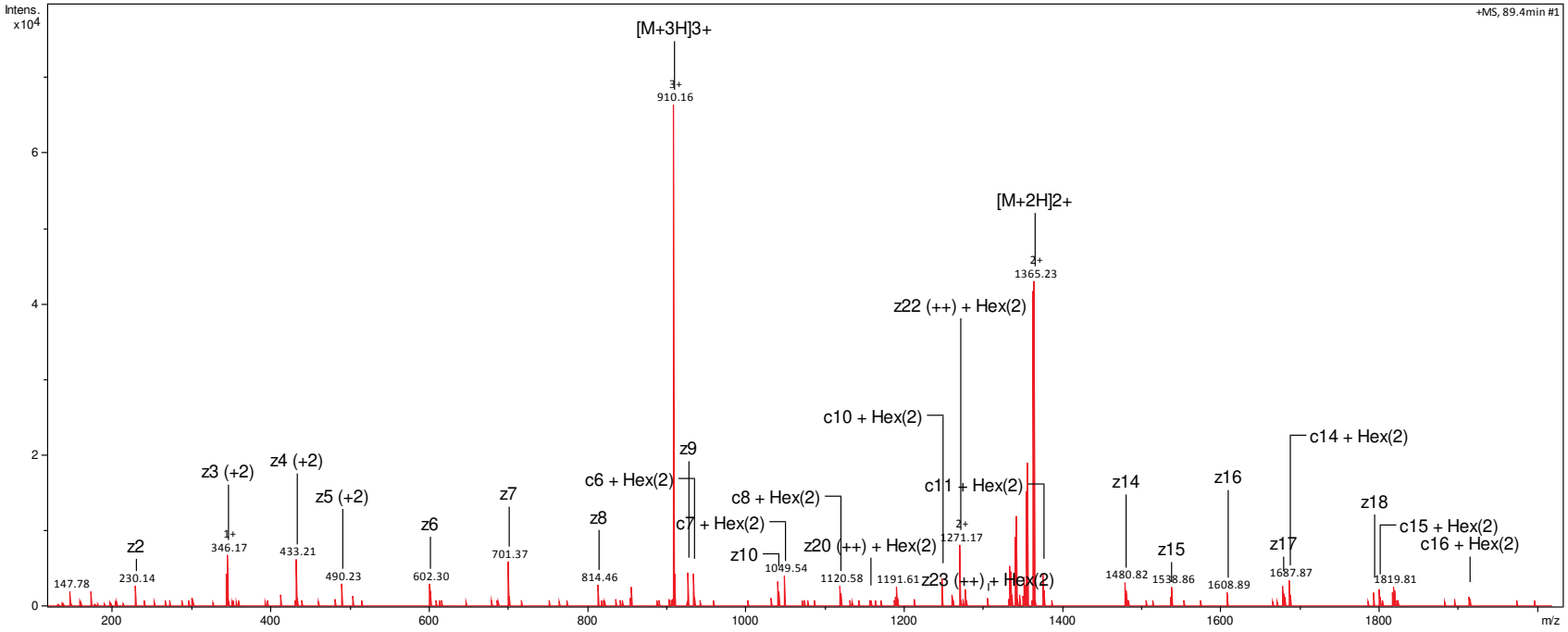

SCO Number	SCO4968
Precursor m/z	811.392
Charge	3
Retention time	31.4
Scan number	6232
Hex on peptide	1
e-value	0.0000091
Site allocated?	Ser65
Method	ETD_OT

V D F K E P A E Q D A HE S A G P E A K P Q R

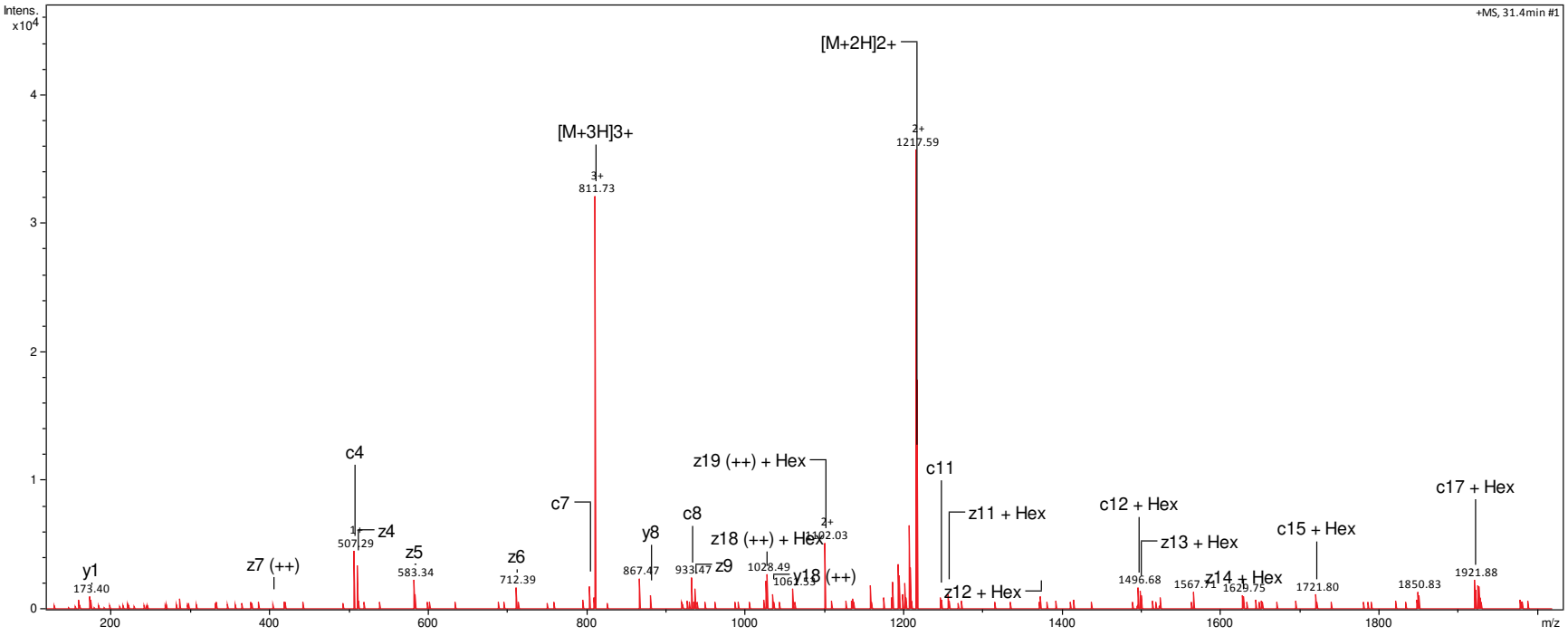

SCO Number	SCO3353
Precursor m/z	626.960
Charge	3
Retention time	17.5
Scan number	2027
Hex on peptide	2
e-value	0.000016
Site allocated?	Thr94
Method	HCD_IT, ETD_IT, ETD_OT

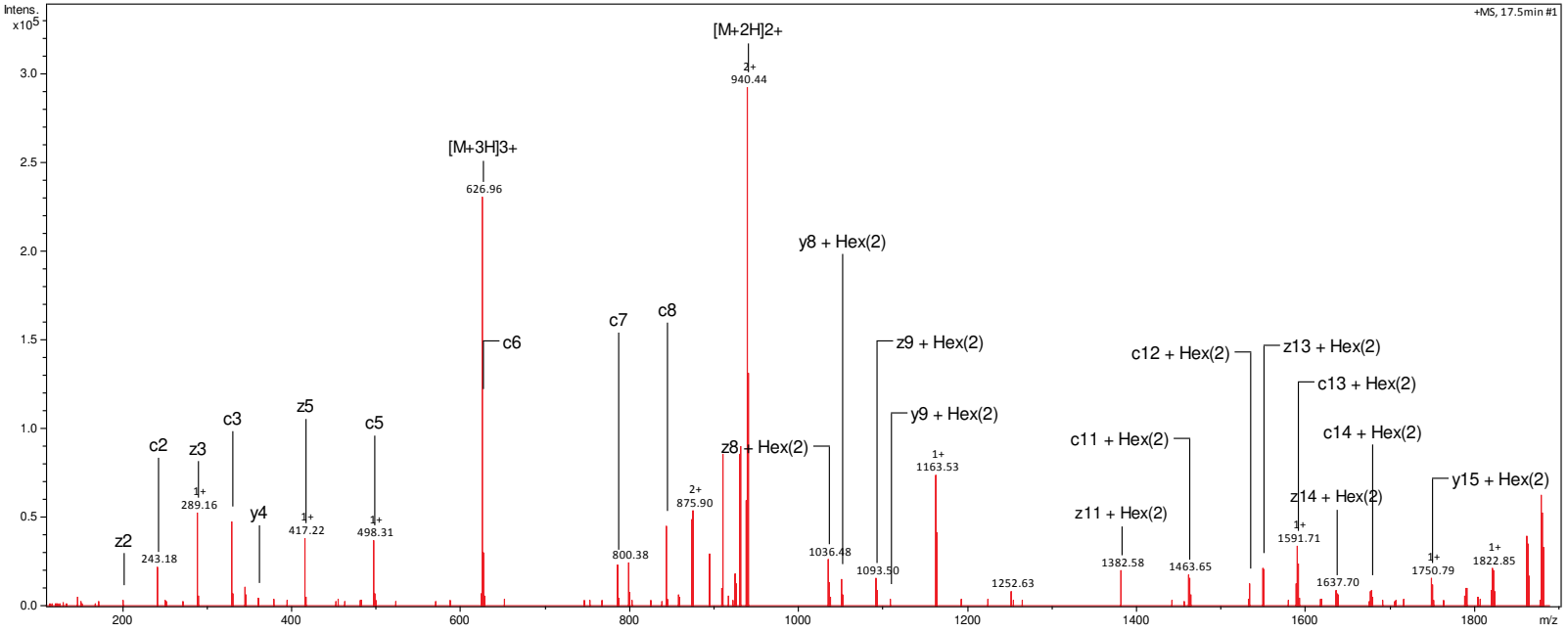

SCO Number	SCO3353
Precursor m/z	680.978
Charge	3
Retention time	17.3
Scan number	4050
Hex on peptide	3
e-value	0.00071
Site allocated?	Thr94
Method	HCD_IT, ETD_IT, ETD_OT

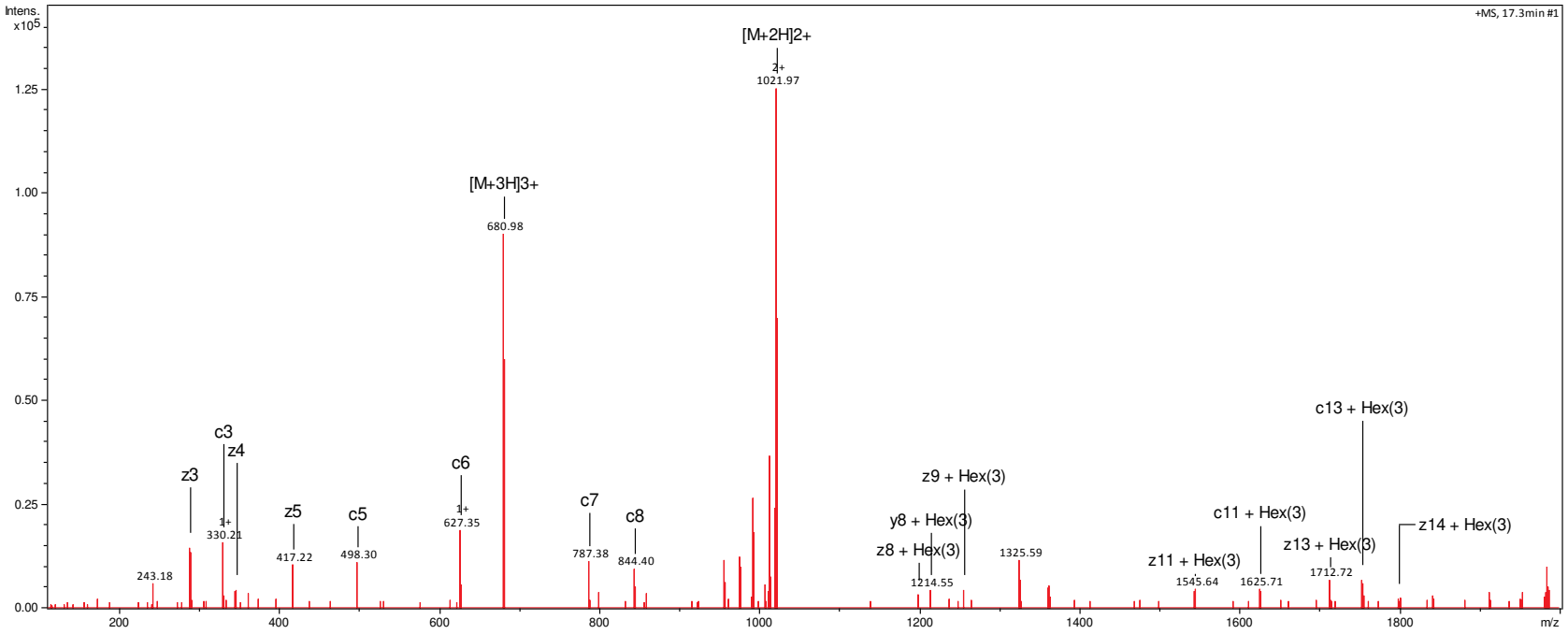

SCO Number	SCO4141
Precursor m/z	562.277
Charge	3
Retention time	18.7
Scan number	2571
Hex on peptide	1
e-value	0.00021
Site allocated?	Thr15
Method	HCD_IT, ETD_IT, ETD_OT

HE

T P Q P P A T E D T R P G R

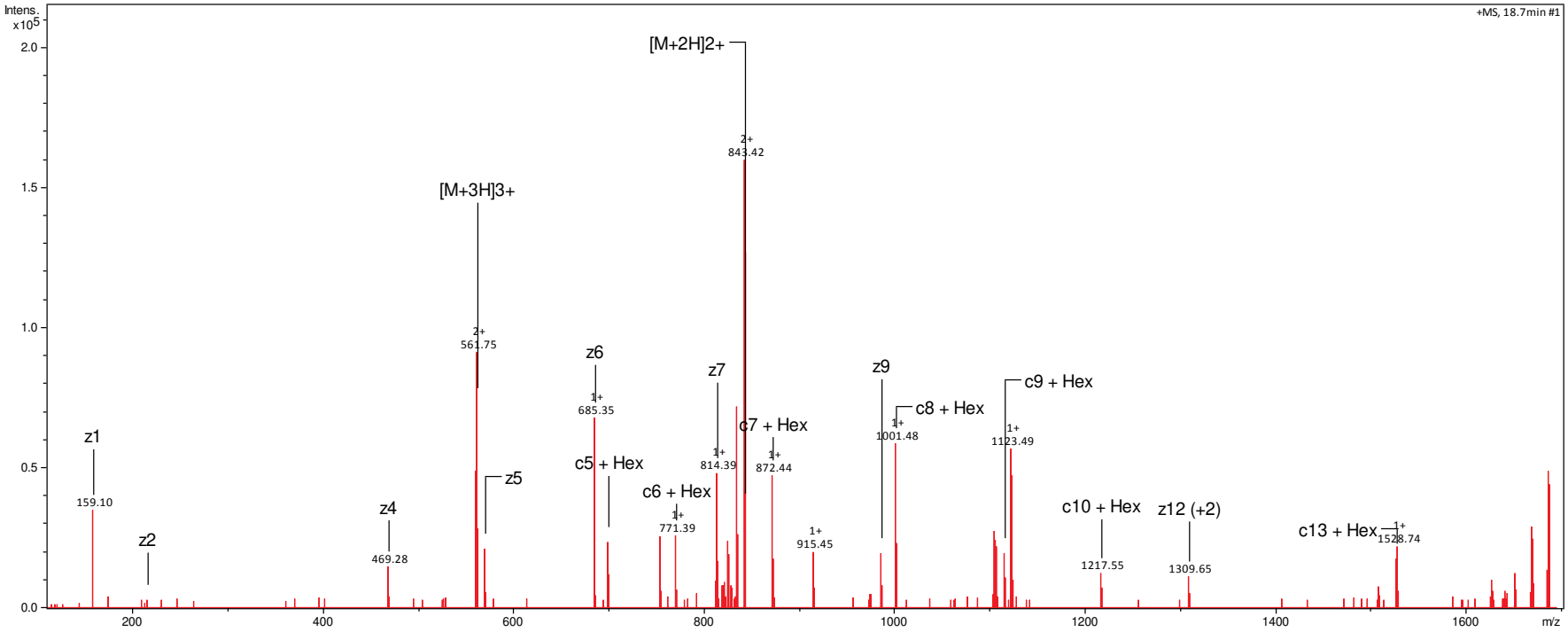

SCO Number	SCO5751
Precursor m/z	695.938
Charge	5
Retention time	26.8
Scan number	4858
Hex on peptide	6
e-value	0.00044
Site allocated?	Ser193, Ser195
Method	ETD_OT

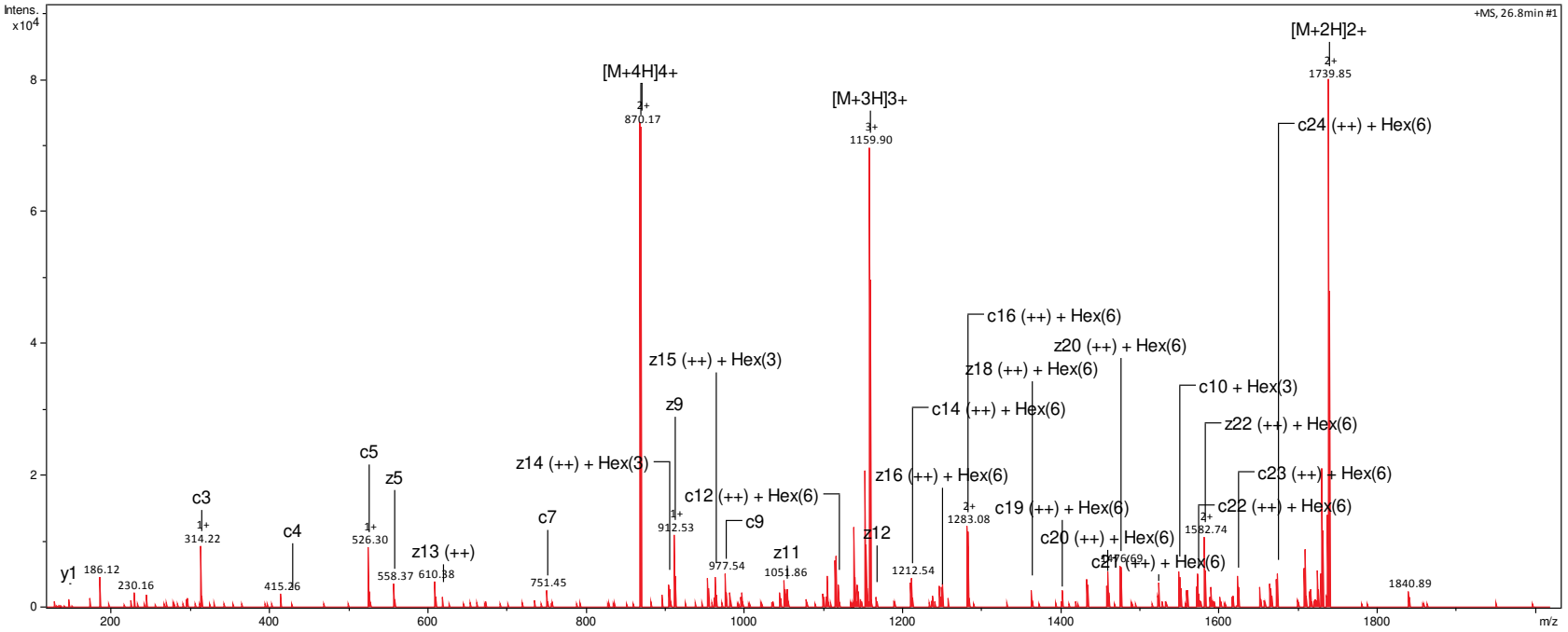

SCO Number	SCO3357
Precursor m/z	938.741
Charge	3
Retention time	20.4
Scan number	2972
Hex on peptide	6
e-value	0.00076
Site allocated?	Ser37, Ser39
Method	ETD_OT

D E G P A H A D A V G G A G S(HE) A S(HE) P A P A A K

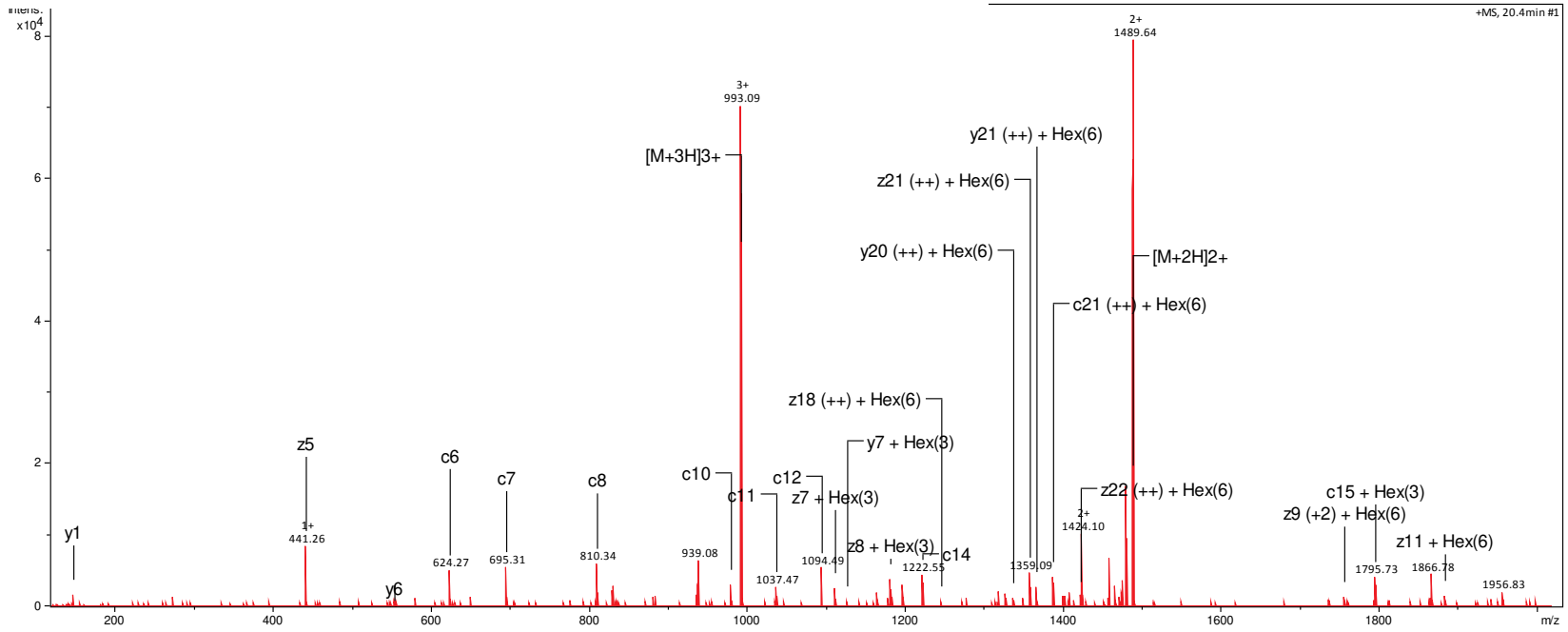

SCO Number	SCO5776
Precursor m/z	609.072
Charge	4
Retention time	94.1
Scan number	60208
Hex on peptide	1
e-value	0.0013
Site allocated?	Ser114
Method	HCD_IT

HE

S E K | V D F A | G P Y L L A H Q D V L | I R

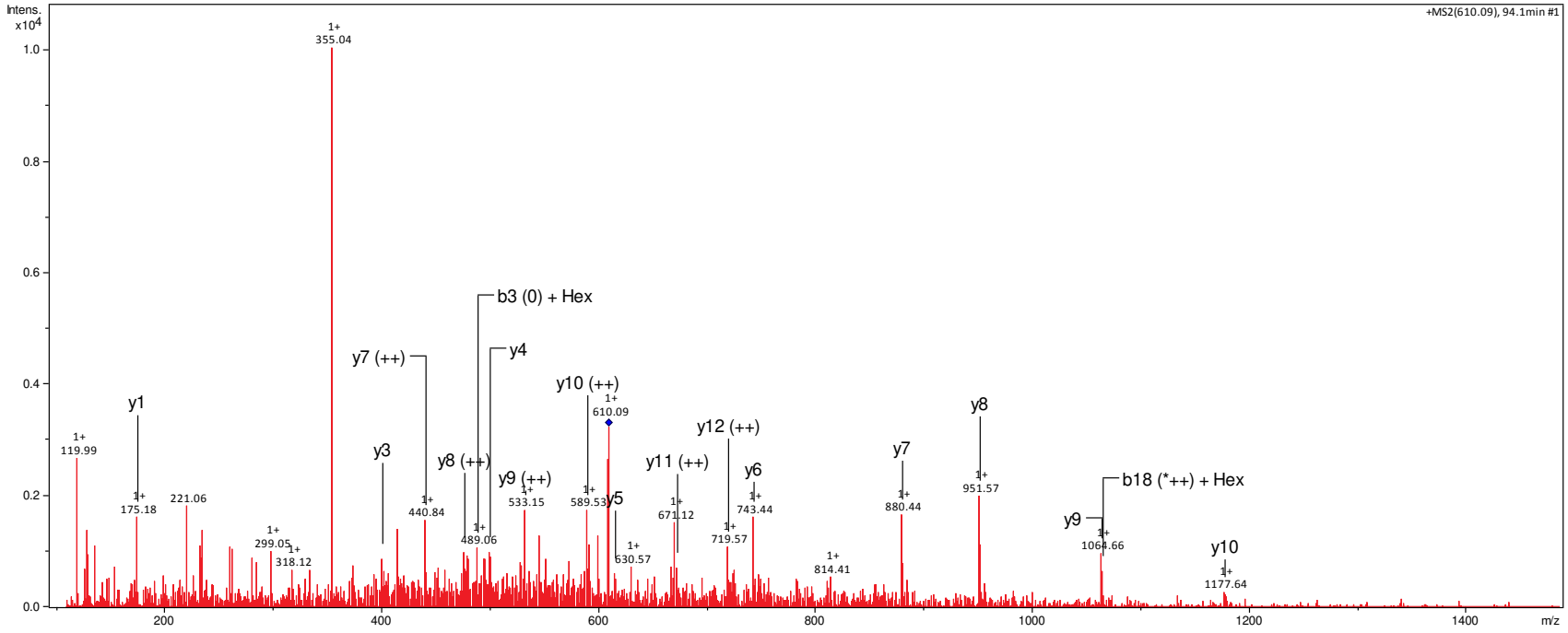

SCO Number	SCO2838
Precursor m/z	683.341
Charge	2
Retention time	18.5
Scan number	2576
Hex on peptide	2
e-value	0.002
Site allocated?	Thr38
Method	ETD_IT

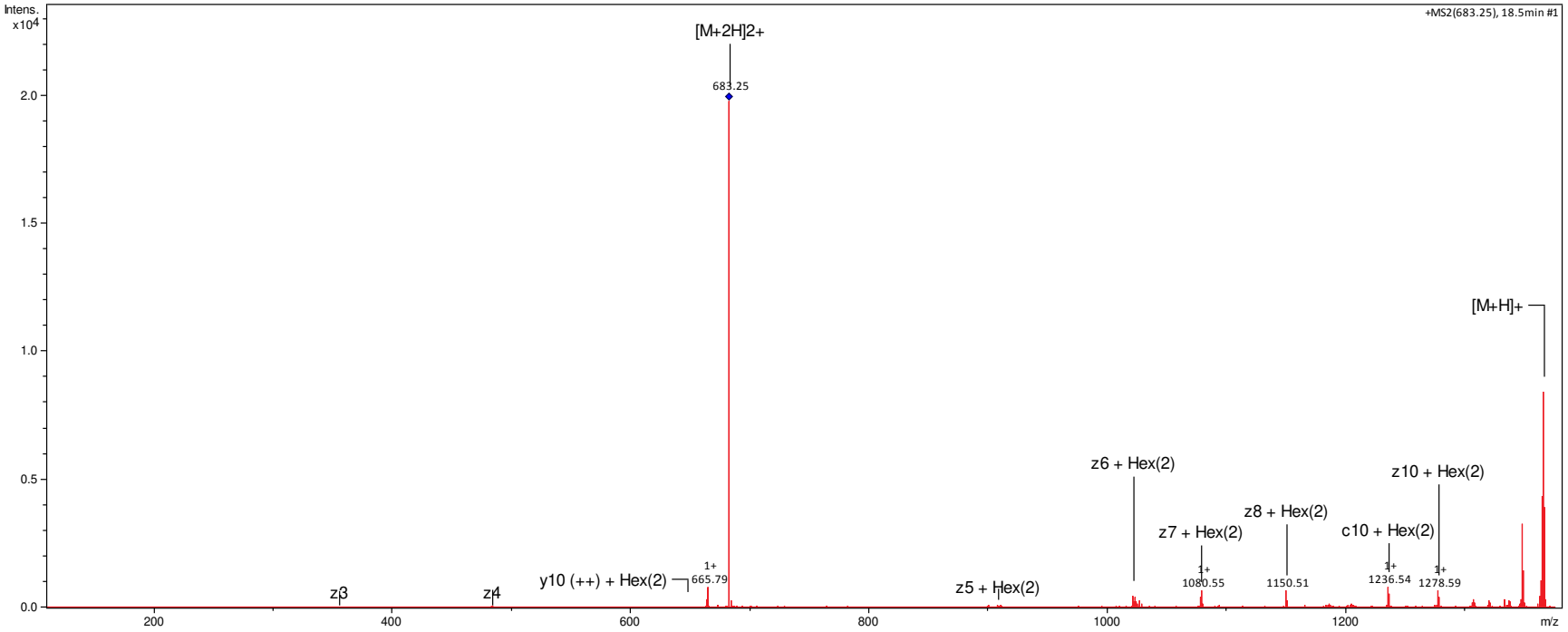

SCO Number	SCO4307
Precursor m/z	404.545
Charge	3
Retention time	32.5
Scan number	6751
Hex on peptide	1
e-value	0.0006
Site allocated?	Thr83
Method	ETD_IT

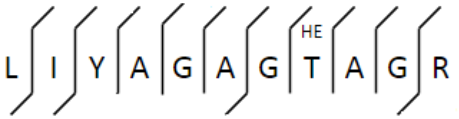

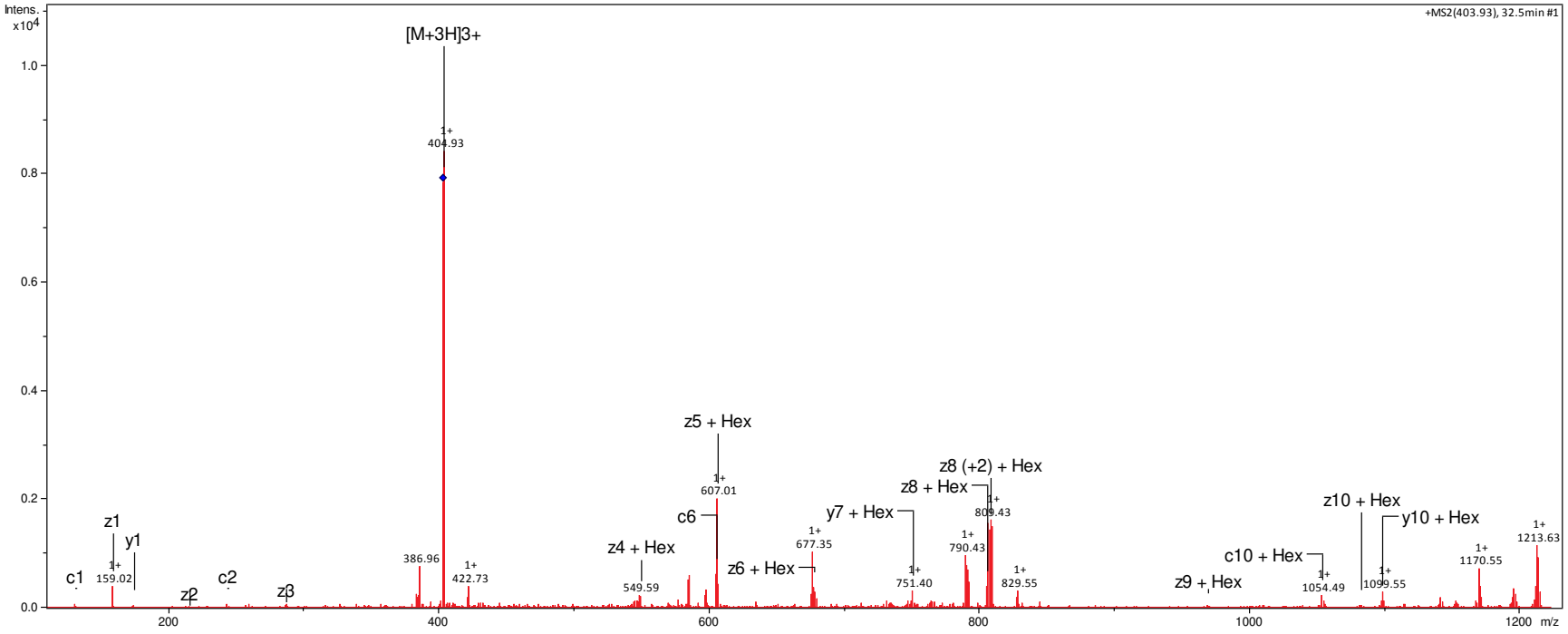

SCO Number	SCO4142
Precursor m/z	379.541
Charge	3
Retention time	23.9
Scan number	3598
Hex on peptide	1
e-value	0.0081
Site allocated?	Thr259
Method	ETD_OT

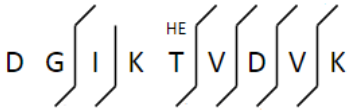

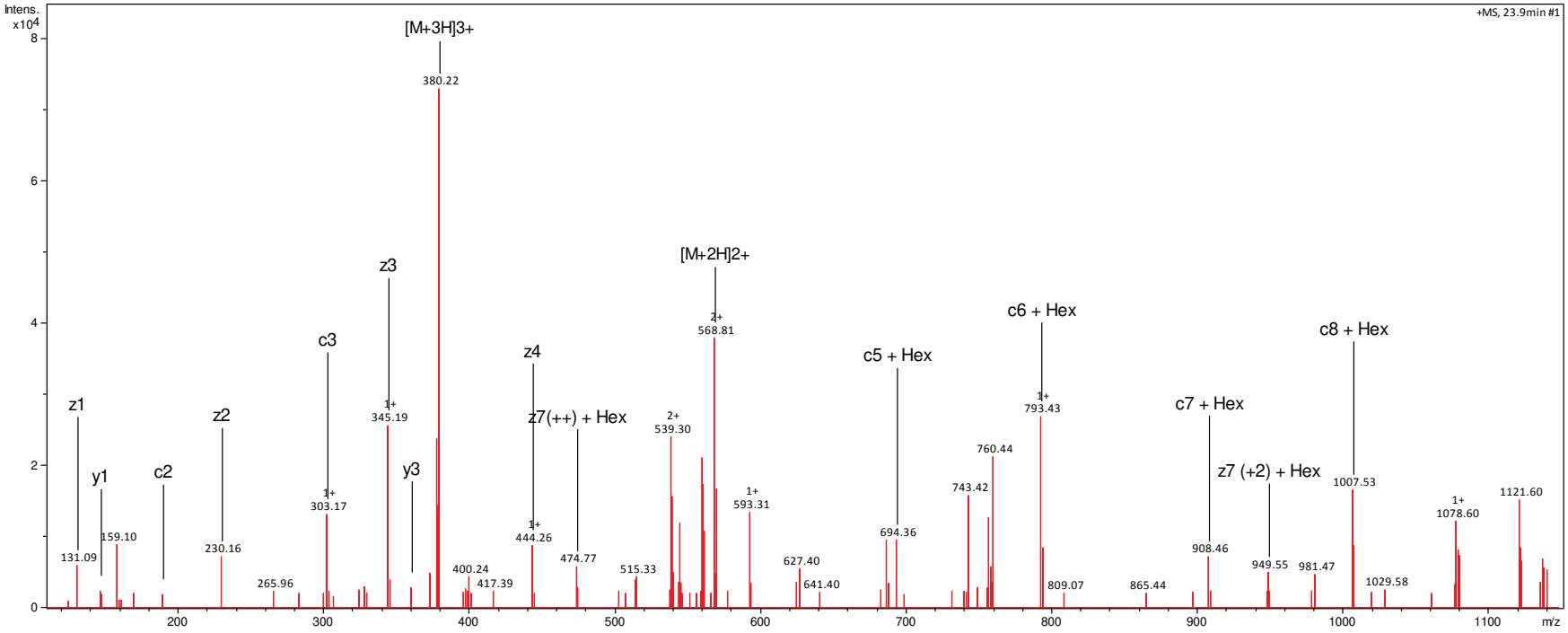

SCO Number	SCO4256
Precursor m/z	527.764
Charge	4
Retention time	15.5
Scan number	1712
Hex on peptide	3
e-value	0.018
Site allocated?	Ser317
Method	ETD_OT

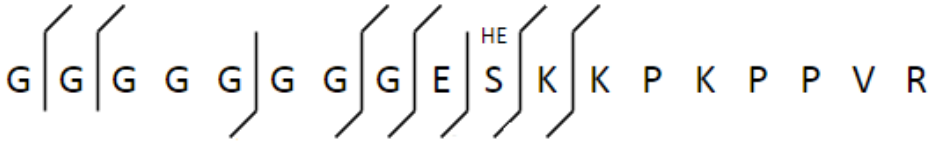

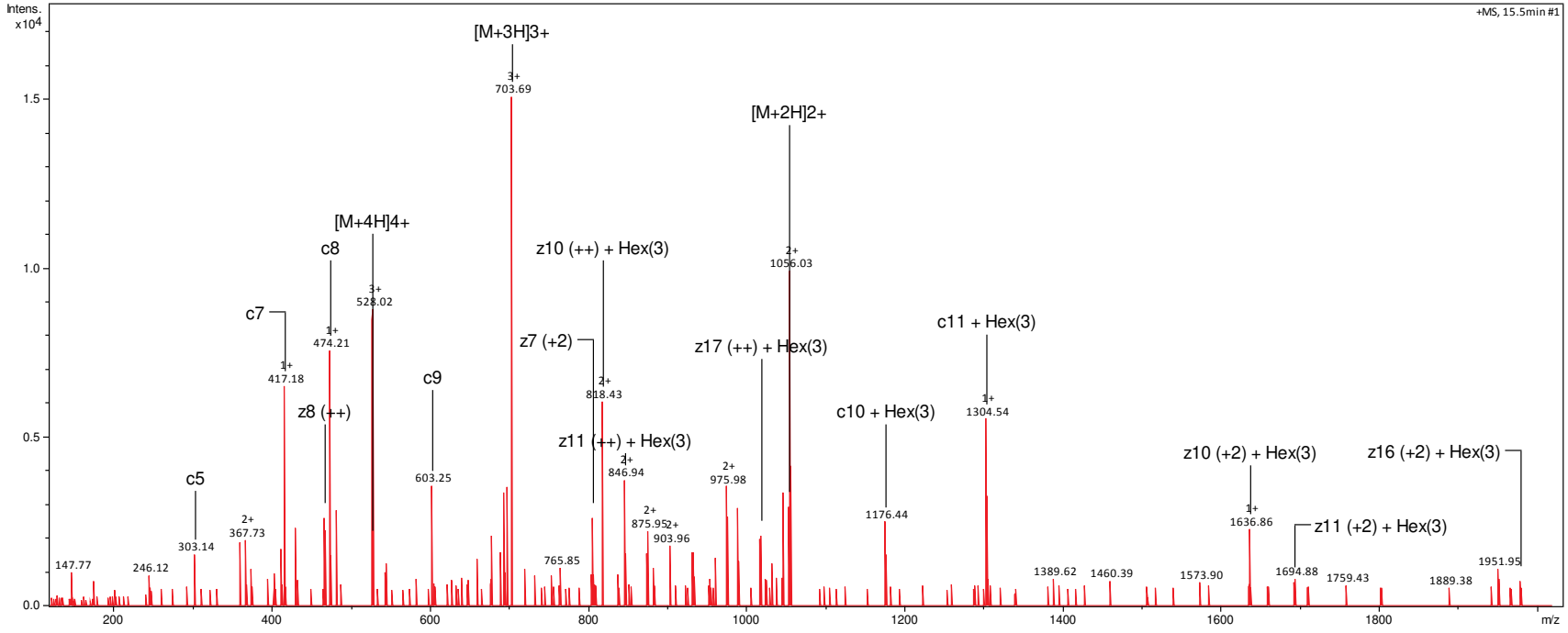

SCO Number	SCO7218
Precursor m/z	759.991
Charge	3
Retention time	22.9
Scan number	3332
Hex on peptide	3
e-value	0.00066
Site allocated?	N
Method	ETD_OT

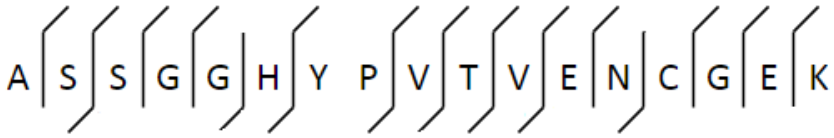

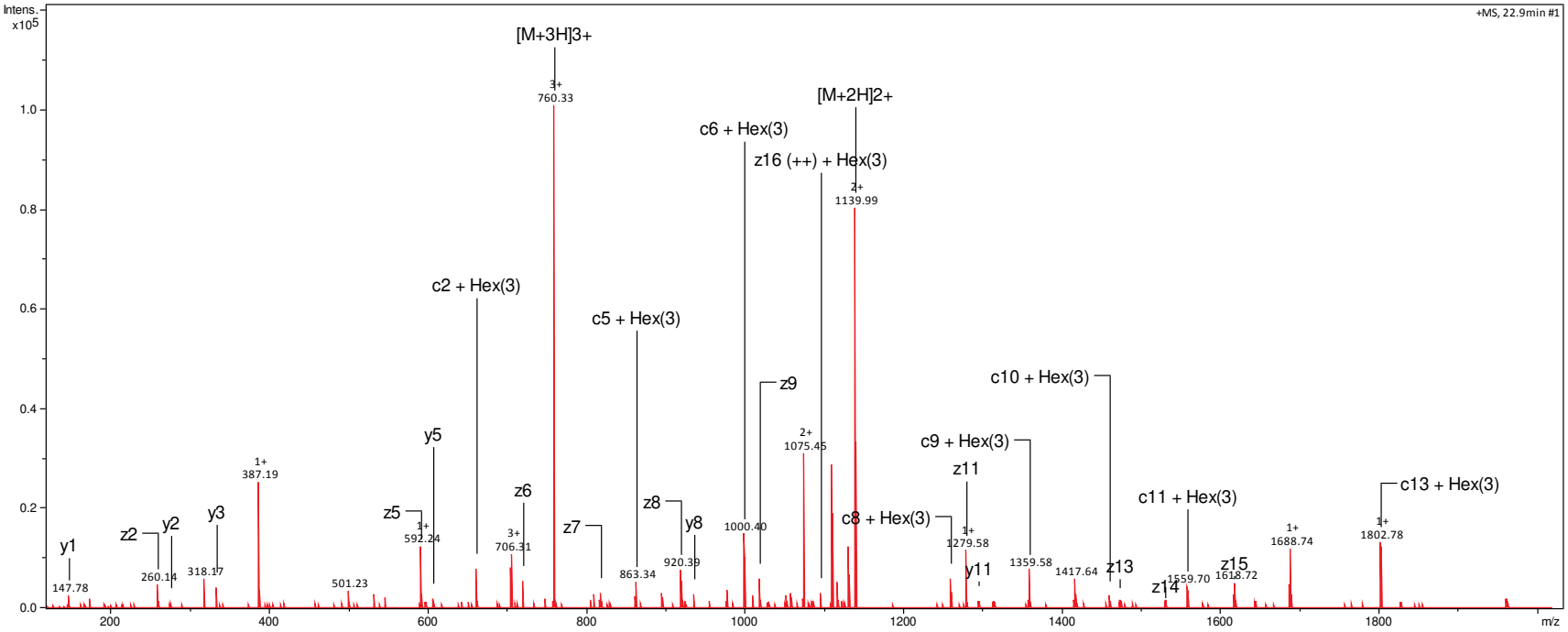

SCO Number	SCO7218
Precursor m/z	724.830
Charge	4
Retention time	49.6
Scan number	11845
Hex on peptide	3
e-value	0.0047
Site allocated?	N
Method	ETD_IT, ETD_OT

A S S G G H Y P V T V E N C G E K L T F E K

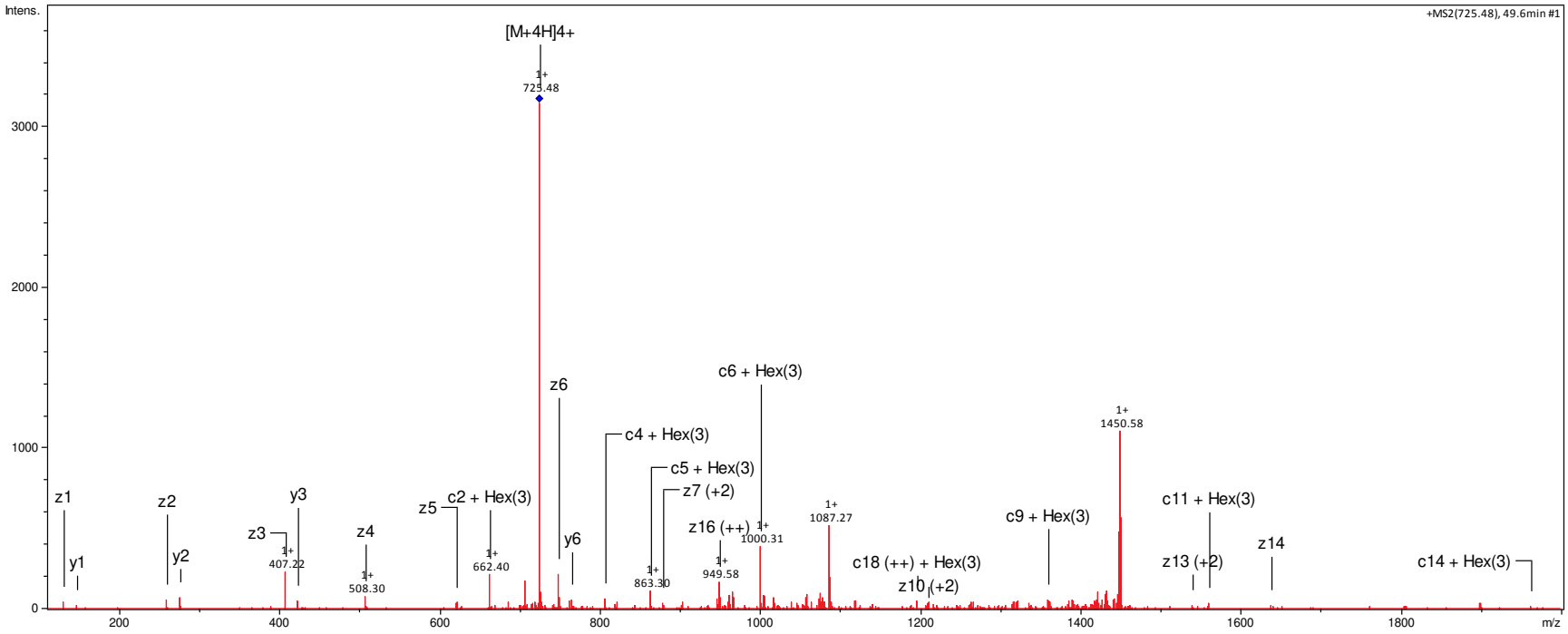

SCO Number	SCO3357
Precursor m/z	814.373
Charge	3
Retention time	17
Scan number	2155
Hex on peptide	6
e-value	0.029
Site allocated?	N
Method	ETD_IT

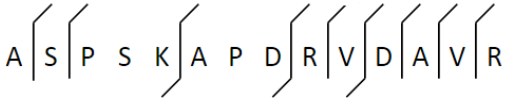

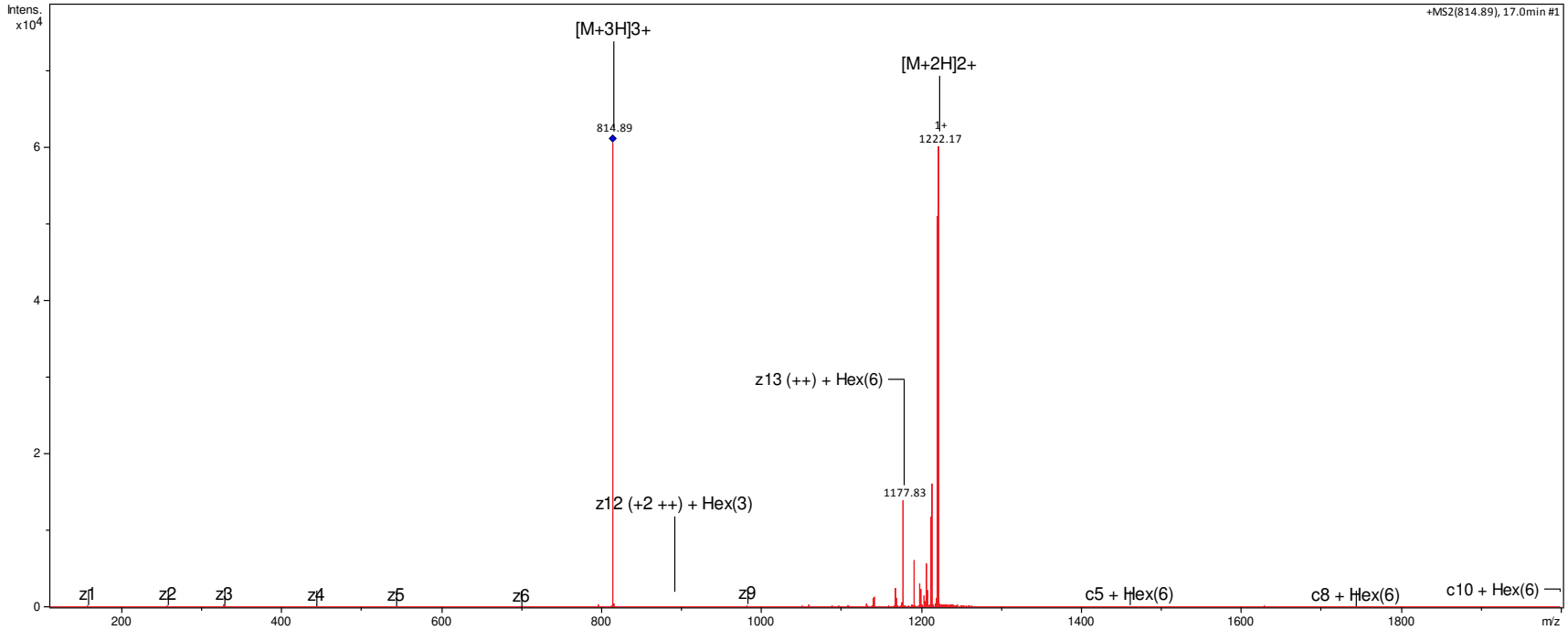

SCO Number	SCO2963
Precursor m/z	541.738
Charge	2
Retention time	39.5
Scan number	8834
Hex on peptide	1
e-value	0.0065
Site allocated?	N
Method	ETD_IT

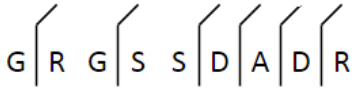

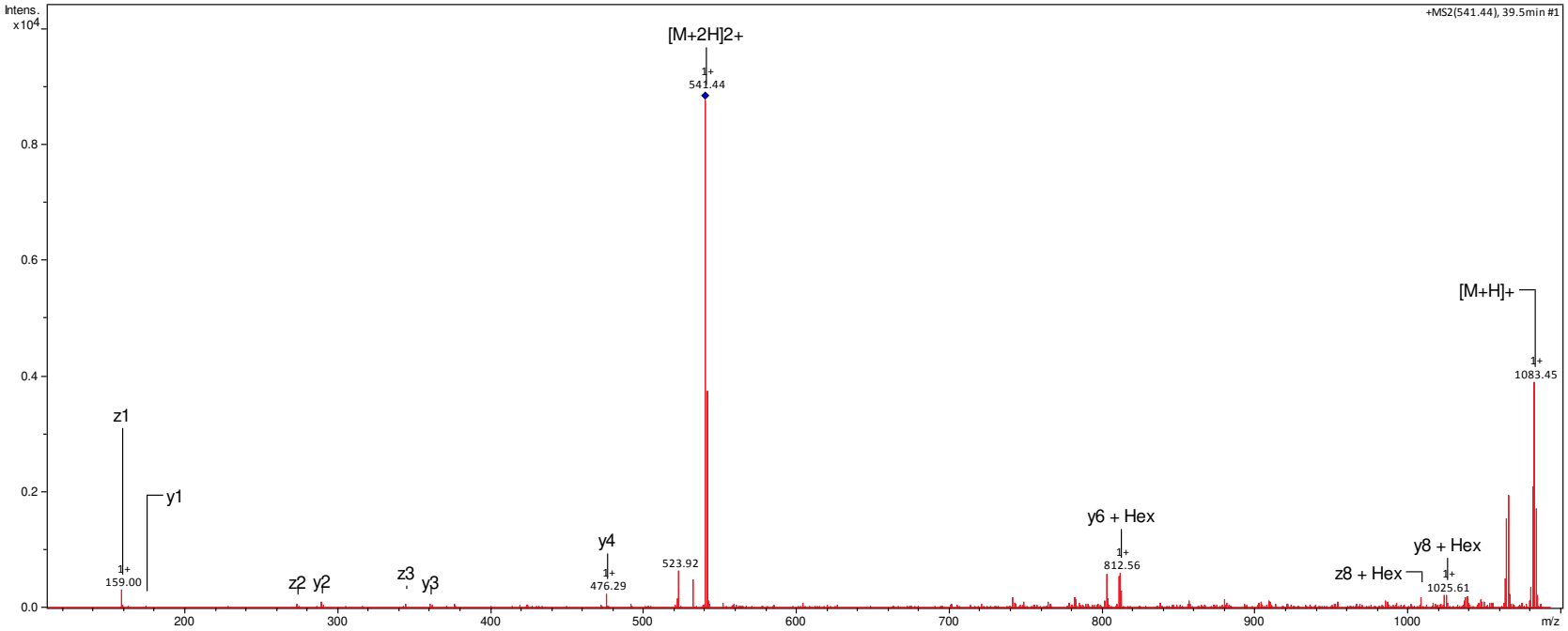

SCO Number	SCO4142
Precursor m/z	739.725
Charge	3
Retention time	71.6
Scan number	32536
Hex on peptide	1
e-value	0.0019
Site allocated?	N
Method	ETD_IT

T A A A E P V K A T V E N A T A A I G A A K

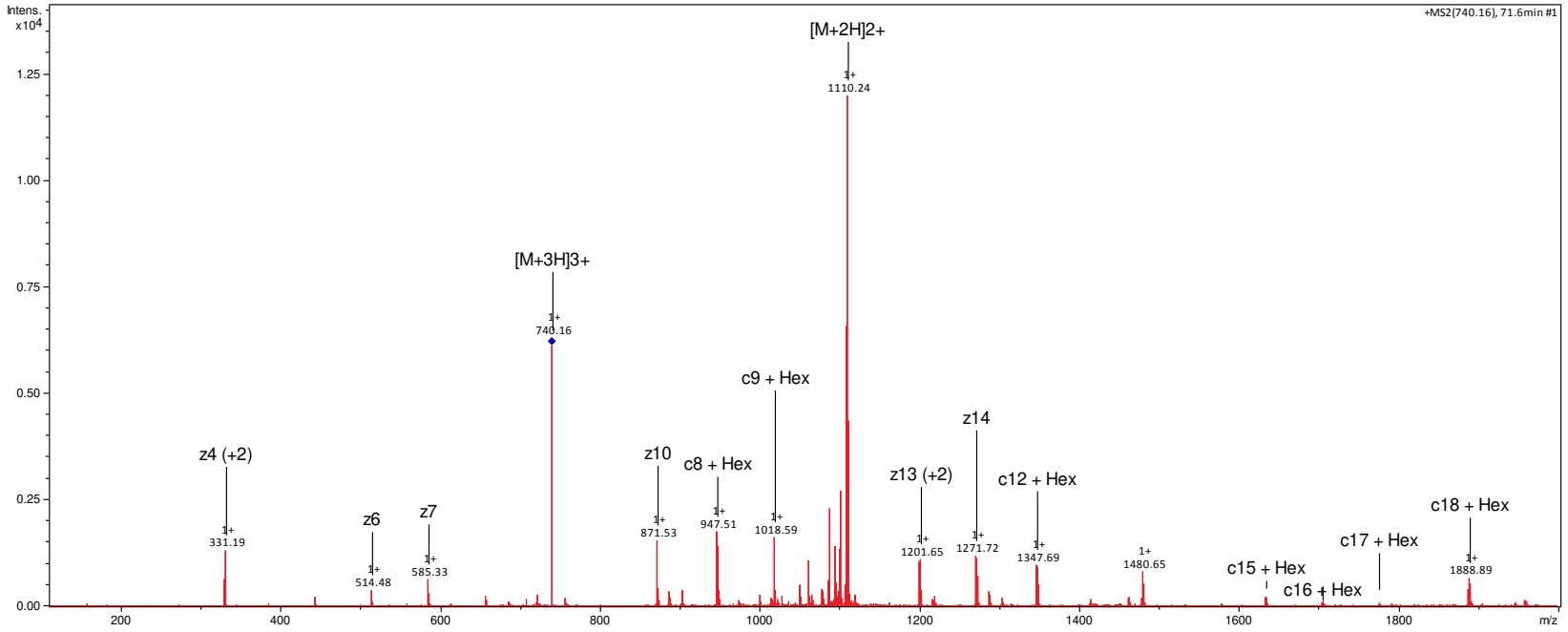

SCO Number	SCO3184
Precursor m/z	694.342
Charge	3
Retention time	23.9
Scan number	46.3
Hex on peptide	1
e-value	0.000011
Site allocated?	N
Method	ETD_IT, ETD_OT

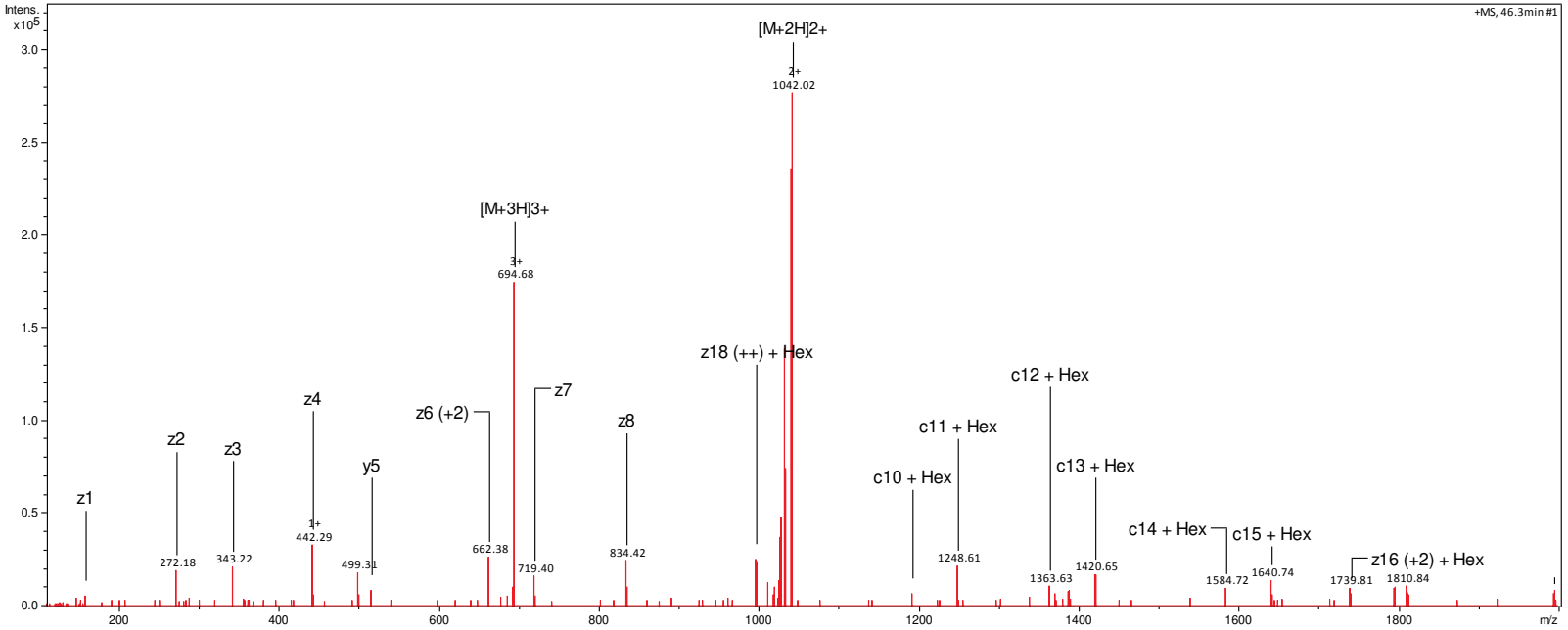

SCO Number	SCO4142
Precursor m/z	956.931
Charge	2
Retention time	17.4
Scan number	4208
Hex on peptide	1
e-value	0.048
Site allocated?	N
Method	HCD_IT

C D D A K G Q L Q A S G S S A Q K

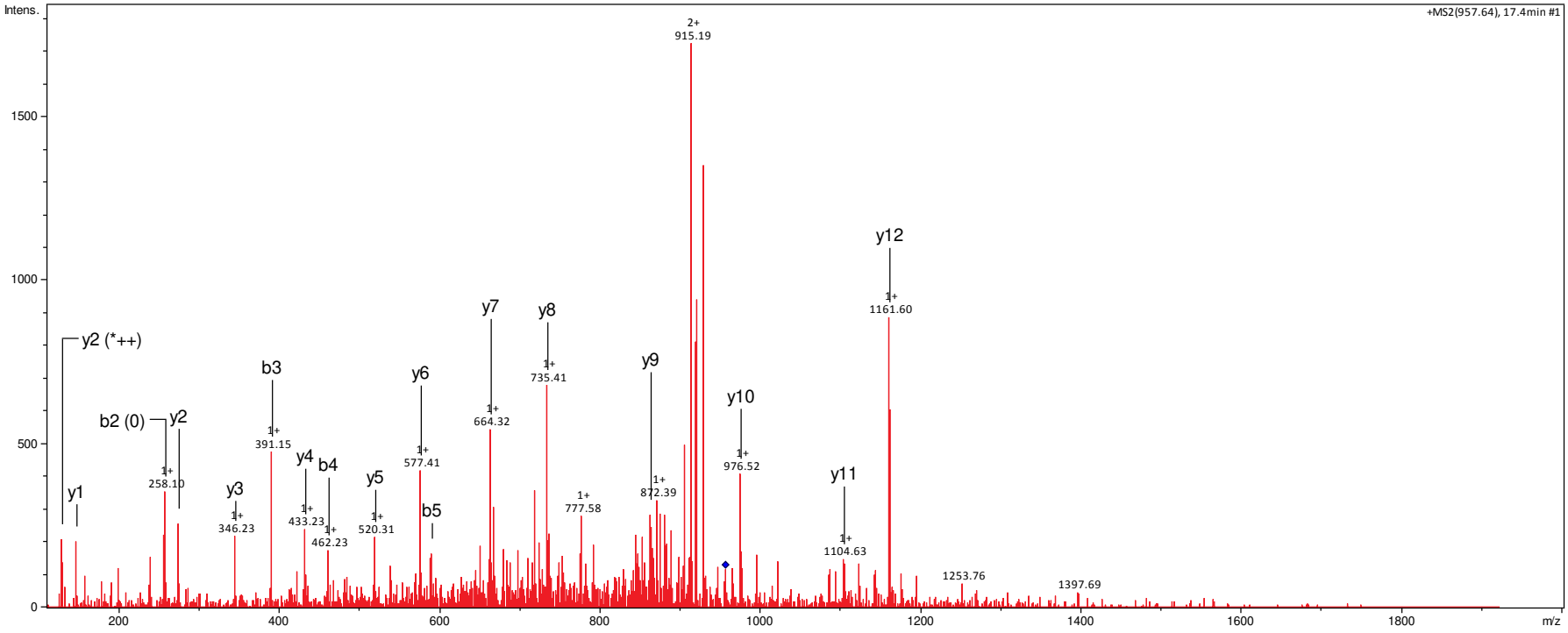

SCO Number	SCO4142
Precursor m/z	1345.343
Charge	3
Retention time	136.9
Scan number	92043
Hex on peptide	1
Other variable mod	Oxidation of M12
e-value	0.014
Site allocated?	N
Method	HCD_IT

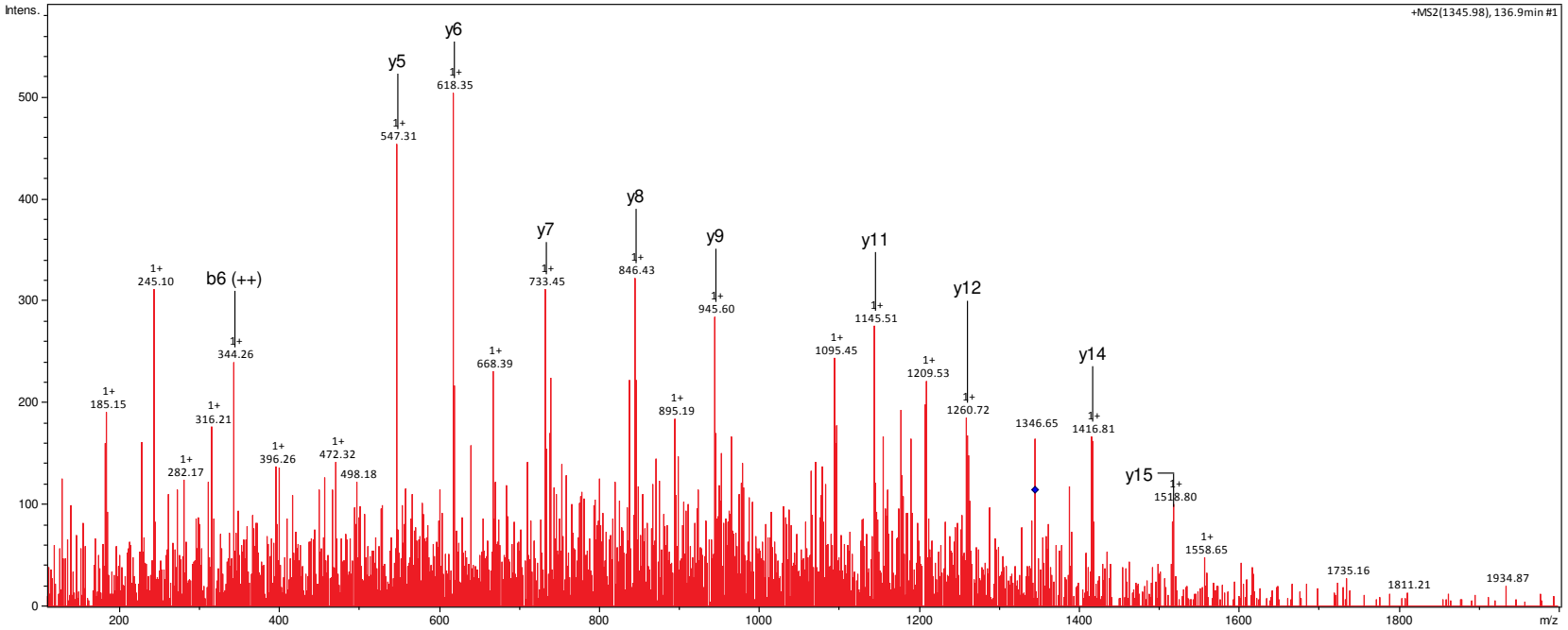

SCO Number	SCO4142
Precursor m/z	1083.868
Charge	3
Retention time	92
Scan number	58627
Hex on peptide	1
e-value	0.000036
Site allocated?	N
Method	HCD_IT

G G Q S A Q G S S G L A G Q V K Q T P G A I S Y F E L S Y A K

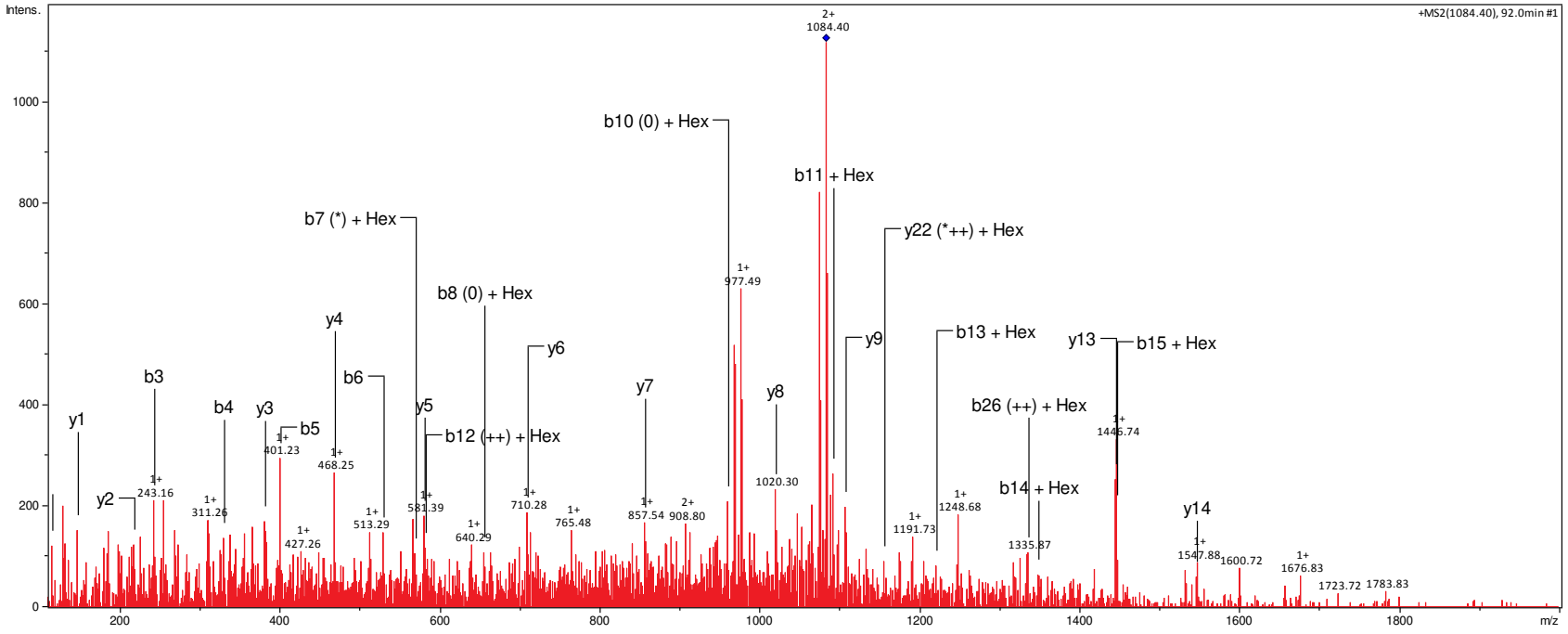

SCO Number	SCO4142
Precursor m/z	1388.343
Charge	3
Retention time	136
Scan number	91188
Hex on peptide	1
e-value	0.00078
Site allocated?	N
Method	HCD_IT

A D T L P A T K S F L N Y M A S E D G Q G L L A D A G Y A P M P T E I I T K

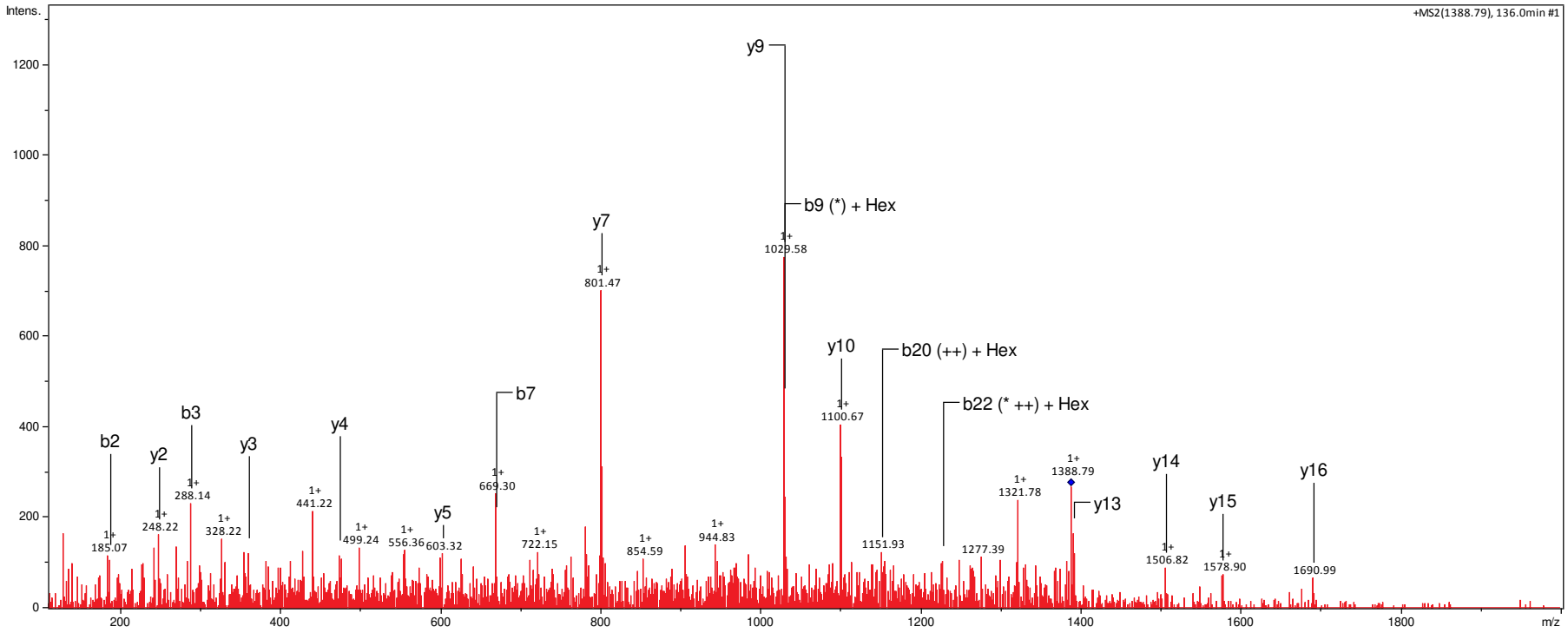

SCO Number	SCO2156
Precursor m/z	733.330
Charge	3
Retention time	48.7
Scan number	25242
Hex on peptide	1
e-value	0.0015
Site allocated?	N
Method	HCD_IT

E G T F L G K C A E L C G V D H S R

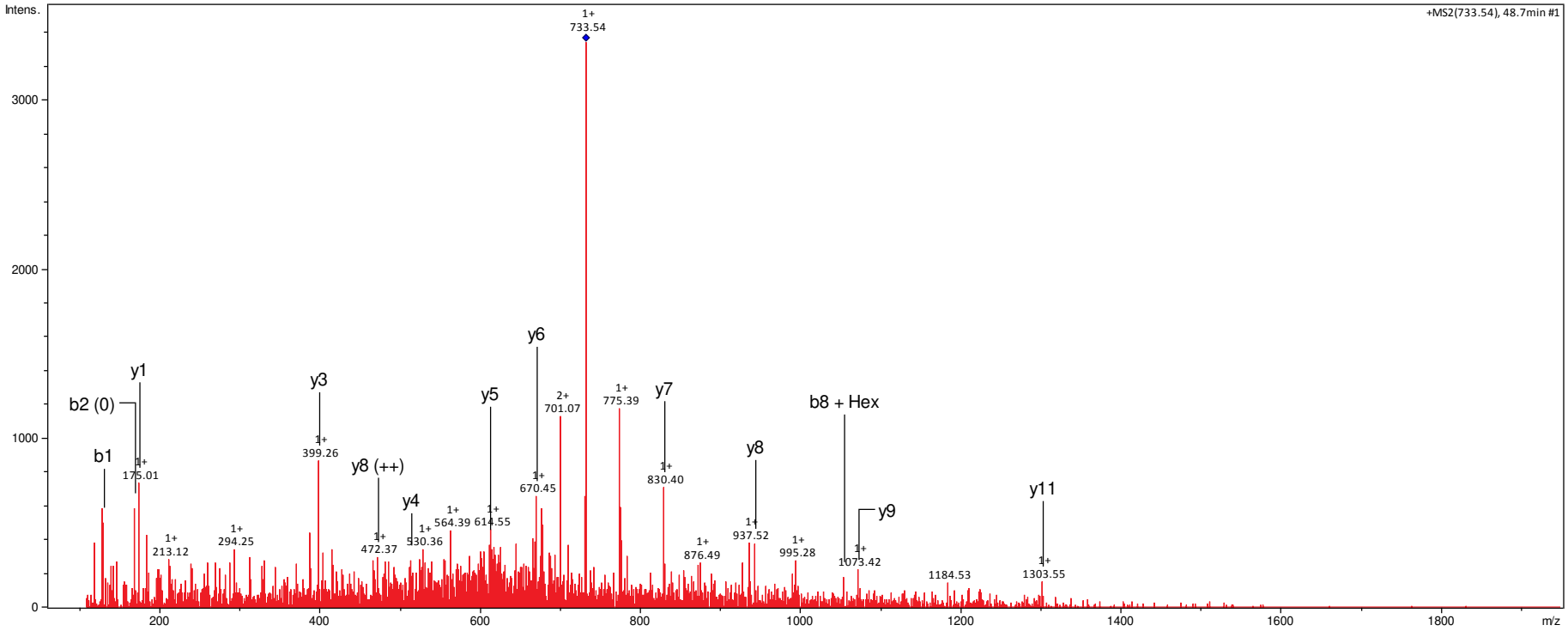

SCO Number	SCO5646
Precursor m/z	894.792
Charge	3
Retention time	109.8
Scan number	72287
Hex on peptide	1
e-value	0.0059
Site allocated?	N
Method	HCD_IT

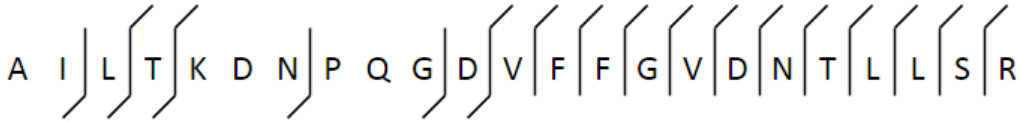

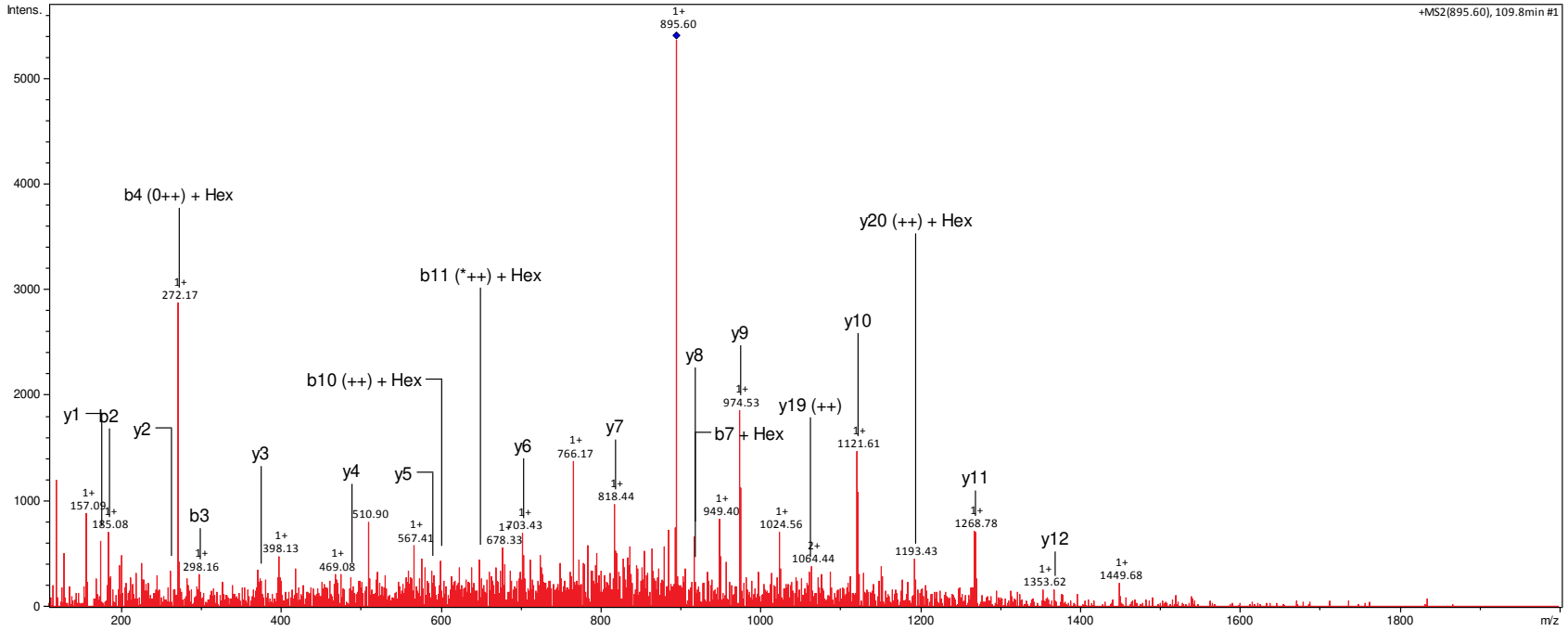

SCO Number	SCO0996
Precursor m/z	753.352
Charge	3
Retention time	76.4
Scan number	46383
Hex on peptide	2
e-value	0.00082
Site allocated?	N
Method	HCD_IT

A T A P S A E G F P V T I D N C G V K

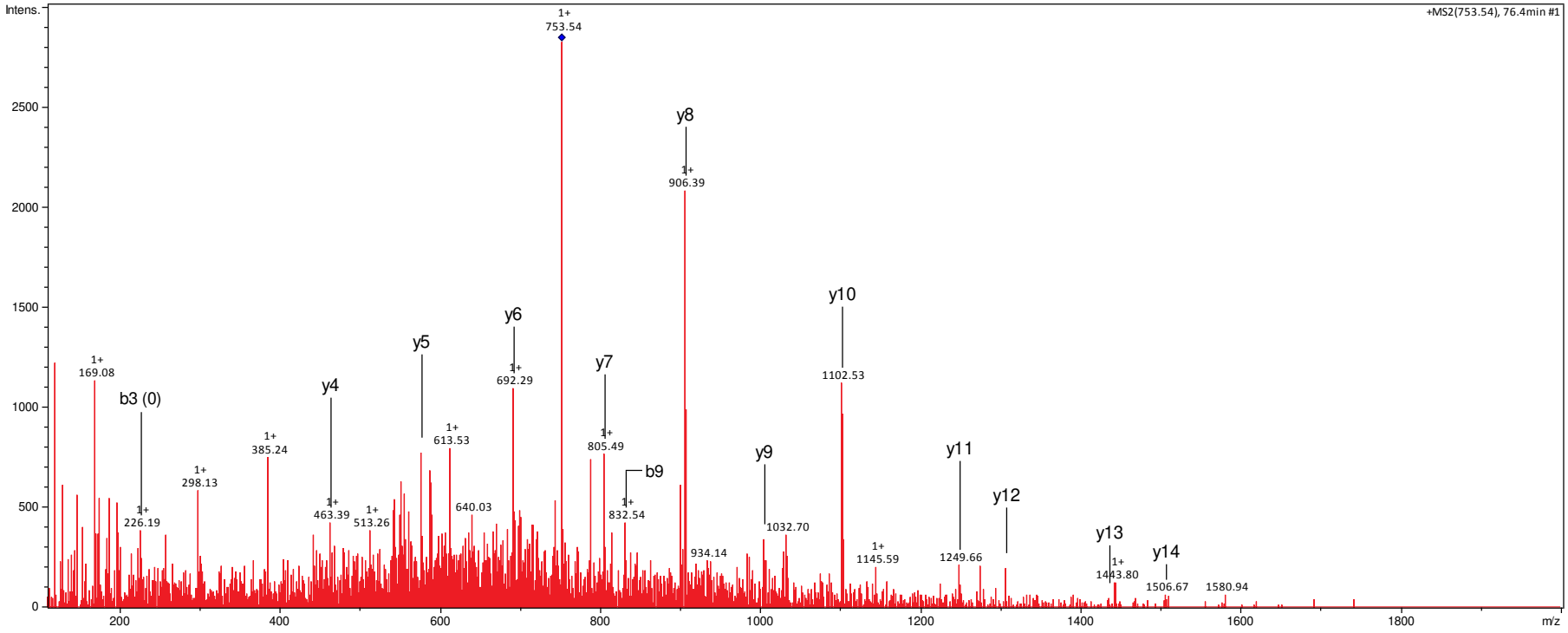

SCO Number	SCO0996
Precursor m/z	1210.550
Charge	2
Retention time	74.7
Scan number	45042
Hex on peptide	3
e-value	0.021
Site allocated?	N
Method	HCD_IT

A T A P S A E G F P V T I D N C G V K

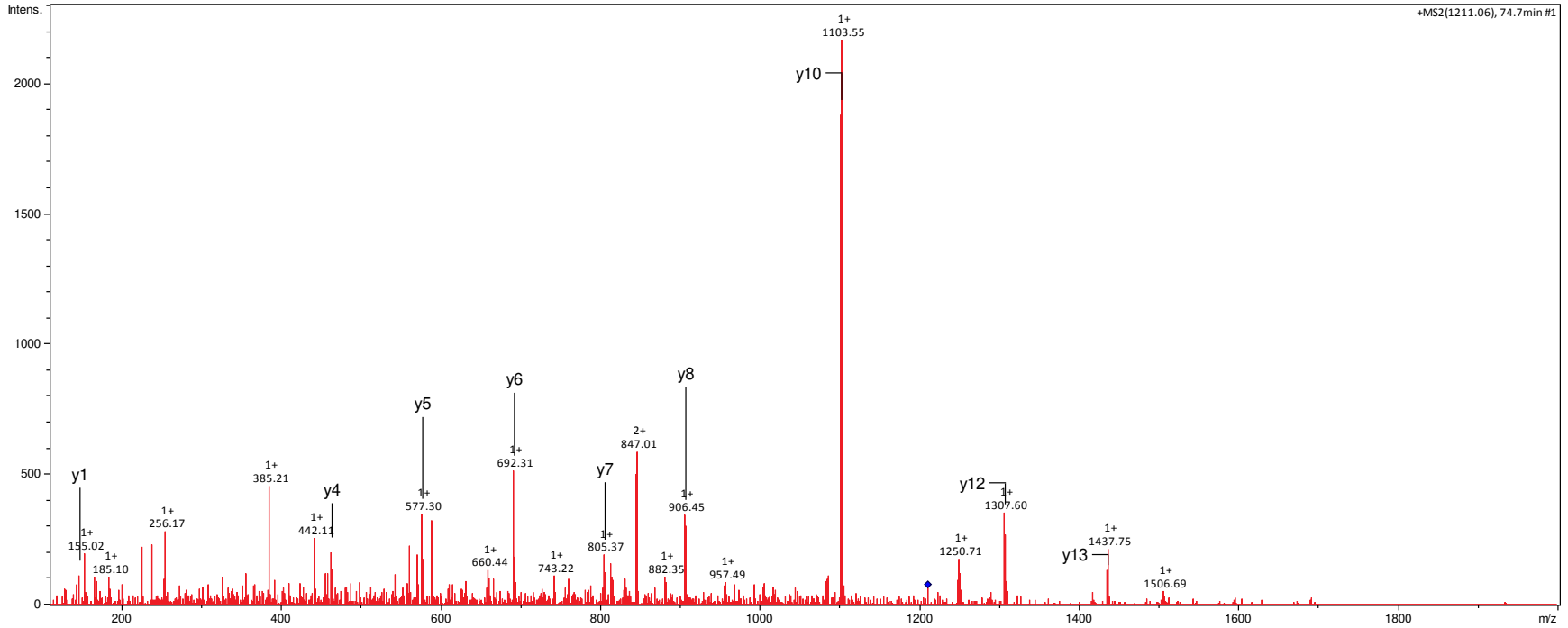

SCO Number	SCO3184
Precursor m/z	737.041
Charge	3
Retention time	35.6
Scan number	16323
Hex on peptide	1
e-value	0.0014
Site allocated?	N
Method	HCD_IT

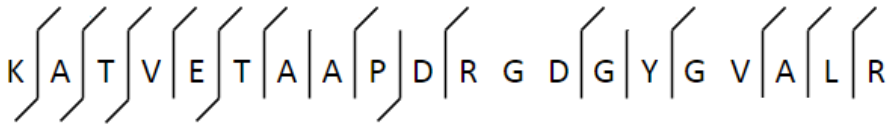

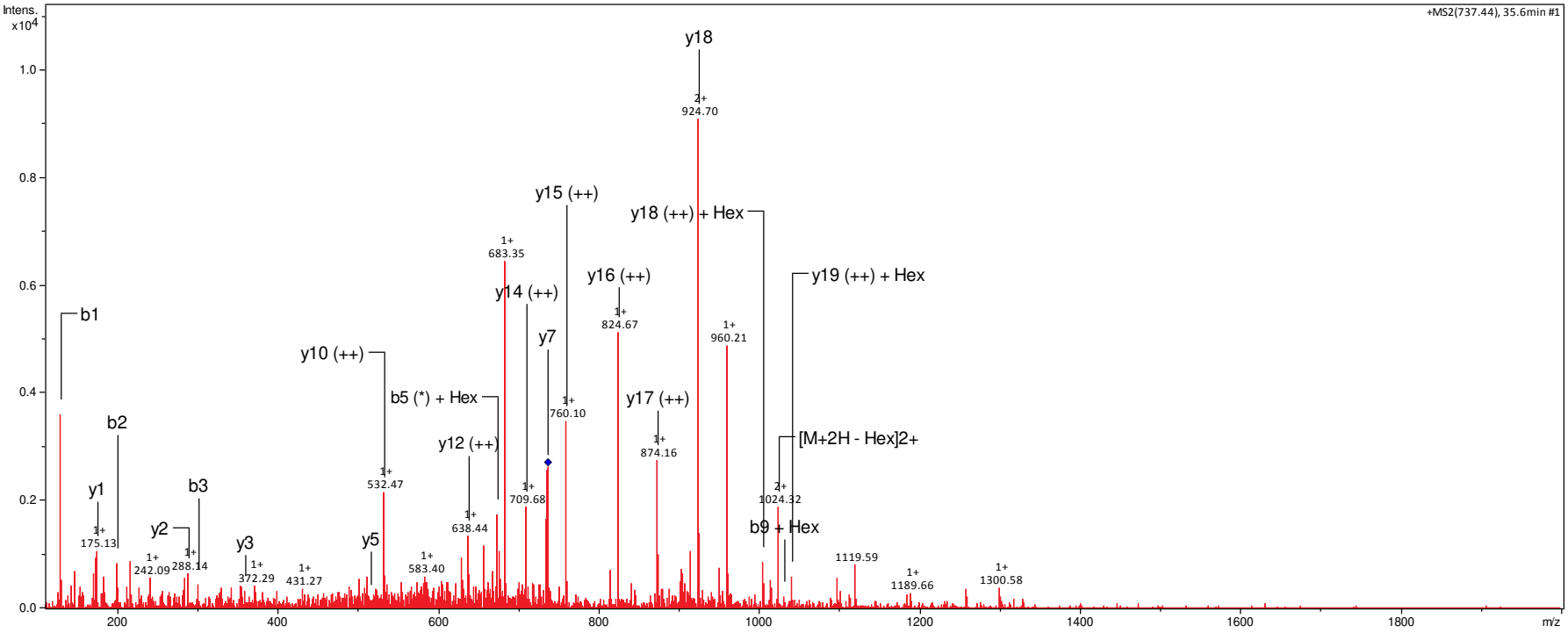

SCO Number	SCO4013
Precursor m/z	890.437
Charge	2
Retention time	54.1
Scan number	29320
Hex on peptide	1
e-value	0.023
Site allocated?	N
Method	HCD_IT

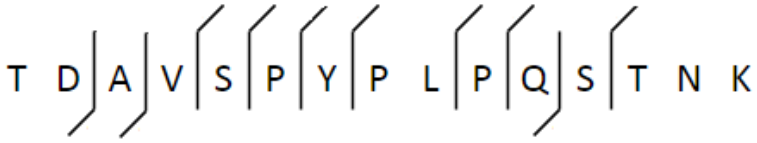

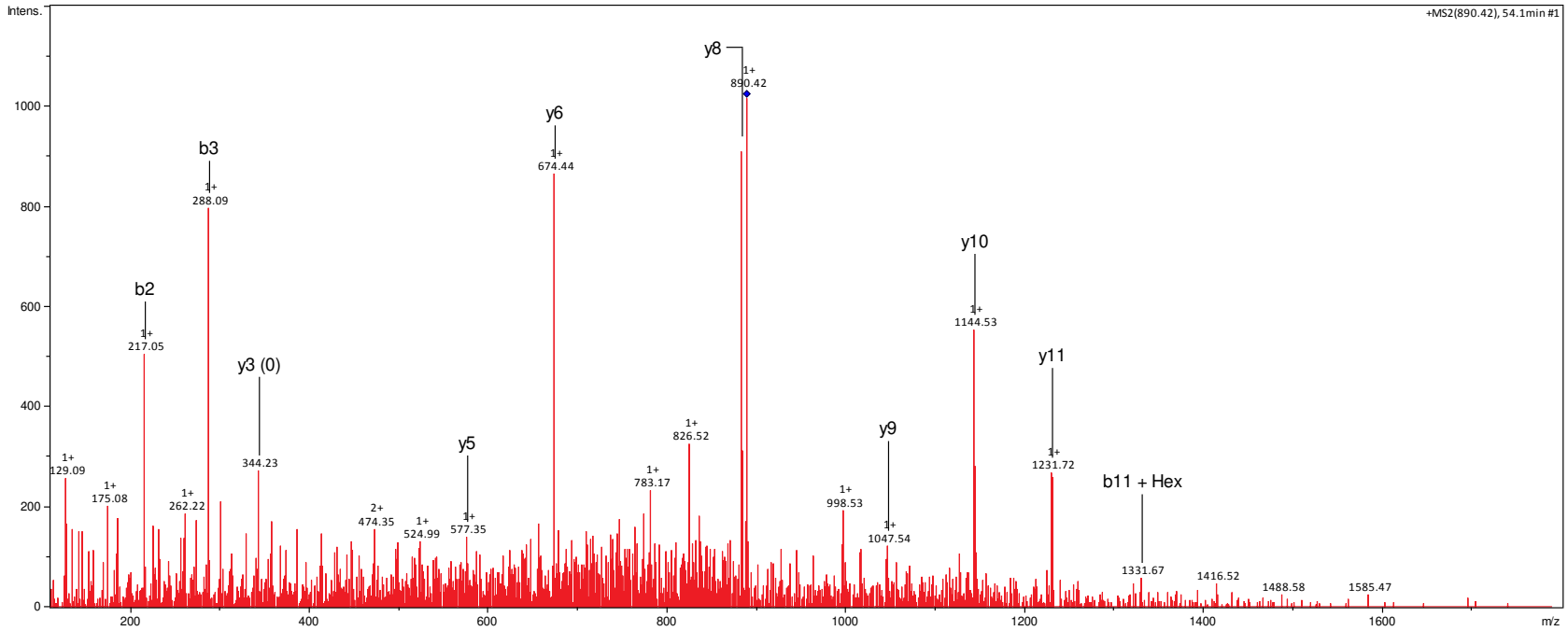

SCO Number	SCO4885
Precursor m/z	1180.552
Charge	2
Retention time	109.3
Scan number	71923
Hex on peptide	1
e-value	0.00000081
Site allocated?	N
Method	HCD_IT

S D Q A P E P G F A D S P Y I T V T F R

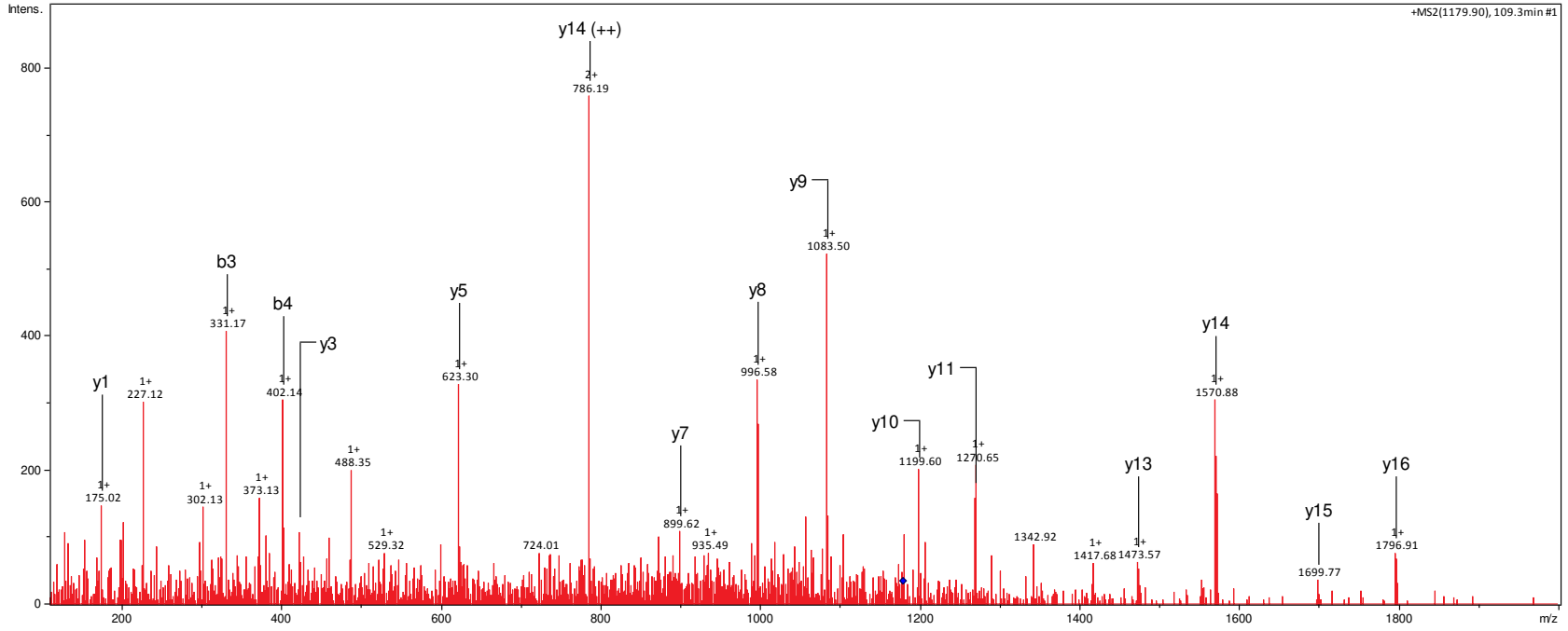

SCO Number	SCO3044
Precursor m/z	995.119
Charge	3
Retention time	98.4
Scan number	63503
Hex on peptide	3
e-value	0.000032
Site allocated?	N
Method	HCD_IT

G D A G Q P S D E P A A D S E I G V L V Q N A T R

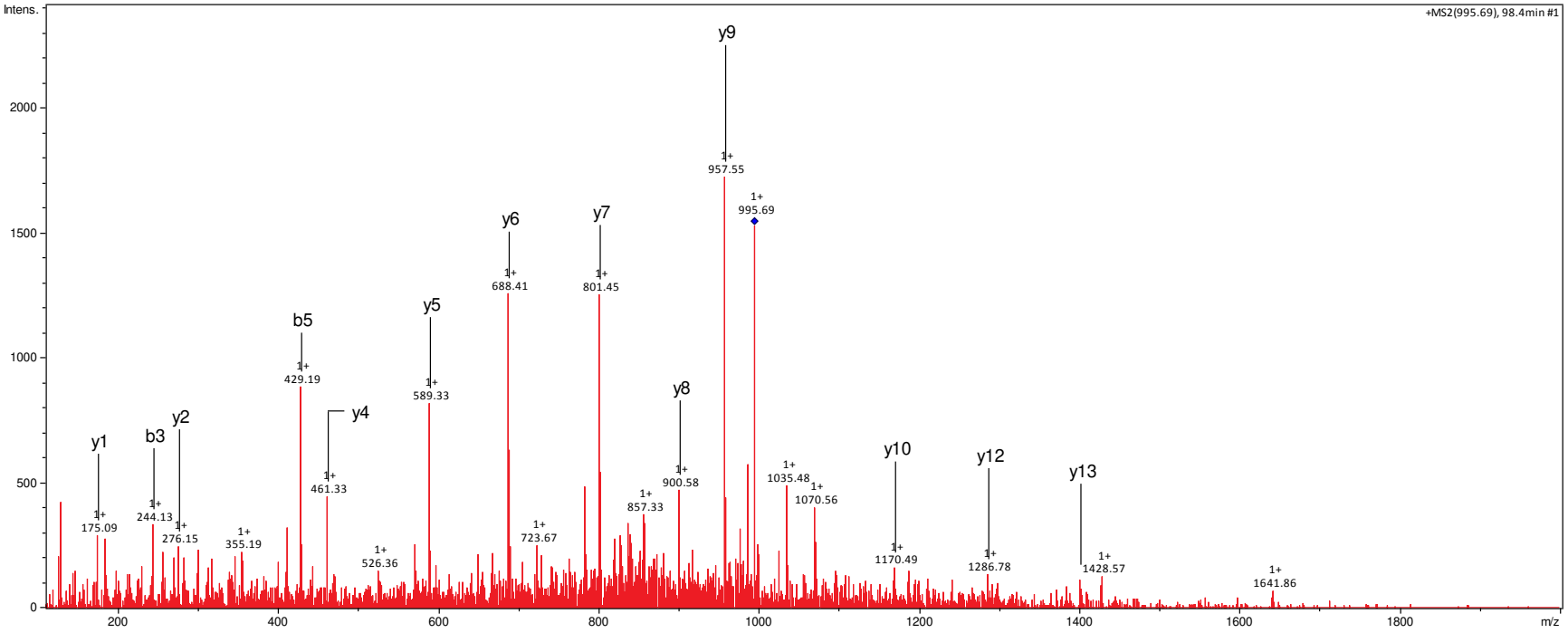

SCO Number	SCO3540
Precursor m/z	954.489
Charge	2
Retention time	57.4
Scan number	31744
Hex on peptide	2
e-value	0.0002
Site allocated?	N
Method	HCD_IT

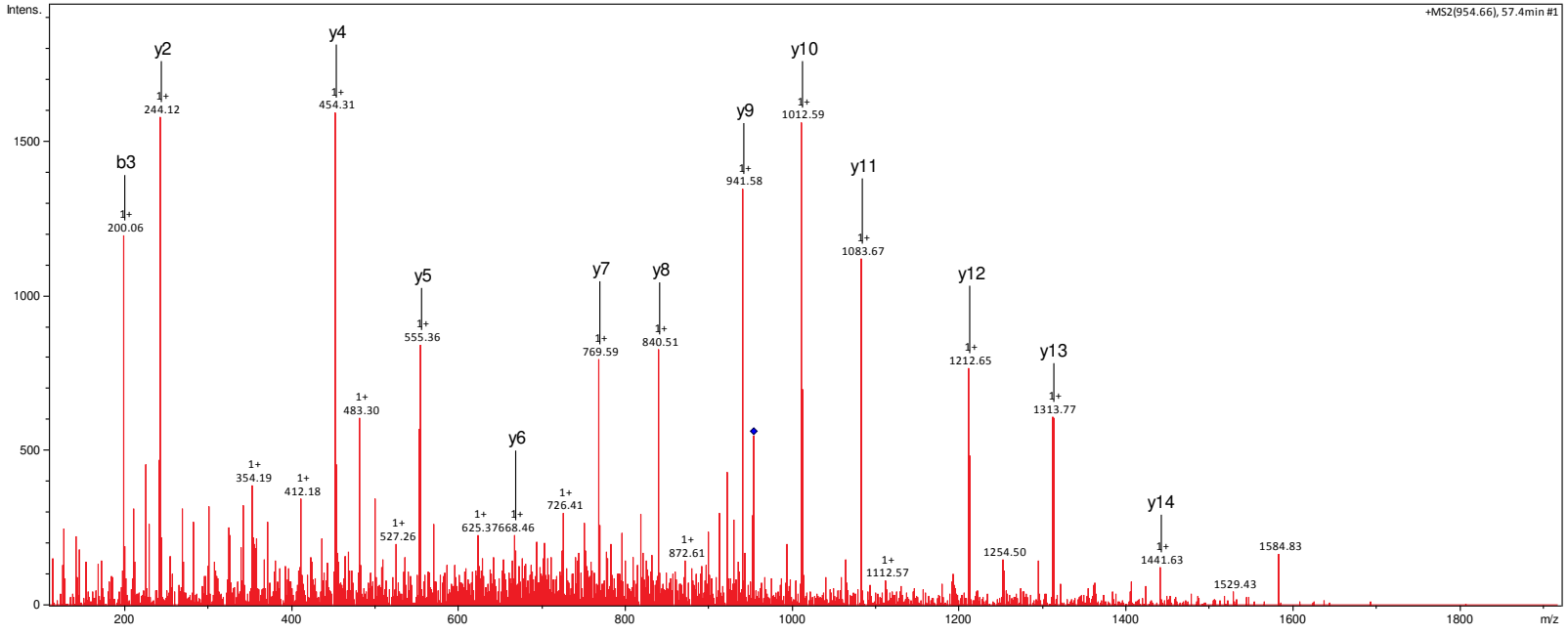

SCO Number	SCO3540
Precursor m/z	1035.515
Charge	2
Retention time	50.7
Scan number	26747
Hex on peptide	3
e-value	0.000022
Site allocated?	N
Method	HCD_IT

A A G A T E A A T A T L T P L P K

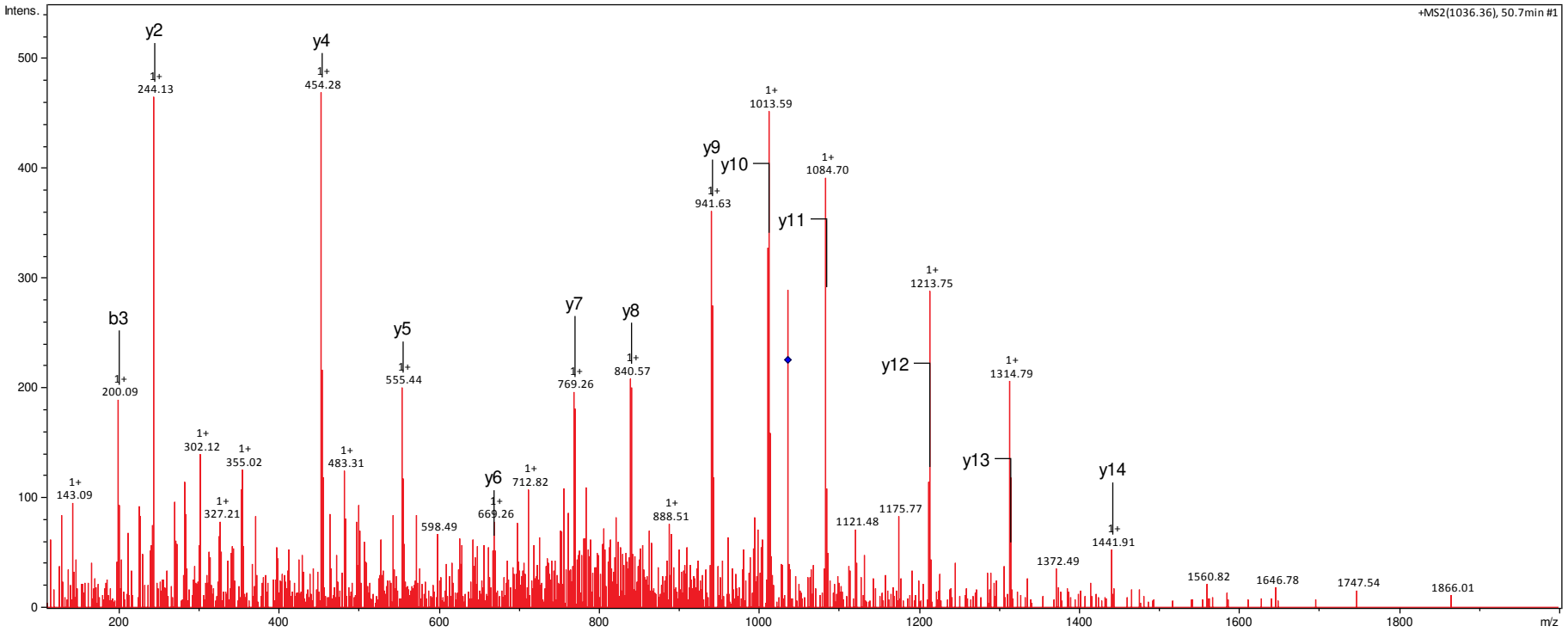

SCO Number	SCO3540
Precursor m/z	910.920
Charge	2
Retention time	46.3
Scan number	23511
Hex on peptide	2
e-value	0.00039
Site allocated?	N
Method	HCD_IT

A T P A E L S P Y Y E Q K

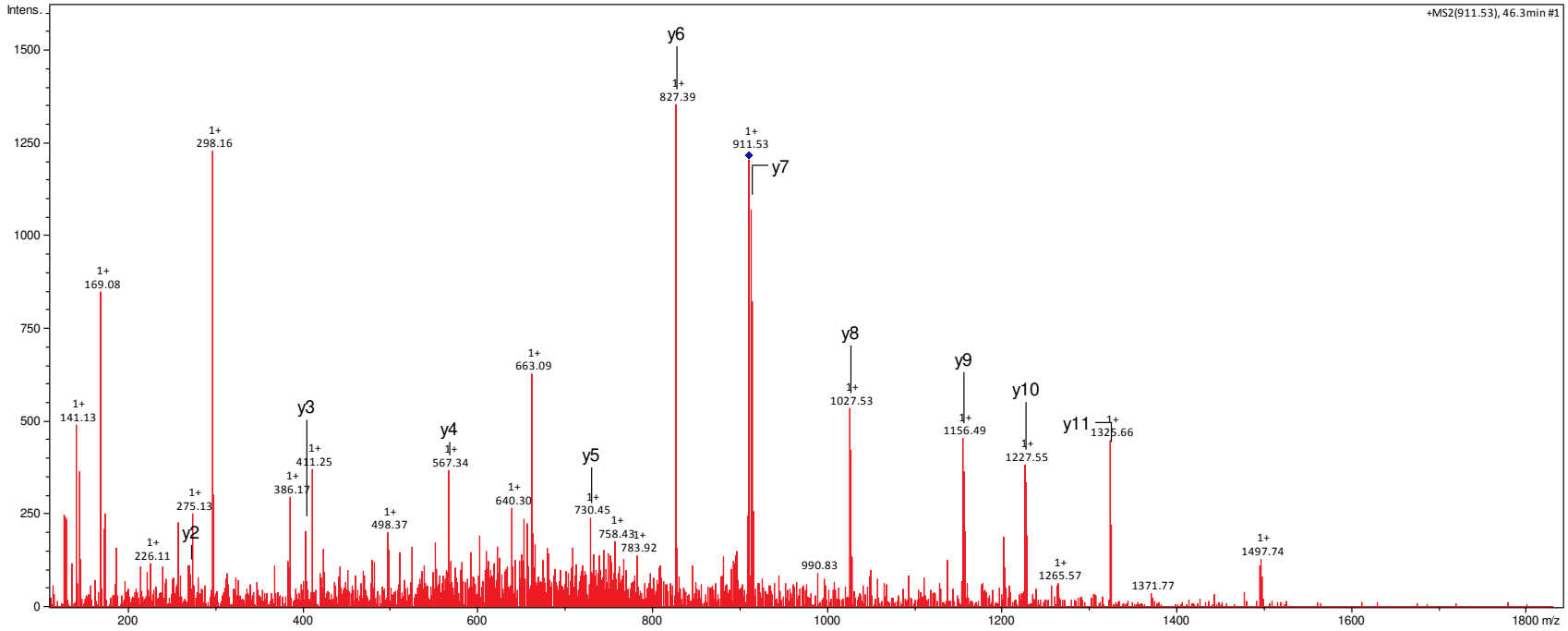

SCO Number	SCO2096
Precursor m/z	909.421
Charge	3
Retention time	51
Scan number	26945
Hex on peptide	3
e-value	0.0059
Site allocated?	N
Method	HCD_IT

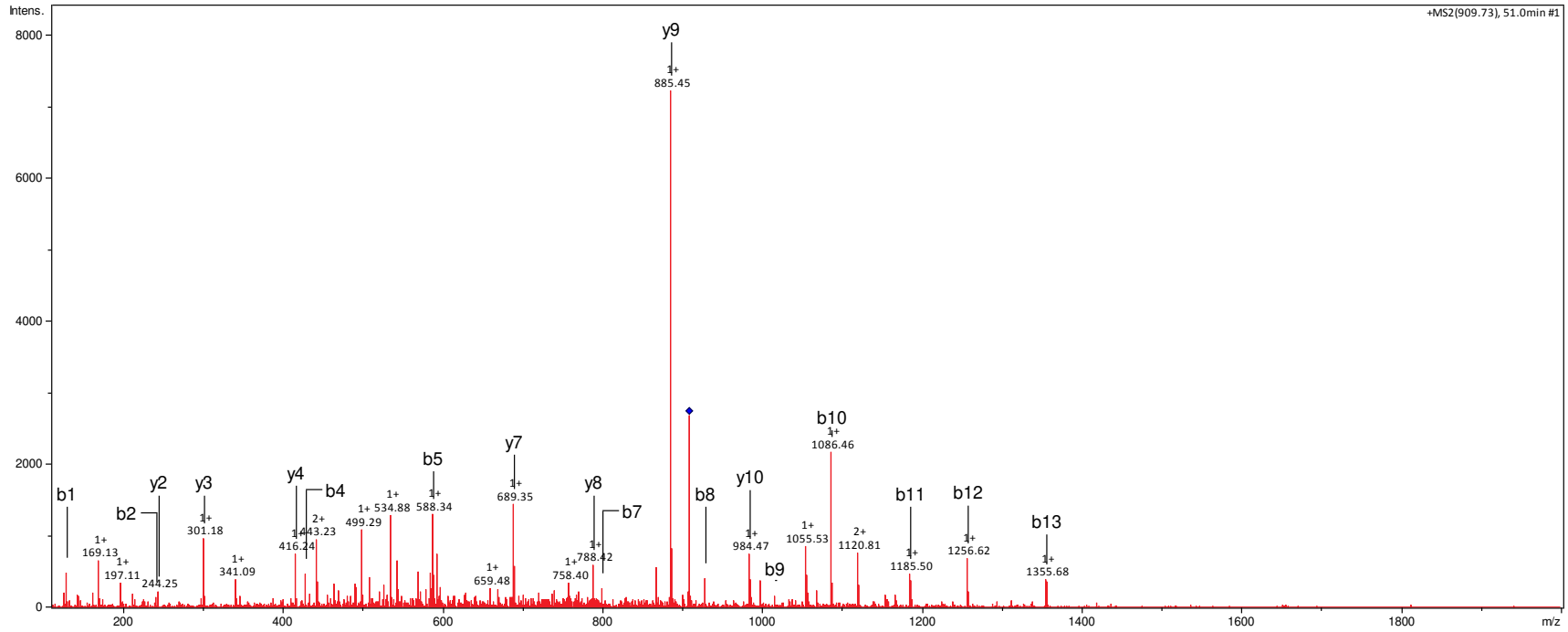

SCO Number	SCO2035
Precursor m/z	1026.959
Charge	2
Retention time	32.4
Scan number	14239
Hex on peptide	2
e-value	0.0066
Site allocated?	N
Method	HCD_IT

D D G S E S A G P V V A P S G A Q G K

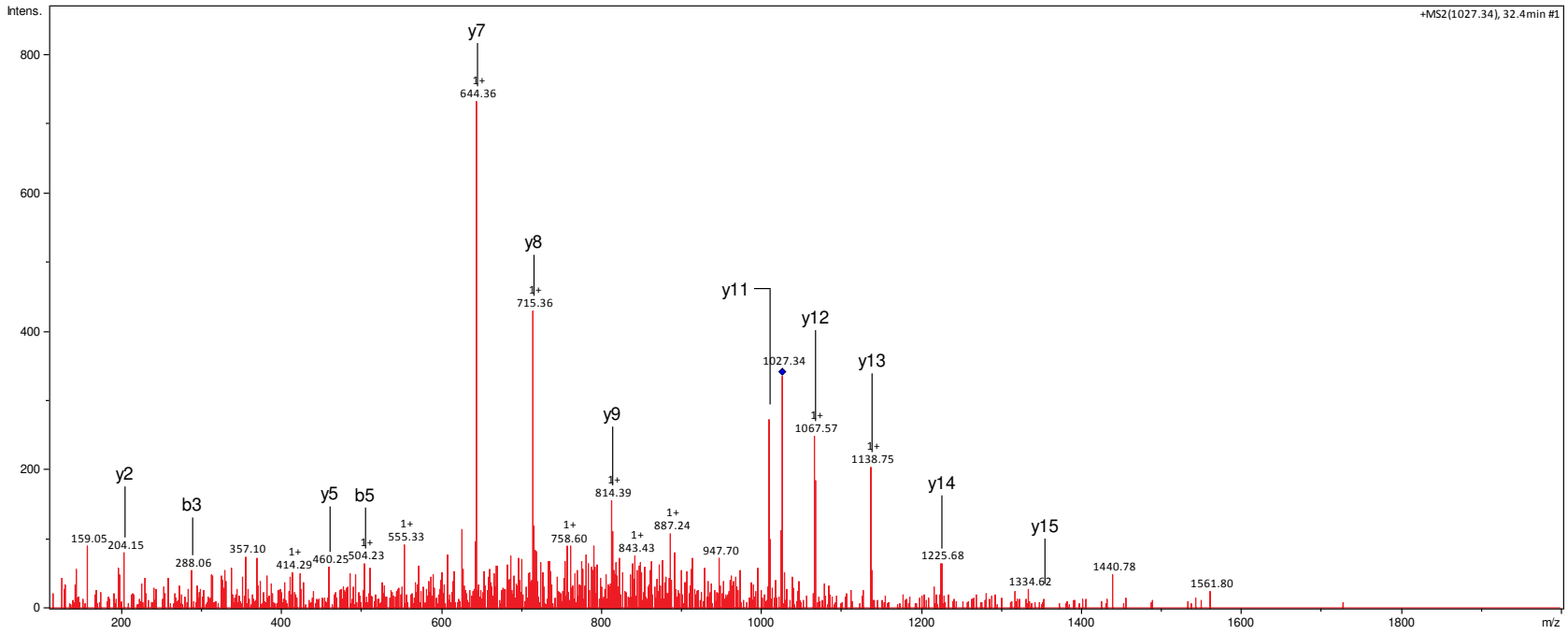

SCO Number	SCO3848
Precursor m/z	769.725
Charge	3
Retention time	53.3
Scan number	28662
Hex on peptide	1
e-value	0.00047
Site allocated?	N
Method	HCD_IT

Q|G T D V D K E S T V|N|L|V|V|S|T|G A|P K

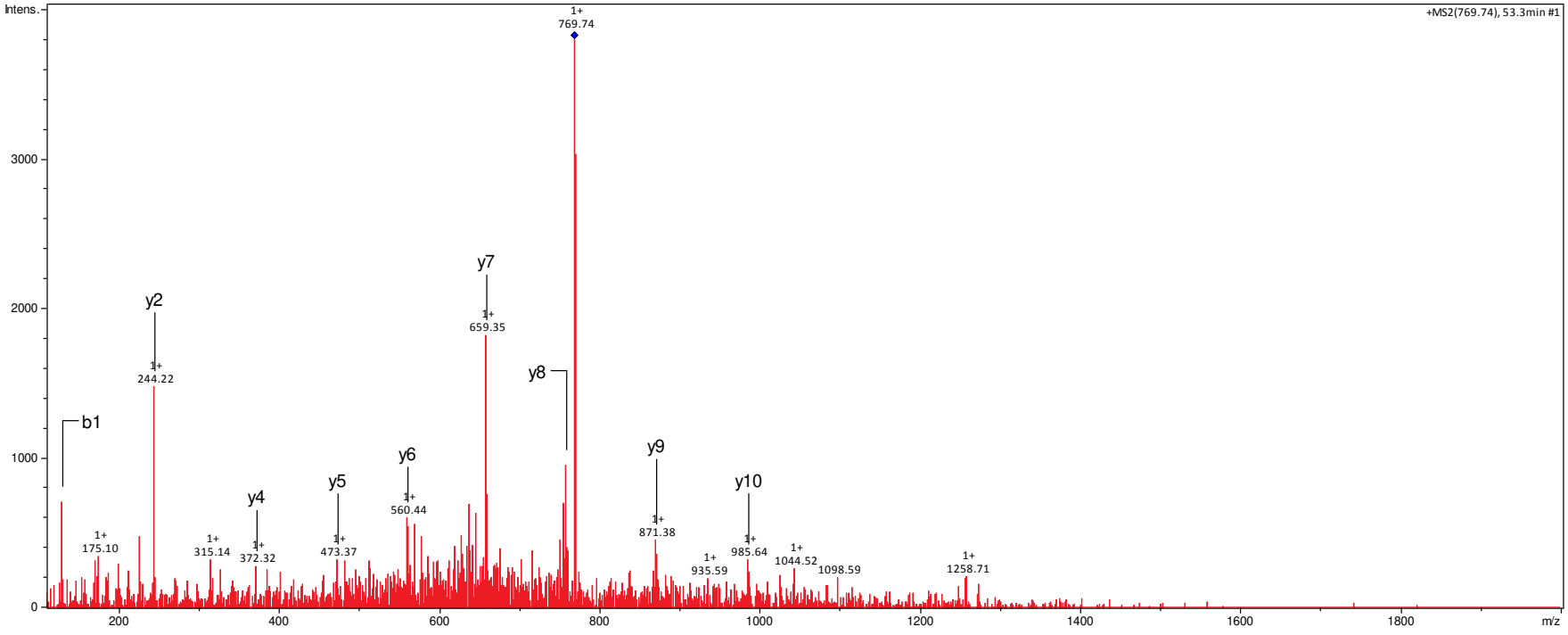

SCO Number	SCO3848
Precursor m/z	823.741
Charge	3
Retention time	52.2
Scan number	27876
Hex on peptide	2
e-value	0.00053
Site allocated?	N
Method	HCD_IT

Q|G T D V D K|E|S T V|N|L|V|V|S|T G A|P K

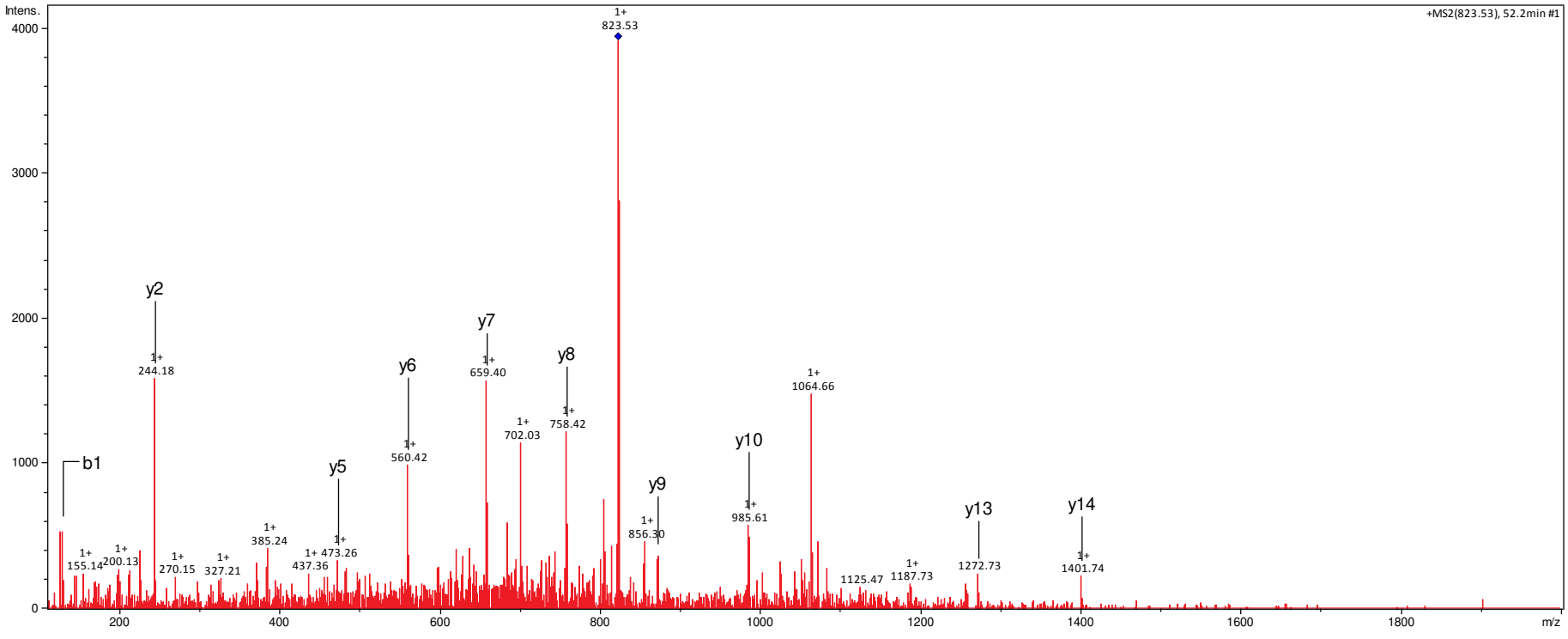

SCO Number	SCO4130
Precursor m/z	1109.514
Charge	4
Retention time	91.9
Scan number	58511
Hex on peptide	2
e-value	0.00036
Site allocated?	N
Method	HCD_IT

T S A T A P S G T R P V Q S G F A H D A Q G A Q S A A A N Y A V A L G S D G M F D K

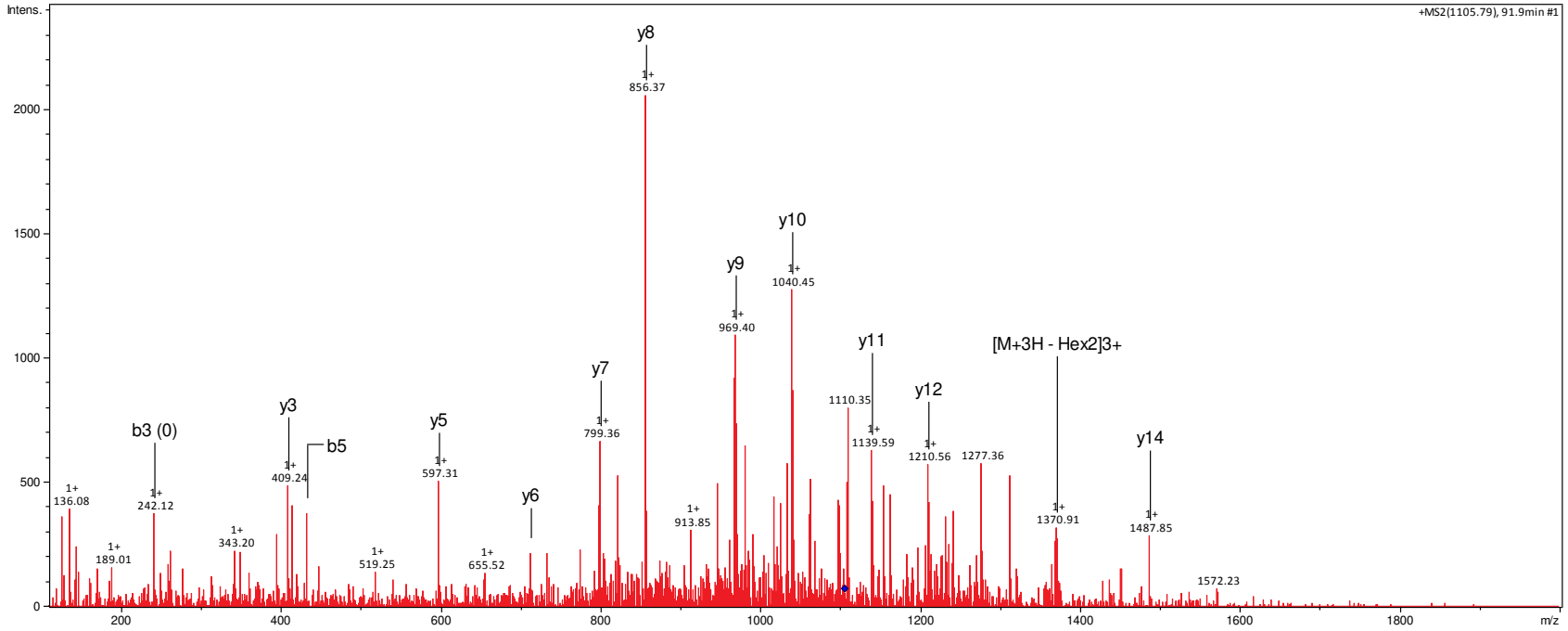

SCO Number	SCO4905
Precursor m/z	919.795
Charge	3
Retention time	132.6
Scan number	4335
Hex on peptide	3
e-value	0.024
Site allocated?	N
Method	HCD_IT

A T P G L P A Q V F L L C G S S L V A V D R

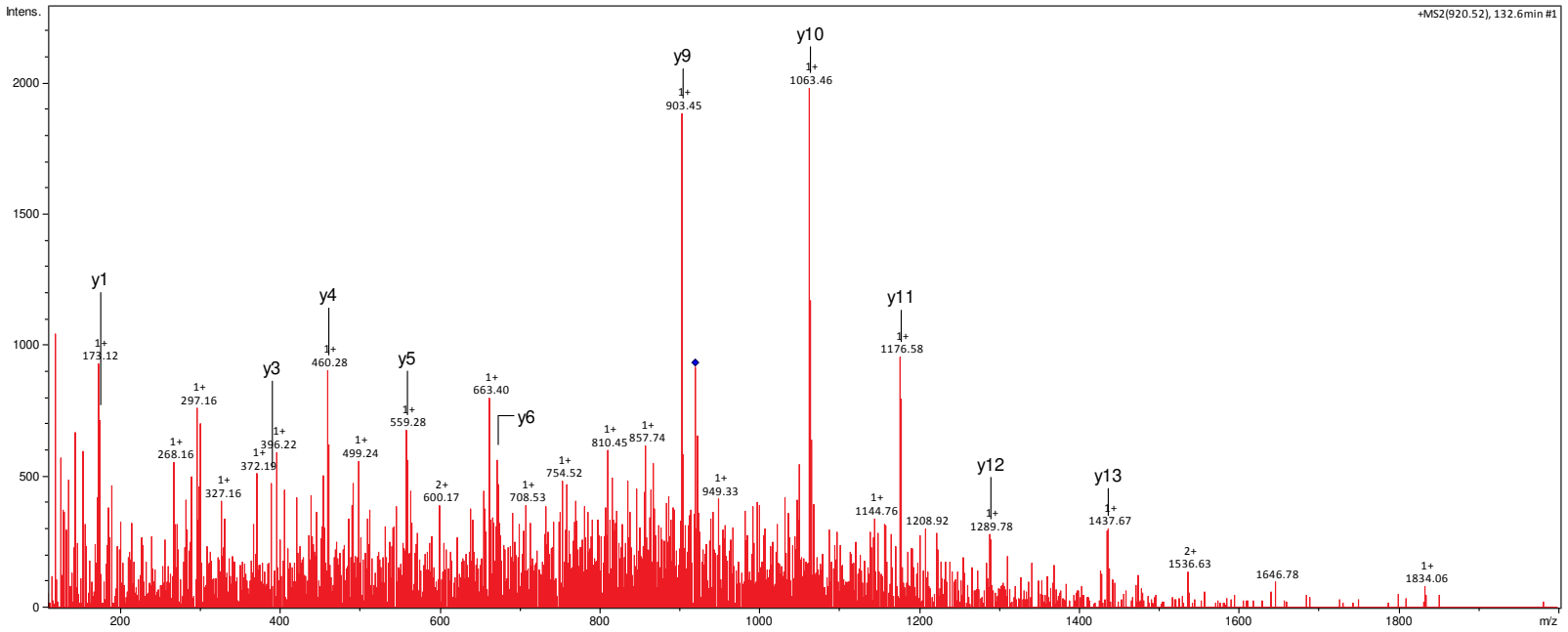

SCO Number	SCO4548
Precursor m/z	877.408
Charge	2
Retention time	20.4
Scan number	6204
Hex on peptide	3
e-value	0.00042
Site allocated?	N
Method	HCD_IT

T T S S S S S T A P S A P S A P R

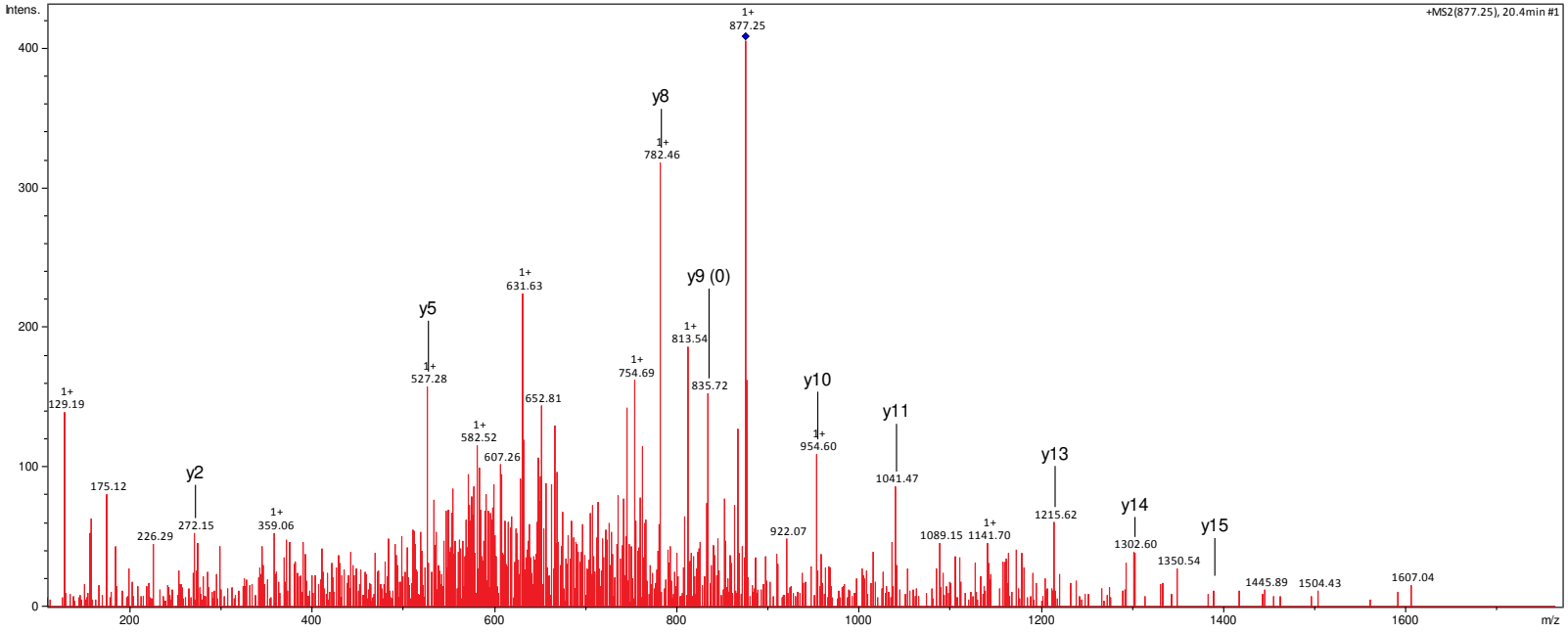

SCO Number	SCO3357
Precursor m/z	933.099
Charge	3
Retention time	50.1
Scan number	26320
Hex on peptide	3
e-value	0.0023
Site allocated?	N
Method	HCD_IT

Q V Y D K G D P V S S P S G E N V I T Y R

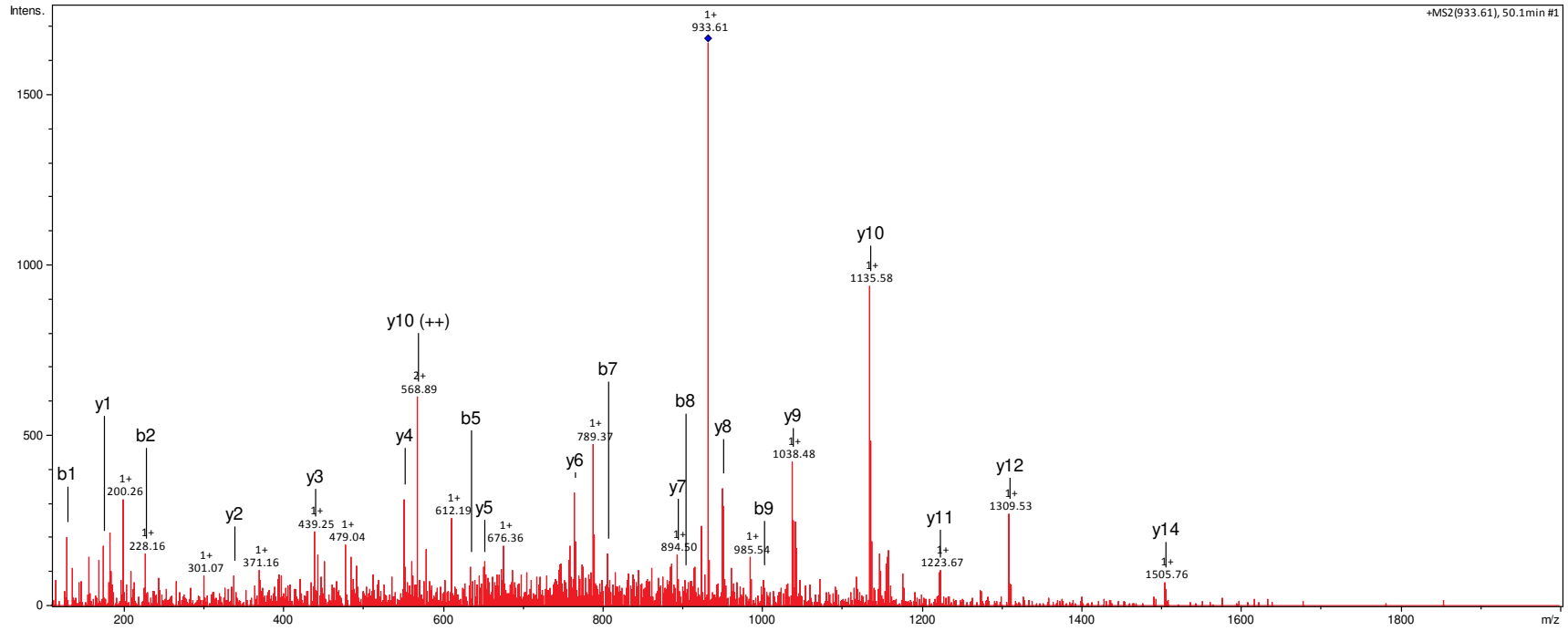

SCO Number	SCO3891
Precursor m/z	938.921
Charge	2
Retention time	45.6
Scan number	22941
Hex on peptide	2
e-value	0.00091
Site allocated?	N
Method	HCD_IT

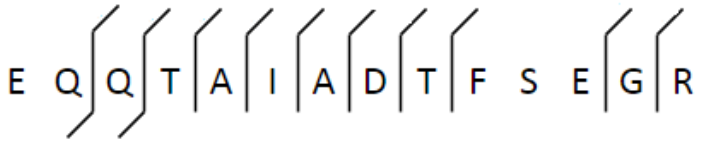

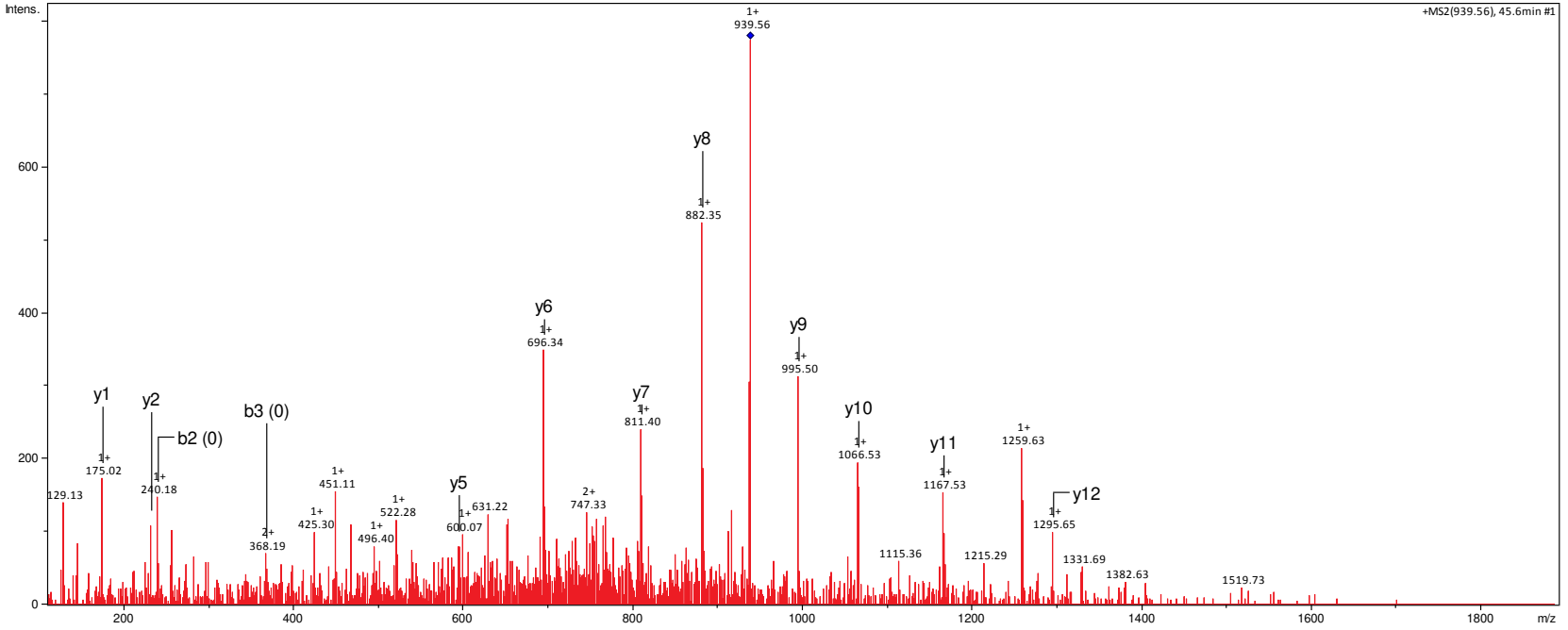

SCO Number	SCO4905
Precursor m/z	865.779
Charge	3
Retention time	133.2
Scan number	4335
Hex on peptide	2
e-value	0.000072
Site allocated?	N
Method	HCD_IT

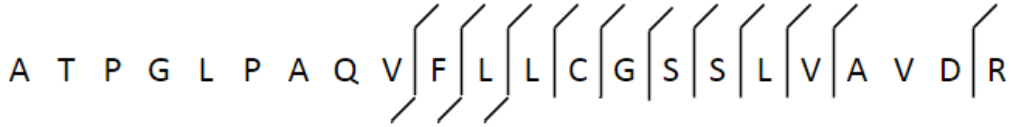

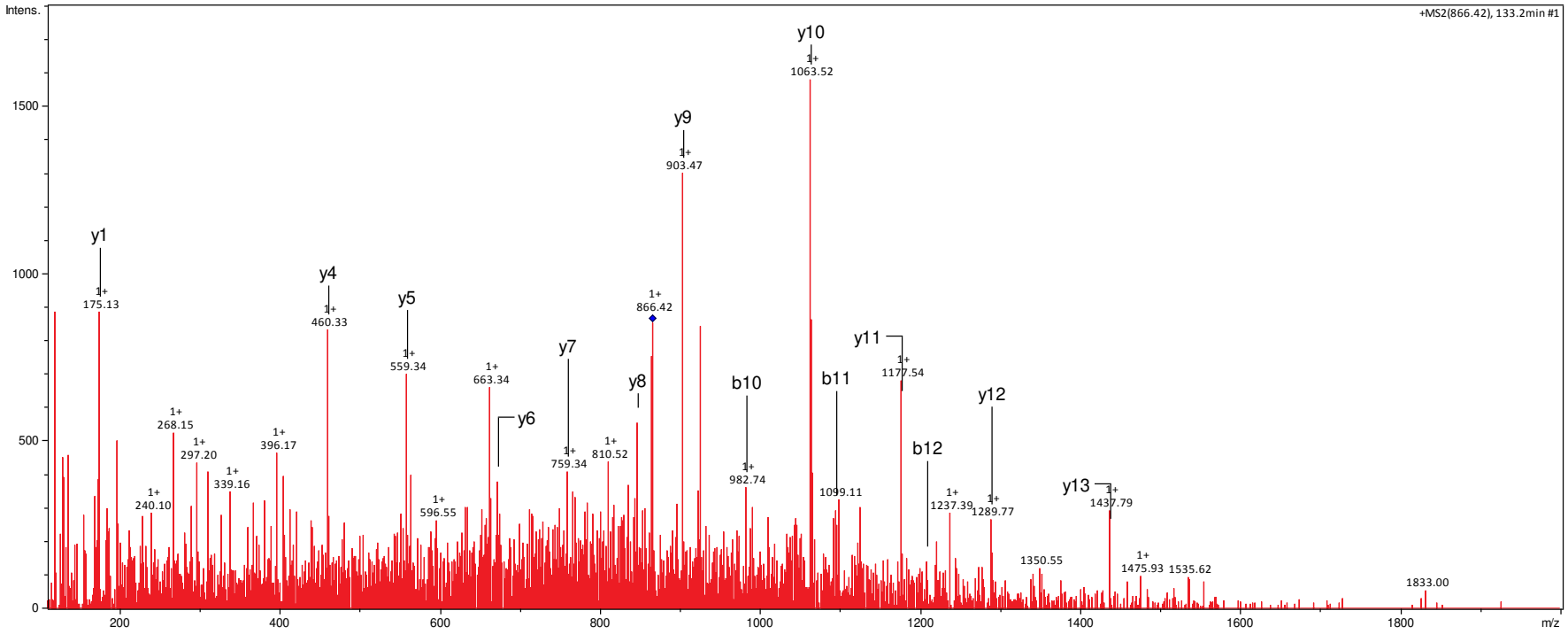

TK008

		J1929					DT1025					DT3017					TK008 (*sco4934-*)					
		Zone of inhibition (mm)			Average	SEM	Zone of inhibition (mm)			Average	SEM	Zone of inhibition (mm)			Average	SEM	Zone of inhibition (mm)			Average	SEM	
Antibiotic	**conc (µg/disc)**	**1**	**2**	**3**			**1**	**2**	**3**			**1**	**2**	**3**			**1**	**2**	**3**			**p-value**
Vancomycin	40	1	1	2	1.3	0.3	2	3	2	2.3	0.3	31	29	25	28.3	1.8	2	2	2	2.0	0.0	0.18
Vancomycin	4	0	0	0	0.0	0.0	0	0	0	0.0	0.0	23	23	20	22.0	1.0	0	0	0	0.0	0.0	-
Vancomycin	0.4	0	0	0	0.0	0.0	0	0	0	0.0	0.0	14	13	11	12.7	0.9	0	0	0	0.0	0.0	-
Vancomycin	0.04	0	0	0	0.0	0.0	0	0	0	0.0	0.0	1	1	3	1.7	0.7	0	0	0	0.0	0.0	-
Rifampicin	40	8	8	11	9.0	1.0	5	8	10	7.7	1.5	27	25	24	25.3	0.9	6	6	7	6.3	0.3	0.10
Rifampicin	4	0	0	0	0.0	0.0	0	0	0	0.0	0.0	7	6	5	6.0	0.6	0	0	0	0.0	0.0	-
Bacitracin	40	10	10	10	10.0	0.0	13	12	10	11.7	0.9	22	22	18	20.7	1.3	10	10	9	9.7	0.3	0.42
Bacitracin	4	3	1	2	2.0	0.6	1	1	2	1.3	0.3	10	10	7	9.0	1.0	2	1	1	1.3	0.3	0.39
Teicoplanin	40	19	21	20	20.0	0.6	19	19	16	18.0	1.0	24	25	22	23.7	0.9	20	21	19	20.0	0.6	1.00
Teicoplanin	4	12	11	12	11.7	0.3	10	11	10	10.3	0.3	15	15	13	14.3	0.7	12	11	12	11.7	0.3	1.00
Teicoplanin	0.4	3	3	2	2.7	0.3	2	2	2	2.0	0.0	6	5	4	5.0	0.6	3	3	3	3.0	0.0	0.42
Imipenem	40	10	13	13	12.0	1.0	23	23	27	24.3	1.3	37	37	35	36.3	0.7	26	29	29	28.0	1.0	0.00
Imipenem	4	0	0	0	0.0	0.0	0	0	0	0.0	0.0	10	8	12	10.0	1.2	4	7	6	5.7	0.9	0.02
Meropenem	40	8	9	10	9.0	0.6	13	13	12	12.7	0.3	29	29	27	28.3	0.7	21	21	20	20.7	0.3	0.00
Penicillin	100	5	6	9	6.7	1.2	9	8	9	8.7	0.3	31	29	17	25.7	4.4	13	13	12	12.7	0.3	0.03
Ampicillin	200	8	7	8	7.7	0.3	12	11	11	11.3	0.3	37	37	21	31.7	5.3	18	18	18	18.0	0.0	0.00
Ampicillin	20	0	0	0	0.0	0.0	0	0	0	0.0	0.0	16	19	0	11.7	5.9	0	0	0	0.0	0.0	-

TK008 and complements

		J1929					DT1025					DT3017					TK008 (*sco4934-*)							TK010 (*sco4934-*: pTAK32)							TK015 (*sco4934-*: pIJ10257)					
		Zone of inhibition (mm)					Zone of inhibition (mm)					Zone of inhibition (mm)					Zone of inhibition (mm)							Zone of inhibition (mm)							Zone of inhibition (mm)					
Antibiotic	**conc (µg/disc)**	**1**	**2**	**3**	**Average**	**SEM**	**1**	**2**	**3**	**Average**	**SEM**	**1**	**2**	**3**	**Average**	**SEM**	**1**	**2**	**3**	**Average**	**SEM**	**vs J1929**	**p-value**	**1**	**2**	**3**	**4**	**Average**	**SEM**	**vs TK008**	**p-value**	**1**	**2**	**3**	**Average**	**SEM**	**vs TK008**
and	40	12	12	14	12.7	0.7	21	20	18	19.7	0.9	37	37	37	37.0	0.0	30	29	29	29.3	0.3	0.00		22	25	19	20	21.5	1.3	0.01		27	25	24	25.3	0.9	0.03
Imipenem	4	6	6	7	6.3	0.3	12	13	13	12.7	0.3	29	29	29	29.0	0.0	23	17	19	19.7	1.8	0.01		12	15	12	12	12.8	0.8	0.04		21	17	16	18.0	1.5	0.52
Imipenem	0.4	0	0	0	0.0	0.0	0	0	0	0.0	0.0	18	16	18	17.3	0.7	13	10	11	11.3	0.9	0.01		10	7	8	7	8.0	0.7	0.04		10	11	6	9.0	1.5	0.27
Meropenem	40	8	8	9	8.3	0.3	15	14	15	14.7	0.3	29	27	26	27.3	0.9	19	19	20	19.3	0.3	0.00		14	14	13	13	13.5	0.3	0.00		17	17	16	16.7	0.3	0.00
Meropenem	4	3	1	4	2.7	0.9	7	8	10	8.3	0.9	20	17	20	19.0	1.0	11	11	11	11.0	0.0	0.01		7	7	8	8	7.5	0.3	0.00		10	11	7	9.3	1.2	0.30
Penicillin	100	6	4	6	5.3	0.7	3	2	9	4.7	2.2	13	16	15	14.7	0.9	12	14	14	13.3	0.7	0.00		7	9	10	9	8.8	0.6	0.00		13	11	9	11.0	1.2	0.17
Ampicillin	200	2	3	5	3.3	0.9	2	1	4	2.3	0.9	0	29	31	20.0	10.0	10	9	10	9.7	0.3	0.01		3	4	8	7	5.5	1.2	0.04		10	5	6	7.0	1.5	0.22
Ampicillin	20	0	0	0	0.0	0.0	0	0	0	0.0	0.0	0	19	23	14.0	7.1	0	0	0	0.0	0.0	-		0	0	0	0	0.0	0.0	-		0	0	0	0.0	0.0	-
Ampicillin	2	0	0	0	0.0	0.0	0	0	0	0.0	0.0	0	11	15	8.7	4.5	0	0	0	0.0	0.0	-		0	0	0	0	0.0	0.0	-		0	0	0	0.0	0.0	-

		J1929					DT1025					DT3017					TK006 (sco4847-)									TK013 (*sco4847-*:pTAK30)							TK016 (sco4847-:pIJ10257)					
		Zone of inhibition (mm)			AVERAGE	SEM	Zone of inhibition (mm)			AVERAGE	SEM	Zone of inhibition (mm)			AVERAGE	SEM	Zone of inhibition (mm)						AVERAGE	SEM	vs J1929	Zone of inhibition (mm)				AVERAGE	SEM	vs TK006	Zone of inhibition (mm)			AVERAGE	SEM	vs TK006
Antibiotic	**conc (µg/disc)**	**1**	**2**	**3**			**1**	**2**	**3**			**1**	**2**	**3**			**1**	**2**	**3**	**4**	**5**	**6**			**p-value**	**1**	**2**	**3**	**4**			**p-value**	**1**	**2**	**3**			**p-value**
Vancomycin	40	0	0	0	0.0	0.0	1	2	2	1.7	0.3	31	31	29	30.3	0.7	0	0.5	1	2	2	2	1.3	0.5	0.02	0	0	1	0	0.3	0.3	0.05	0	1	1	0.7	0.3	0.28
Vancomycin	4	0	0	0	0.0	0.0	0	0	0	0.0	0.0	29	28	27	28.0	0.6	0	0	0	0	0	0	0.0	0.0	-	0	0	0	0	0.0	0.0	-	0	0	0	0.0	0.0	-
Vancomycin	0.4	0	0	0	0.0	0.0	0	0	0	0.0	0.0	25	25	26	25.3	0.3	0	0	0	0	0	0	0.0	0.0	-	0	0	0	0	0.0	0.0	-	0	0	0	0.0	0.0	-
Vancomycin	0.04	0	0	0	0.0	0.0	0	0	0	0.0	0.0	23	23	23	23.0	0.0	0	0	0	0	0	0	0.0	0.0	-	0	0	0	0	0.0	0.0	-	0	0	0	0.0	0.0	-
Rifampicin	40	8	8	11	9.0	1.0	5	8	10	7.7	1.5	27	25	24	25.3	0.9	11	10	10	12	11	11	10.8	0.4	0.20	7	4	7	-	6.0	1.0	0.03	6	3	7	5.3	1.2	0.04
Rifampicin	4	0	0	0	0.0	0.0	0	0	0	0.0	0.0	7	6	5	6.0	0.6	0	0	0	0	0	0	0.0	0.0	-	0	0	0	0	0.0	0.0	-	0	0	0	0.0	0.0	-
Bacitracin	40	12	12	12	12.0	0.0	12	12	12	12.0	0.0	19	20	19	19.3	0.3	13	12	13	12	10	13	12.2	0.7	0.74	12	12	12	-	12.0	0.0	0.74	12	13	11	12.0	0.6	0.83
Bacitracin	4	0.5	2	2	1.5	0.5	1	0.5	2	1.2	0.4	6	6	5	5.7	0.3	2	2	1	2	1	2	1.7	0.3	0.78	1	1	1	-	1.0	0.0	0.03	2	1	0.5	1.2	0.4	0.38
Teicoplanin	40	18	18	20	18.7	0.7	20	18	20	19.3	0.7	22	24	23	23.0	0.6	19	19	20	19	19	19	19.2	0.2	0.53	18	16	18	-	17.3	0.7	0.10	18	18	18	18.0	0.0	0.00
Teicoplanin	4	10	10	11	10.3	0.3	9	9	11	9.7	0.7	13	15	15	14.3	0.7	9	10	12	10	11	11	10.5	0.6	0.77	10	9	10	-	9.7	0.3	0.17	11	9	11	10.3	0.7	0.84
Teicoplanin	0.4	0	0	0	0.0	0.0	0	0	0	0.0	0.0	4	3	5	4.0	0.6	0	0	0	0	0	0	0.0	0.0	-	0	0	0	-	0.0	0.0	-	0	0	0	0.0	0.0	-
Imipenem	40	7	8	5	6.7	0.9	20	21	21	20.7	0.3	41	37	41	39.7	1.3	27	27	27	25	28	28	27.0	0.6	0.00	18	17	19	17	17.8	0.5	0.00	27	28	30	28.3	0.9	0.27
Imipenem	4	0	0	0	0.0	0.0	12	14	14	13.3	0.7	29	33	33	31.7	1.3	17	16	16	18	18	19	17.3	0.7	0.00	12	10	12	12	11.5	0.5	0.00	19	15	16	16.7	1.2	0.65
Imipenem	0.4	0	0	0	0.0	0.0	0	0	0	0.0	0.0	25	27	27	26.3	0.7	0	0	0	0	0	0	0.0	0.0	-	0	0	0	0	0.0	0.0	-	0	0	0	0.0	0.0	-
Imipenem	0.04	0	0	0	0.0	0.0	0	0	0	0.0	0.0	19	23	15	19.0	2.3	0	0	0	0	0	0	0.0	0.0	-	0	0	0	0	0.0	0.0	-	0	0	0	0.0	0.0	-
Meropenem	40	5	7	5	5.7	0.7	12	11	12	11.7	0.3	30	33	29	30.7	1.2	16	18	15	17	17	17	16.7	0.6	0.00	12	10	12	10	11.0	0.6	0.00	16	15	16	15.7	0.3	0.11
Meropenem	4	0	0	0	0.0	0.0	5	6	5	5.3	0.3	25	23	23	23.7	0.7	5	7	5	8	8	9	7.0	1.0	0.00	3	3	3	3	3.0	0.0	0.00	5	6	5	5.3	0.3	0.07
Meropenem	0.4	0	0	0	0.0	0.0	0	0	0	0.0	0.0	10	12	15	12.3	1.5	0	0	0	0	0	0	0.0	0.0	-	0	0	0	0	0.0	0.0	-	0	0	0	0.0	0.0	-
Penicillin	100	15	15	17	15.7	0.7	15	17	16	16.0	0.6	35	33	33	33.7	0.7	20	20	20	19	19	20	19.7	0.3	0.02	15	15	17	15	15.5	0.5	0.00	22	18	22	20.7	1.3	0.53
Penicillin	10	0	2	0	0.7	0.7	3	7	7	5.7	1.3	29	23	25	25.7	1.8	8	10	6	10	9	12	9.2	1.2	0.00	3	0	8	8	4.8	2.0	0.11	8	9	9	8.7	0.3	0.60
Penicillin	1	0	0	0	0.0	0.0	0	0	0	0.0	0.0	19	19	19	19.0	0.0	0	0	0	0	0	0	0.0	0.0	-	0	0	0	0	0.0	0.0	-	0	0	0	0.0	0.0	-
Penicillin	0.1	0	0	0	0.0	0.0	0	0	0	0.0	0.0	10	7	4	7.0	1.7	0	0	0	0	0	0	0.0	0.0	-	0	0	0	0	0.0	0.0	-	0	0	0	0.0	0.0	-
Ampicillin	200	0	0	0	0.0	0.0	0	0	0	0.0	0.0	24	26	28	26.0	1.2	10	11	9	11	10	10	10.2	0.4	0.00	6	3	7	-	5.3	1.2	0.05	9	8	8	8.3	0.3	0.01